SVENSKA GEOFYSISKA FÖRENINGEN

VOLUME 3, NUMBER 4 **Tellus** NOVEMBER 1951

A QUARTERLY JOURNAL OF GEOPHYSICS

Vilhelm Bjerknes in Memoriam

By H. U. SVERDRUP, Professor of Geophysics, Director, Norsk Polarinstitutt

(Presented at joint meeting of the International Associations of Meteorology and Physical Oceanography, Brussels, 27. August 1951)

It is with great humility that I stand here today in order to attempt an evaluation of the contributions to the advance of meteorology and oceanography which my late teacher and friend, Vilhelm Bjerknes, made during his long and active life. He laid an ambitious plan for his work, he followed his plan with great consistency — and he lived to see many of his ideas bear fruit.

To Bjerknes the prediction of the weather soon became the central problem towards which he directed his attention. In his entrance lecture at the University of Leipzig, which in 1913 had called him to the chair of professor of geophysics and director of the new Geophysical Institute, he formulated his programme by saying:

"From the observed state of the atmosphere at one moment we must compute the state at a later moment. The problem of the exact computation of a future state, which long ago has been solved in astronomy, must now be tackled in all seriousness in meteorology.

"The problem is of immense dimensions. It can be solved only as result of a long development. One single research worker cannot get far, no matter how great his efforts are. However, I am convinced that in spite of all this it is not too early to point at this problem as the goal of the research. One does not always select a goal in the hope of reaching it soon. To steer towards a distant goal determines the course. In this case the far-away goal will give us an indispensable plan for our work."

Fifteen years earlier the name of Bjerknes had been unknown in meteorology. During his early years he had mainly been working in the field of classical hydrodynamics and had brought part of the remarkable work of his father, C. A. Bjerknes, to a conclusion. At this time he had frequently felt that the assumptions defining an ideal fluid placed too great limitation upon the character of the problems to which the results could be applied. In his search for an expansion he discovered in 1898 his famous theorem of circulation that later on became the core of what he called physical hydrodynamics. Unknown to Bjerknes the same theorem had been discovered already in 1886 by Silberstein who had published his findings but had failed to draw any further conclusions. The very great merit of Bjerknes is that he immediately realised the importance of the theorem to the dynamics of the atmosphere and the ocean, and drew attention to the applications in his first paper on the subject. In this first paper he did not consider circulation relative to the earth, but this matter was taken up a few years later, in 1902.

From the very beginning Bjerknes' papers

aroused great interest among meteorologists and oceanographers. One reason why Bjerknes' work became rapidly known was that by a happy coincidence his ideas, which opened up new possibilities for dealing with the three-dimensional problems of the atmosphere, were advanced just at the time when the exploration of the free atmosphere started. Around year 1900 this fascinating field, for which Köppen proposed the name aerology, was suddenly being developed. In the 1890-s systematic meteorological observations from manned balloons had been organized in Germany by R. Assmann. From 1892 paper balloons with recording instruments had been sent up by the French meteorologists, Hermite, Besançon and Teisserenc de Bort, and in 1894 A. Lawrence Rotch had started using kites at the Blue Hill observatory, Mass. In 1901 Assmann introduced the rubber balloon, which Teisserenc de Bort immediately took into use, and in the following year, 1902, he and Assmann announced independently the discovery of the stratosphere.

In the midst of all this activity Bjerknes' ideas of tackling the problem of the computation of the future weather as a three-dimensional problem naturally aroused great hopes. The meteorologists who had turned with enthusiasm to the study of the free atmosphere foresaw the possibility that the observations gathered by their efforts might revolutionize the forecasting procedure.

In oceanography the situation was similarly favourable. Around 1900 the accuracy of oceanographic observations was greatly improved and the technique of deep sea measurements perfected. Numerous observations were being collected, and now Bjerknes' theoretical contribution promised to render the needed tools for the rational use of the observations.

Still another fortunate circumstance contributed to the furthering of Bjerknes' work. In this case I do not refer to a coincidence, but to a development for which Bjerknes himself has a great deal of the credit because he understood how to impart his own enthusiasm to others. In 1904 he visited the at that time recently established Carnegie Institution of Washington where he gave a number of lectures which created such an interest that from 1906 and until shortly before his death Bjerknes received an annual grant from the Carnegie Institution in order to continue the development of his theories and apply them to the atmosphere and the ocean.

I believe it will be difficult to point at any modest grant which has rendered greater returns than the one given Bjerknes. There are two reasons for this. One is that thanks to the grant Bjerknes could employ the assistants he needed in his work. He did need assistants, because his own work centered completely around the further development of the theoretical tools. He has to my knowledge never attempted to draw a weather map, nor has he ever discussed actual meteorological observations. In the course of the years many of his assistants worked with the data, they tried to interpret the observed conditions, and, step by step, to gain better understanding of the physical processes in the atmosphere or the ocean. Bjerknes gave them complete freedom in their work. He was no hard taskmaster, but he laid the course. He was himself a very independent thinker, who in his writings rarely quoted results obtained by other authors. His papers are characterized by their elegant mathematics and clear style, because he never published a paper before he had corrected every ambiguous sentence and removed every superfluous word. He expected the same clarity from his assistants, and to some degree he wanted his assistants to be as independent in their research as he himself was. There were instances when he was openly displeased by finding his assistants spending too much time studying meteorological literature. In all events, Bjerknes' assistants helped to advance his ideas, partly when they were working with him, and partly in later years, when many of them had students who worked under their direction. In this manner the Bjerknes influence has spread like rings in the water, reaching to ever greater distances.

The other reason for the importance of the grant from the Carnegie Institution was that his grant was given during years when it was difficult for a young man to start on a scientific career. Bjerknes was free to offer assistantships to any interested student and could select among the more promising ones. Several of the young men who for some periods became his "Carnegie assistants" did not continue in meteorology or oceanography,

but most of them did, and could later on, as already mentioned, bring Bjerknes' view points to their own students.

I have dealt to such an extent with Bjerknes' assistants and his relation to them, partly because Bjerknes' attitude to them was characteristic of him, and partly because speaking of Bjerknes' influence on the development of meteorology and oceanography the contributions of his assistants cannot be overlooked, although Bjerknes was the dominating leader. He laid out the course, and his thinking exerted the greatest influence upon those who came in contact with him.

After Bjerknes turned to the application of hydrodynamics to the problems of geophysics his activity falls in four different periods. The first was the period from 1898 to 1912 when he was in Stockholm until 1907 and in Oslo from 1907 until 1912. During these years the first two volumes of the broadly planned work 'Dynamic Meteorology and Hydrography", the "Static" and the "Kinematic", were published by the Carnegie Institution, and during these years the impact of Bjerknes' thoughts started to become apparent in the meteorological and oceanographic literature. Thus, in a paper of 1909 Bjerknes lists a dozen papers in which his theorem of circulation has been applied.

He conducted an intensive campaign for the use of rational units in aerological research, and after he had urged his case at several meetings of the International Aerological Commission this body recommended in 1912 to the Directors' Conference that in the aerological publications pressure should be reported in millibar and that geopotential should be used as the vertical co-ordinate.

The second phase is covered by the years in Leipzig, from 1913 to 1917. Bjerknes accepted the offer from Leipzig for two reasons. In the first place because he could expect to obtain more students and, therefore, might hope to develop a school in meteorology; in the second place because facilities were promised him for the working up of the aerological data that were being accumulated on agreed-upon

international days. Bjerknes would use these for a three-dimensional analysis of the state of the free atmosphere partly to develop methods for representing the state of the atmosphere by means of a series of charts, partly to gain experience as to the extent to which that particular material was suited for a study of the changes in the state of the free atmosphere. His stay in Leipzig became much shorter than he had anticipated, and the results were less because only one and one half year after his appointment the first world war started, he lost his German students and also the needed assistance for preparing the aerological charts. As an interesting side-light on the role of meteorology during the first war, as contrasted to its part during the last war, I may mention that no demands for participation in meteorological research related to military problems were made on Bjerknes or on his two or three Norwegian assistants, who continued their strictly academic work and were paid by the grant from the Carnegie Institution in Washington even after the United States had entered the war.

The Leipzig period was terminated in 1917 when Bjerknes was asked to return to Norway and to accept the chair of professor of theoretical meteorology at the Geophysical Institute which recently had been established in Bergen. There he entered the most exciting period in his life, the period in which the importance of the fronts was recognized by his young collaborators, when the structure of the cyclones was discovered and the term polar front was coined. The credit for the actual discovery of the structure of the cyclones and of the polar front goes to his collaborators, but Bjerknes himself had long been interested in the lines of convergence and divergence which appear on charts on which the wind direction is shown by means of stream lines. He had early conceived the idea that a cyclone starts as a wave-like disturbance at a discontinuity surface, and one of his most important papers from the Leipzig period represents his first attempt at approaching that problem, the paper "Über Wellenbewegung in kompressiblen, schweren Flüssigkeiten".

In Bergen he had, however, to neglect his theoretical work because he and his assistants started immediately the organisation of a unique weather forecasting service, basing it on inadequate observations, but using the newly gained insight in the importance of the fronts. This development exercised a considerable influence on Bjerknes' approach to the whole problem of forecasting, as evident from an address he gave at the meeting of Scandinavian geophysicists in Gothenburg in August 1918. He started by saying:

"It is possible that different roads may lead to the solution of the problem of a satisfactory and practical method for weather forecasting. It is conceivable that among these there may be convenient roads which may lead around the strict requirement as to complete understanding of the events whose development shall be predicted. Personally I am not interested in such roads. I am only interested in the road that leads straight through the inexorable demand of complete understanding."

But then he went on to say:

"If we formulate the task (of predicting) as a mathematical problem, we may have no hope of finding a solution in a foreseeable future. But if we transfer it into a more practical form we find that we may advance simply by following consistently the road that the meteorologists started on when they first made the synoptic charts the basis of the study of the weather processes and by means of these found Bar's law and so on. We do not need to doubt that along this road we may reach results which will give us increased understanding and thus will influence the meteorological practice."

In his Leipzig address in 1913 he had stressed the direct application of the laws of hydrodynamics to given initial conditions. Now, after having been more in contact with the practical aspects of forecasting, he recognized the value of the step-wise approach, but he never relaxed his demand for complete understanding of the physical processes. He held his banner high and under this banner meteorologists and oceanographers from all parts of the world gathered.

During the Leipzig and Bergen periods the applications to meteorology came into the foreground, and Bjerknes himself and his direct collaborators gave little thought to oceanography. Still, his influence on oceanography has been equally great because for nearly fifty years Bjerknes' demand as to

striving towards understanding of the physics of the events has directed the progress.

The fourth and last period in Bjerknes' life started in 1926, when he returned to the University of Oslo as professor of mechanics and applied mathematics. He retired in 1932, but remained active until shortly before his death. During these years he returned to his theoretical work. For a long time the third volume, "Dynamics", of his great work, "Dynamic Meteorology and Hydrography" had been in preparation. Drafts had been written to parts of the volume, but had been discarded because new ideas were advanced. Many of these appeared in the "Physikalische Hydrodynamik" which was published in 1933 by himself and three of his collaborators, but the work with the "Dynamics" continued.

I said that Bjerknes lived long enough to see many results of his life's work. He saw aerology being developed to a degree which even in his most optimistic moments he had hardly considered possible, he saw the three-dimensional analysis of the atmosphere be made part of the routine work in forecasting, he experienced an expansion beyond expectation of meteorological research and, best of all, he saw that most of this research was carried out along the lines he had advocated, aiming towards interpretation of events in terms of physics. Shortly before his death he had also the great satisfaction of seeing the manuscript of the "Dynamics" completed by himself and some of his early collaborators.

I cannot close a brief appreciation of Bjerknes' activities without mentioning his very broad cultural interests. In Norway he was an untiring advocate for an expansion of the facilities of the university both in order to train better teachers and in order to create better conditions for scientific research. Along these lines he did not achieve as much as in his special field, but during the last years of his life he had at least the satisfaction that in Norway the possibilities for young men to use their abilities were increased greatly as compared to the years when he himself was nearly the only professor at the university who, thanks to the Carnegie grant, could offer a student an opportunity to attempt entering upon a scientific career.

He was fortunate in retaining his clear mind to the last. Less than eight months ago he took active part in scientific meetings, and on his 89th birthday, only three weeks before his death, he was weak and had to stay in bed, but he insisted on seeing the many of the friends who called upon him to pay their respects.

I am tempted to close with a poor translation from the old Norse "Haavamaal" in which much of the wisdom of our forebears is condensed:

> "Cattle dies, man dies,
> you yourself shall die.
> Your name never dies."

Age Determination of Pacific Chalk Ooze by Radiocarbon and Titanium Content

By G. ARRHENIUS[1], G. KJELLBERG[2], and W. F. LIBBY[3]

(Manuscript received 1 november 1951)

Abstract

Measurements have been carried out on the average radiocarbon activity of a sediment core of eupelagic chalk ooze and the age of the lower boundary was calculated by integration of the radiocarbon decay function.

In such cores where constancy of the rate of minerogenous accumulation is indicated and can be checked by lateral control, the titanium content, calibrated in terms of absolute age by means of radiocarbon measurement, can be used for dating as far back in time as the constancy of the rate of minerogenous sedimentation can be proved.

1. Principles of age measurement in core 61 B of the Swedish Deep Sea Expedition

In the works of JOLY (1908), PETTERSSON (1930), PIGGOT (1944) and URRY (references in URRY 1948) the possibilities have been demonstrated for dating samples of pelagic clays on the basis of their content of ionium supported radium. The radiocarbon method (LIBBY, ANDERSON, ARNOLD, ENGELKEMEIR, GROSSE, HAMILL, INGHRAM, KIRSHENBAUM, REID and WEINHOUSE 1946—51) has opened new possibilities especially with regard to the dating of highly calcareous deep sea deposits.

If cores of deep sea sediments are to be used for geochronological purposes their facies relationships and stratigraphy should be well known. Furthermore such cores ought to be correlated members of coherent profiles through the deep sea bottom, as this makes it possible to recognize layers deposited under abnormal conditions. Finally, if the half-life of the radioelement used is comparatively short, an area with a comparatively high rate of accumulation has to be chosen for sampling.

The sediment cores raised by the Swedish Deep Sea Expedition under the leadership of Professor H. Pettersson provide an excellent material for studies of deep sea sedimentation. The closely spaced samples from the vast, stable Central Pacific area (cf. GUTENBERG and RICHTER 1949, p. 90) have been investigated and the results have made it possible to find a series of sequences which correspond in detail to the demands put forth above (ARRHENIUS 1950 a and b). For the present purpose a member of this series was chosen, which had an exceptionally high rate of calcium carbonate accumulation, viz. the core 61 (10.3 m long, raised with the Kullen-

[1] Kagghamra, Grödinge.

[2] Matematikmaskinnämndens Arbetsgrupp, Stockholm 6.

[3] University of Chicago.

berg piston corer) together with 61 B (0.5 m long, raised with a short open tube corer according to PHLEGER 1951), both from lat. 0° 6′ S, long. 135° 58′ W and 4437 m depth. In core 61 the uppermost layer is missing, owing to the sampling technique, but in 61 B the topmost layer is also present. This material was prepared for radiocarbon analysis in the spring of 1949.

The cores 61—61 B have been closely correlated with other cores in a profile extending from lat. 6° 44′ N to 3° 00′ S and it has been possible to prove that at the locality 61 the changes in the rate of minerogenous sedimentation were smaller than the analytical error during the time of deposition of core 61 B. This conclusion is based upon measurements of the total amount of biogenous material on one hand and of minerogenous material on the other hand, accumulated at different localities along the section and between definite relative time limits.

A closer description of the sedimentation in the East and Central Pacific will be published in the Reports of the Swedish Deep Sea Expedition, Vol. V.

As a measure of the minerogenous component the concentration of titanium recalculated for salt free sediment has been used. Titanium is especially useful for this purpose as its concentration in the minerogenous component appears to be practically constant over the area in question and high enough to allow an easy and accurate determination. Furthermore titanium does not appear to be affected by secondary dissolution in this environment.

The close proportionality between the concentration of titanium and minerogenous matter in eupelagic deposits was first demonstrated in the fundamental works of CORRENS (1935) and REVELLE (1944) and was later stressed by KOCZY (1950 and 1951) who used Correns' measurements. With regard to the possibilities of estimating the rate of minerogenous sedimentation, which were conspicuous from these works, the analysis of titanium was included in the 1948 working program for treating the sedimentary material of the Swedish Deep Sea Expedition (G. ARRHENIUS, 1950 a).

In connection with his work on the core 241 from the Equatorial Atlantic Ocean, WISEMAN (1950) has also pointed out the possibility of using the concentration of titanium for estimating the clay component. He apparently based an interpretation of Late Pleistocene chronology (1951) on the vertical distribution of minerogenous matter assuming a constant rate of deposition of such matter.

It should be emphasized in this connection that a constant rate of sedimentation and a constant titanium content of the minerogenous component should not be looked upon as a general rule for deep sea sediments but must be proved in all cases. A section through the East Pacific from lat. 0° to 17° N and at an approximate distance of 800 nautical miles from the American coast did not reveal the high regularity of minerogenous sedimentation found in the Central Equatorial area. Frequent examples of irregularities in the rate of minerogenous deposition are found on rises and ridges and in throughs and pits of the Atlantic, Pacific and Indian Oceans.

It should also be pointed out that a smooth bottom topography or freedom from volcanism, as in parts of the stable Central Pacific area or in parts of the Indian and Atlantic oceans, might considerably reduce the probability for tectonic disturbances, sediment slumping and abnormal dilution with pyroclastic material but is by no means a guarantee for a constant rate of minerogenous sedimentation. Redepositional changes in this rate by as much as 50 % appear in the eupelagic environment generally not to be accompanied by changes in grain size or by qualitative changes in the composition of the clay material. The only possibility of checking changes in the rate of minerogenous sedimentation in a pelagic environment therefore seems to be a quantitative comparison of corresponding layers in several sediment cores along a profile of wide geographical range.

The biogenous components of the sediment consist mainly of skeletal remains of calcium carbonate from foraminifera and coccolithophoridae and of silica from radiolaria and diatoms. The aim of the present investigation was to use the radiocarbon of the calcium carbonate for dating purposes. The possibility, however, that the calcium carbonate had exchanged ions with the bottom water after deposition could not be ignored. In such a case it would not be possible to use the radio-

carbon content of the carbonate for age calculations. An important means for controlling secondary exchange is furnished by the palaeothermometric method of UREY based upon the temperature sensibility of the ratio between the oxygen isotopes O^{16} and O^{18} (UREY, LOWENSTAM, EPSTEIN and MCKINNEY, 1951). If the calcite had exchanged all its carbonate with carbonate ions from the deep sea bottom water or from the interstitial sediment water, a temperature of a few degrees centigrade ought to be indicated by the oxygen isotope distribution of the calcite. If, on the other hand the shells have not been subjected to any exchange of carbonate after the death of the organisms, the temperature indicated should be that of the surface layer of the ocean. If partial replacement of the original calcite had taken place some intermediate temperature would be found.

Measurements of the oxygen isotope distribution carried out by Dr S. Epstein gave the following results in core 61: 0—2 cm 21° C, 10—11.5 cm 21°, 20 cm 19.5°, 200 cm 17.5°; all measurements with an estimated standard deviation of 5° C. All temperatures found thus coincide within the limits of the experimental error with an assumed average temperature for the biotope of tropical planktonic foraminifera which are most abundant in the uppermost 100 m layer of the ocean (PHLEGER 1951). It is thus very probable that no considerable exchange of the shell carbonate took place after deposition on the deep sea bottom and the radiocarbon measurements might safely be used as a basis for age calculations. This conclusion refers to core 61 only and the results may not directly be applied to other types of deep sea deposits or other localities. It is, however, probable that the stability of the carbonate characterizes all bathyal pelagic deposits with a very high content of calcite, poor in humus and not affected by rising juvenile solutions.[1]

The stratigraphy of core 61 and 61 B indicated 3 cm/1,000 years as the order of magnitude of the average rate of Post-Glacial sedimentation at this locality. The half life level of C^{14} would under such conditions be found at approx. 17 cm depth. For the radiocarbon analysis approx. 100 g of calcium carbonate are required. Due to the small dimensions of the core (3 cm diameter) and to the fact that material had to be used also for other analyses it was, in this case, impossible to extract and analyse samples from definite time levels and to construct a decay curve from the results. Instead a coherent sample from 0 to 45 cm depth in core 61 B was subjected as a whole to radiocarbon analysis and the result was used as a basis for the age calculation. The principles of this calculation appear from fig. 1. If N_m is the average activity value obtained from analysis of a homogenous sediment column, deposited with a constant rate of accumulation and if T is the age of the lower boundary of the column then the product

$$N_m \cdot T = \int_0^T N_0 \cdot e^{-\lambda t} \cdot dt \quad \text{if} \quad N_t = N_0 \cdot e^{-\lambda t}$$

is the disintegration function.

In the actual case, however, the rate of sedimentation has not been constant, the changes being caused by changes in the rate of biogenous sedimentation. As the minerogenous rate of sedimentation appears to have

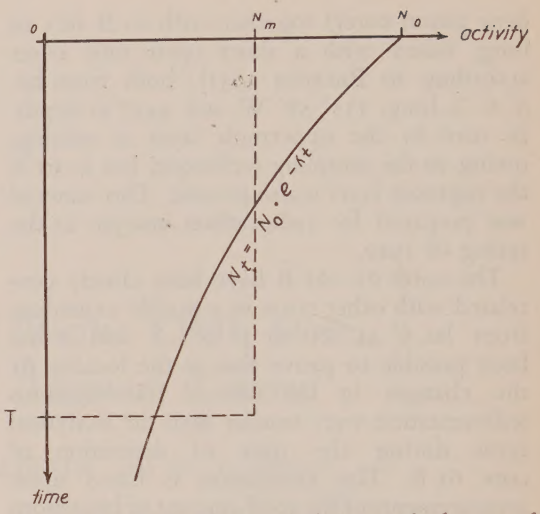

Fig. 1. Principles of age calculation. T is the age of the lower boundary of an ideal sediment column, which, subjected as a whole to radiocarbon analysis, yields the activity N_m. The curve represents the radiocarbon decay function. As is easily seen, the surface of the rectangle $N_m \cdot T$ is equal to the surface limited by the coordinate axes, the line $y = T$ and the decay curve.

[1] It might be pointed out in this connection that radiocarbon measurements in autochtonous eupelagic carbonate deposits are not affected by the source of error recently indicated by BARTLETT (1951) as influencing the isotopic composition of tufa and lake marl.

been constant in the case of core 61 B and its neighbours and as the concentration of titanium is proportional to the concentration of minerogenous matter (see above pp 223—224 and Vol. V, Rep. Swed. Deep Sea Exp.), the integral over the titanium concentration as a function of the depth in the sediment will be proportional to the time interval between the integration limits. The relative age of any level in core 61 B is thus expressed by the titanium integral from the present sediment surface to the level in question.

A factor which must be taken into consideration in the age calculation is, that due to the changes in the balance between the biogenous production of calcium carbonate and of silica the amount of calcium carbonate and therefore of radiocarbon deposited per time unit varies with time. As the calcium carbonate concentration has been measured in closely spaced samples from core 61 B, corrections for the varying carbonate deposition can easily be applied.

The calculation must also take into account the fact that at different levels of the sediment column samples of varying size had been extracted for other chemical and palaeontological analyses previous to the radicarbon analysis. The corrections for this stepwise variation in size of the samples were applied in the same way as the corrections for carbonate content.

The variations in composition of the samples investigated were not big enough to require a correction for the varying specific gravity of the deposit.

2. Constants and experimental values

Assay of modern calcium carbonate shell $N_0 = 16.2 \pm 0.5$ disintegrations/min/g of C.

Half life of $C^{14} = 5\,568 \pm 30$ years.

Assay of column 61 B $N_m = 6.18 \pm 0.24$ disintegr/min/g of C.

The results of the measurements of carbonate, titanium and mass of sediment are shown in table 1 together with the calculated cumulative fractions of the total time T. The core was divided into 22 elementary samples, or strips, for each of which the same measurements were made. The concentrations of carbonate and titanium and the mass values all refer to salt free sediment.

Table 1

Sample depth cm	$[CaCO_3] \cdot 10^3$ (q_i)	$[TiO_2] \cdot 10^5$	Mass of sample in dg (p_i)	Cumul. fraction of total time T (f_i)
0 — 2	762	33	12	0.054
2 — 4	764	31	55	0.104
4 — 5.5	766	30	13	0.141
5.5— 7	780	24	42	0.170
7 — 8.5	795	18	32	0.192
8.5—11.5	795	18	83	0.236
11.5—13.5	794	19	24	0.267
13.5—15.5	805	18	55	0.296
15.5—17	817	17	21	0.316
17 —17.5	840	22	14	0.325
17.5—19	862	27	27	0.358
19 —21	808	44	55	0.430
21 —22.5	755	61	14	0.504
22.5—23	757	57	13	0.527
23 —25.5	760	38	138	0.604
25.5—27.5	763	22	79	0.640
27.5—32	768	22	248	0.738
32 —33.5	773	23	71	0.766
33.5—38.5	778	26	275	0.872
38.5—40	783	29	73	0.908
40 —43	799	25	166	0.969
43 —45	815	20	55	1.000

3. Calculation of the results

Notations:

mass of material in the i:th strip p_i
fraction of carbonate in ,, ,, q_i
time limits of ,, ,, t_{i-1}, t_i
$t_i = f_i \cdot T$

T is the age of the lowest level of the column. The index i varies from 1 through 22, and $f_0 = 0$, $f_{22} = 1$.

To derive an equation that will permit the determination of T, it is simplest to start with the assumption that the quantities needed are known as continuous functions of the time t along the column.

Suppose that $c(t)dt$ is the mass of the carbonate contained between the levels of the core that correspond to times t and $t + dt$. With N_0 = the radioactivity of modern carbonate per unit mass, the total activity of the core becomes:

$$N_{tot} = N_0 \cdot \int_0^T c(t)\, e^{-\lambda t}\, dt \qquad (1)$$

and the activity per mass unit carbonate:

$$N_m = N_0 \cdot \frac{\int_0^T c(t)\, e^{-\lambda t}\, dt}{\int_0^T c(t)\, dt} \qquad (2)$$

But $c(t)dt = q(t) \cdot m(t)dt$, where $m(t)dt$ is the mass of all material between the levels t and $t + dt$, and $q(t)$ the fraction of carbonate in the same portion. The variation of $m(t)$ thus accounts both for the variations in the rate of sedimentation and for the variations in the area of the cross-section which occur because material was extracted from the core for other experimental purposes, prior to this investigation. $q(t)$ depends also on the variation of the rate of accumulation of silica.

Inserting this in (2) and removing the denominators we get:

$$N_m \int_0^T q(t)\, m(t)\, dt = N_0 \int_0^T q(t)\, m(t)\, e^{-\lambda t} dt \qquad (3)$$

or, by writing the integrals as sums of integrals over the elementary strips:

$$N_m \sum_{i=1}^{i=22} \int_{t_{i-1}}^{t_i} q(t)\, m(t)\, dt =$$

$$= N_0 \sum_{i=1}^{i=22} \int_{t_{i-1}}^{t_i} q(t)\, m(t)\, e^{-\lambda t} dt \qquad (4)$$

Supposing now that $q(t)$ and $m(t)$ are constant over each strip, we get:

$$N_m \sum_{i=1}^{i=22} q_i m_i (t_i - t_{i-1}) =$$

$$= \frac{N_0}{\lambda} \sum_{i=1}^{i=22} q_i m_i [\exp(-\lambda t_{i-1}) - \exp(-\lambda t_i)] \qquad (5)$$

As $m_i(t_i - t_{i-1}) = p_i$, and $t_i = f_i \cdot T$, we finally get:

$$\frac{N_m}{N_0} \cdot \lambda T \cdot \sum_{i=1}^{i=22} p_i q_i =$$

$$= \sum_{i=1}^{i=22} \frac{p_i q_i}{f_i - f_{i-1}} [\exp(-\lambda T f_{i-1}) - \exp(-\lambda T f_i)] \qquad (6)$$

Putting:

$$u(t) = \sum_{i=1}^{i=22} p_i q_i \left\{ \frac{N_m}{N_0} \lambda t - \frac{\exp(-\lambda t f_{i-1}) - \exp(-\lambda t f_i)}{f_i - f_{i-1}} \right\},$$

the upper age limit T is the positive root of the equation $u(t) = 0$.

Although this equation might conceivably have several positive roots, it can be shown that this is not the case by study of the exact equation (3), which can have only one positive root. This conclusion is valid also for discontinuous $q(t)$, $m(t)$, such as we have assumed here, and the equation $u(t) = 0$ does therefore determine T unambiguously.

The value of T was found to be 14 162 years. The accuracy of this result is discussed in the next section.

For the numerical work, the digital relay computer BARK was used.[1] A program for the evaluation of u was so arranged that, with only slight modifications, it could also be used to calculate the different partial derivatives necessary for the error estimation. (See next section). Once this program had been set up, each new value of u was computed in about 5 1/2 minutes. It was therefore easy to compute both u and the derivatives for several neighbouring values of t, which gave a convincing guarantee against accidental errors of computation.

4. Sources of error and their influence

If, for the purposes of the present section, we introduce the notation:

dx = the standard deviation of x, we get the following formula for dT.

$$dT^2 = \left(\frac{\partial T}{\partial \tau}\right)^2 d\tau^2 + \left(\frac{\partial T}{\partial N_0}\right)^2 dN_0^2 +$$

$$+ \left(\frac{\partial T}{\partial N_m}\right)^2 dN_m^2 + \sum_{i=1}^{i=22} \left(\frac{\partial T}{\partial p_i}\right)^2 dp_i^2 +$$

$$+ \sum_{i=1}^{i=22} \left(\frac{\partial T}{\partial q_i}\right)^2 dq_i^2 + \sum_{i=1}^{i=21} \left(\frac{\partial T}{\partial f_i}\right)^2 df_i^2$$

[1] For a description of the BARK and its performance, see G. KJELLBERG and G. NEOVIUS, (1951).

or,

$$dT^2 = \left(\frac{\partial T}{\partial \tau}\right)^2 d\tau^2 + \frac{1}{\left(\frac{\partial u}{\partial t}\right)^2_{t-T}} \cdot$$

$$\cdot \left\{ \left(\frac{\partial u}{\partial N_0}\right)^2 dN_0^2 + \left(\frac{\partial u}{\partial N_m}\right)^2 dN_m^2 + \right.$$

$$+ \sum_{i=1}^{i=22} \left(\frac{\partial u}{\partial p_i}\right)^2 dp_i^2 + \sum_{i=1}^{i=22} \left(\frac{\partial u}{\partial q_i}\right)^2 dq_i^2 +$$

$$\left. + \sum_{i=1}^{i=21} \left(\frac{\partial u}{\partial f_i}\right)^2 df_i^2 \right\}_{t-T}$$

The derivatives were computed according to the formulae:

$$\frac{\partial T}{\partial \tau} = \frac{T}{\tau}$$

$$\frac{\partial u}{\partial N_0} = - \sum_{i=1}^{i=22} p_i q_i \frac{N_m \lambda T}{N_0^2}$$

$$\frac{\partial N_m}{\partial u} = \sum_{i=1}^{i=22} p_i q_i \frac{\lambda T}{N_0}$$

$$\left(\frac{\partial u}{\partial t}\right)_{t-T} = \lambda \sum_{i=1}^{i=22} p_i q_i \left\{ \frac{N_m}{N_0} + \right.$$

$$\left. + \frac{f_{i-1} \cdot \exp(-\lambda T f_{i-1}) - f_i \cdot \exp(-\lambda T f_i)}{f_i - f_{i-1}} \right\}$$

$$\frac{\partial u}{\partial p_i} = q_i \cdot \left\{ \frac{N_m}{N_0} \cdot \lambda T - \right.$$

$$\left. - \frac{\exp(-\lambda T f_{i-1}) - \exp(-\lambda T f_i)}{f_i - f_{i-1}} \right\}$$

$$\frac{\partial u}{\partial q_i} = \frac{p_i}{q_i} \cdot \frac{\partial u}{\partial p_i}$$

$$\frac{\partial u}{\partial f_i} = \frac{p_i q_i}{f_i - f_{i-1}} \cdot$$

$$\cdot \left\{ \frac{\exp(-\lambda T f_{i-1}) - \exp(-\lambda T f_i)}{f_i - f_{i-1}} - \right.$$

$$\left. - \lambda T \exp(-\lambda T f_i) \right\} - \frac{p_{i+1} q_{i+1}}{f_{i+1} - f_i} \cdot$$

$$\cdot \left\{ \frac{\exp(-\lambda T f_i) - \exp(-\lambda T f_{i+1})}{f_{i+1} - f_i} - \right.$$

$$\left. - \lambda T \exp(-\lambda T f_i) \right\}$$

(For the computation of the derivatives $\frac{\partial u}{\partial t}$, $\frac{\partial u}{\partial p_i}$, $\frac{\partial u}{\partial q_i}$, $\frac{\partial u}{\partial f_i}$ the BARK was used.)

The following numerical results were obtained. The units employed are: τ and T in years, N_m and N_0 in disintegrations per min per g C, p_i in hectograms, q_i and f_i dimensionless fractions.[1]

$$\frac{\partial T}{\partial \tau} = 2.54$$

$$\frac{\partial u}{\partial t} = 0.48712 \cdot 10^{-4}$$

$$\frac{\partial u}{\partial N_0} = -0.0509$$

$$\frac{\partial u}{\partial N_m} = 0.1333$$

and

i	$\frac{\partial u}{\partial p_i}$	$\frac{\partial u}{\partial q_i}$	$\frac{\partial u}{\partial f_i}$
1	−0.7689	−0.0121	+0.0716
2	−0.6577	−0.0474	+0.0675
3	−0.5743	−0.0097	+0.0526
4	−0.5204	−0.0280	+0.0660
5	−0.4844	−0.0195	+0.0996
6	−0.4270	−0.0446	+0.0900
7	−0.3637	−0.0110	+0.0613
8	−0.3223	−0.0220	+0.0554
9	−0.2913	−0.0075	+0.0242
10	−0.2785	−0.0046	+0.0330
11	−0.2530	−0.0079	+0.0552
12	−0.1680	−0.0114	+0.0410
13	−0.0766	−0.0014	+0.0128
14	−0.0294	−0.0005	+0.0683
15	+0.0165	+0.0030	+0.0896
16	+0.0635	+0.0066	+0.1219
17	+0.1141	+0.0368	+0.1078
18	+0.1576	+0.0145	+0.1045
19	+0.1992	+0.0704	+0.0942
20	+0.2389	+0.0223	+0.0590
21	+0.2680	+0.0557	+0.0504
22	+0.2946	+0.0199	

[1] In section 3 N_0 and N_m were defined as disintegrations per min. per g $CaCO_3$. It is, however, obvious that the choise of unit does not matter, as long as N_0 and N_m are measured with the same unit.

The value of the standard deviation of each variable is known from the measurements, except for p_i and q_i, where one should also take into account the error involved in the assumption that $q(t)$ and $m(t)$ are constant over each strip. This leads to estimated s.d.:s for the q_i, larger than would result from the measurements alone, while the errors of the p_i are not affected. The argument proving this, and the procedure by which the standard deviations of the q_i were estimated (with the aid of differences from table 1), will be omitted, as it will soon appear that neither group of errors contributes appreciably to the total error dT.

After these corrections had been made, the standard deviations of the p_i, q_i and f_i were taken to be, respectively:

$1 \cdot 10^{-3}$, between $3 \cdot 10^{-3}$ and $9 \cdot 10^{-3}$, $1 \cdot 10^{-3}$

The standard deviations of the other variables are given in section 2. Inserting the values of derivatives and s.d.:s in equation (7), one obtains:

$$dT = 843$$

and we should therefore write:

$$T = 14\,200 \pm 900 \text{ years.}$$

The following list gives the influence of each separate source of error.

$$\left| \frac{\partial T}{\partial \tau} \cdot d\tau \right| = 76$$

$$\left| \frac{\partial T}{\partial N_0} \cdot dN_0 \right| = 522$$

$$\left| \frac{\partial T}{\partial N_m} \cdot dN_m \right| = 657$$

$$\sqrt{\sum_{i=1}^{i=22} \left(\frac{\partial T}{\partial p_i} \right)^2 \cdot dp_i^2} = 35$$

$$\sqrt{\sum_{i=1}^{i=22} \left(\frac{\partial T}{\partial q_i} \right)^2 \cdot dq_i^2} = 8$$

$$\sqrt{\sum_{i=1}^{i=21} \left(\frac{\partial T}{\partial f_i} \right)^2 \cdot df_i^2} = 7$$

It is evident that the errors dN_m and dN_0 dominate completely, and in particular that the errors in p, q and f are negligible.

5. Possibilities for extrapolation of the results and further use of the integration method for age determination

The possibilities of extrapolating laterally the results gained from core 61 B depend upon whether isochronous key levels can be found and traced through the sedimentary sequence of the oceans. The investigations of the Swedish Deep Sea Expedition has shown that this condition is fulfilled in certain types of calcium carbonate lithofacies where detailed correlation can be carried out over distances exceeding 1 700 nautic miles. The world encircling net of stations of the Swedish Deep Sea Expedition provides a material which is highly promising for the establishment of a global marine geochronology (cf. PETTERSSON, 1950).

The possibilities for extrapolating backwards in time from the radiocarbon age determination of core 61 B depend upon the ability to evaluate the rate and changes of rate of biogenous and minerogenous sedimentation in the same way as was done with core 61 B. This work has not yet been completed but as far as can be judged from present results, the vertical extrapolation can be carried down to the lower Pleistocene or upper Pliocene in the East Pacific chalk ooze profile. This mostly corresponds to the entire depth of the sequence sampled with the Kullenberg piston corer.

The easiest way of extending the radiocarbon time scale backwards in time appears to be to control the constancy of minerogenous sedimentation and, in such cases where constancy is found, to calibrate the titanium integral in terms of absolute time. The age of any depth level can thereafter be calculated from the corresponding titanium integral. Constancy of minerogenous sedimentation can be expected and proved only in exceptional cases. In regions where no such constancy is found the dating can be acquired through correlation with key localities such as number 61 of the Swedish Deep Sea Expedition. Correlation methods for deep sea sequences will be described in detail in Vol. V of the Reports of the Expedition.

Acknowledgments

The authors are indebted to Professor H. Pettersson and Dr O. Arrhenius for having made the present investigation possible. They should also like to thank Dr H. C. Urey for making the oxygen isotope analyses possible and Dr S. Epstein for carrying them out and the Swedish Natural Science Research Council as well as the Knut and Alice Wallenberg Foundation for sponsoring the investigation. The relay computer BARK was made available through the courtesy of the Swedish Board for Computing Machinery and the Director of the Boards computing center, Dr Conny Palm.

REFERENCES

ANDERSON, E. C., LIBBY, W. F., WEINHOUSE, S., REID, A. F., KIRSHENBAUM, A. D., and GROSSE, A. V., 1947: Radiocarbon from cosmic radiation. *Science* **105**, 576.

ANDERSON, E. C., LIBBY, W. F., WEINHOUSE, S., REID, A. F., KIRSHENBAUM, A. D., and GROSSE, A. V., 1947: Natural radiocarbon from cosmic radiation. *Phys. Rev.* **72**, 931.

ANDERSON, E. C., ARNOLD, J. R., and LIBBY, W. F., 1951: Measurement of low level radiocarbon. *Rev. Sci. Instr.* **22**, 225.

ANDERSON, E. C., and LIBBY, W. F., 1951: World-wide distribution of natural radiocarbon. *Phys. Rev.* **81**, 64.

ARNOLD, J. R., and LIBBY, W. F., 1949: Age determination by radiocarbon content; checks with samples of known age. *Science* **110**, 678.

ARNOLD, J. R. and LIBBY, W. F., 1951: Radiocarbon dates. *Science* **113**, 111.

ARRHENIUS, G., 1950 a: The Swedish Deep Sea Expedition. The geological material and its treatment with special regard to the Eastern Pacific. *Geol. Fören. Förhandl.* **72**, 185.

— 1950 b: Late Cenozoic climatic changes as recorded by the Equatorial Current System. *Tellus* **2**, 83.

BARTLETT, H. H., 1951: Radiocarbon datability of peat, marl, caliche and archaeological materials. *Science* **114**, 55.

CORRENS, C. W., 1937: Die Sedimente des Äquatorialen Atlantischen Ozeans. *Wiss. Ergebn. d. Deutschen Atlant. Exp. 1925—1927* **3**, 3.

ENGELKEMEIR, A. G., HAMILL, W. H., INGHRAM, M. G., and LIBBY, W. F., 1949: The half-life of radiocarbon (C^{14}). *Phys. Rev.* **75**, 1825.

ENGELKEMEIR, A. G., and LIBBY, W. F., 1950: End and wall corrections for absolute beta-counting in gas counters. *Rev. Sci. Instr.* **21**, 550.

GROSSE, A. V., and LIBBY, W. F., 1947: Cosmic radiocarbon and natural radioactivity of living matter. *Science* **106**, 88.

GUTENBERG, B., and RICHTER, C. F., 1949: Seismicity of the Earth and associated phenomena. *Princeton University Press.*

JOLY, J., 1908: On the content of radium and thorium in deep sea deposits. *Phil. Mag.* **6**, 190.

KJELLBERG, G., and NEOVIUS, G, 1951: The BARK, a Swedish general purpose relay computer. *Mathematical Tables and Other Aids to Computation* **5**, 29.

KOCZY, F. F., 1950: Zur Sedimentation und Geochemie im Äquatorialen Atlantischen Ozean. *Medd. Oceanogr. Inst. Göteborg* **17**.

— 1951: Factors determining the element concentration in sediments. *Geochimica et Cosmochimica Acta* **1**, 73.

LIBBY, W. F., 1946: Atmospheric helium three and radiocarbon from cosmic radiation. *Phys. Rev.* **69**, 671.

LIBBY, W. F., ANDERSON, E. C., and ARNOLD, J. R., 1949: — Age determination by radiocarbon content; world-wide assay of natural radiocarbon. *Science* **109**, 227.

PETTERSSON, H., 1930: Teneur en radium des dépôts de mer profonde. *Résult. Camp. Sci. Monaco* **91**.

— 1949: Geochronology of the deep ocean bed. *Tellus* **1**, 1.

PHLEGER, F. B., 1951: Ecology of Foraminifera, Northeast Gulf of Mexico. Part 1. *Geol. Soc. Am. Mem.* **46**.

PIGGOT, C. S., 1944: Radium content of ocean bottom sediments. *Carnegie Inst. Wash. Publ.* **556**.

REVELLE, R. R., 1944: Marine bottom samples collected in the Pacific Ocean by the Carnegie on its seventh cruise. *Carnegie. Inst. Wash. Publ.* **556**.

SCHOTT, W., 1935: Die Foraminiferen in dem Äquatorialen Teil des Atlantischen Ozeans. *Wiss. Ergebn. d. Deutschen Atl. Exp. 1925—1927* **3**, 3.

UREY, H. C., LOWENSTAM, H. A., EPSTEIN, S., and MC KINNEY, C. R., 1951: Measurement of paleotemperatures and temperatures of the Upper Cretaceous of England, Denmark and the Southern United States. *Bull. Geol. Soc. Am.* **62**, 399.

URRY, W. D., 1948: Radioactivity of ocean sediments., 7, Rate of deposition of deep sea sediments. *Jour. Marine Research*, **7** 3 618.

WISEMAN, J. D. H., 1950: Secrets of the ocean bed. — Dating the changing climate of the past. The Times, Friday September 22.

WISEMAN, J. D. H., and OVEY, C. D., 1950: Recent investigations on the deep sea floor. *Proc. Geol. Ass.* **61**, 50.

Multiple Currents in the Gulf Stream System*

By F. C. FUGLISTER, Woods Hole Oceanographic Institution

(Manuscript received 20 September 1951)

Abstract

A new interpretation of the accumulated temperature and salinity data from the Gulf Stream Area indicates that the System is made up of a series of overlapping currents. These currents are separated by relatively weak countercurrents. Data from a recent survey are presented as supporting this hypothesis.

In nearly all discussions of the Gulf Stream and of the North Atlantic Current the terms countercurrent and eddy are frequently employed, (ISELIN 1936, 1940, and SVERDRUP et al. 1942). Many temperature and salinity profiles across the currents indicate the presence of countercurrents and/or eddies and certain theoretical considerations require that they exist (ROSSBY 1936). On the other hand charts showing the average distribution of temperature and salinity (WÜST and DEFANT 1936 and FUGLISTER 1947, etc.) and charts showing the currents in the western North Atlantic do not indicate that countercurrents or eddies are permanent features of the system.

It is the purpose of this paper to suggest that, by eliminating the averaging processes, countercurrents can be introduced as, at least, semi-permanent features of the circulation and a new picture of the current system will evolve. The existing current charts fall into two general classes, those that show a relatively narrow current flowing from Cape Hatteras to the Grand Banks area where the current is shown to fork or branch, and those charts that depict a current at Cape Hatteras that gradually broadens as it moves toward the mid-Atlantic. The data used for these charts interpreted in a different manner shows that, in the Gulf Stream and North Atlantic Current areas, there is no one continuous current but a series of overlapping easterly currents separated by countercurrents.

The averaging processes tend to obscure certain details that are known to exist. Perhaps the most important of these details, in the present connection, is the very narrow zone of minimum temperatures or low pressure generally found on the left-hand side, facing downstream, of a strong current. In an attempt to show this zone and to illustrate what seems a more logical interpretation of the accumulated sub-surface data, a schematic chart of temperatures at a depth of 200 meters in the Gulf Stream area has been drawn. The data used are from various sources but primarily from the multiple ship survey of 1950, (FUGLISTER and WORTHINGTON 1951). This chart (see fig. 1) shows three easterly currents between Cape Hatteras and the longitude of Flemish Cap. There is a minimum temperature

* Contribution No. 584 from the Woods Hole Oceanographic Institution.

This research was sponsored by the Office of Naval Research under Contract N6onr-277, T. O. I.

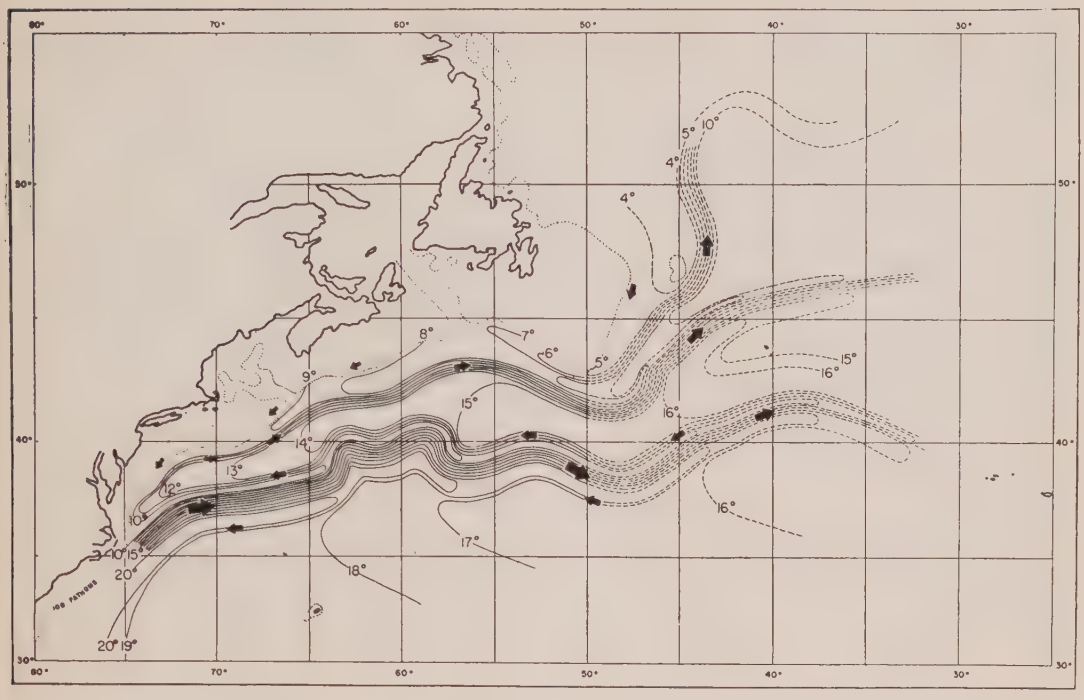

Fig. 1. Schematic chart of temperatures (° C.) at a depth of 200 meters in the Gulf Stream Area.

zone inshore of the sharp gradient off Cape Hatteras. The temperatures in this zone increase to the east. This increase in temperature is balanced by a corresponding decrease in temperature in the warm zone to the right of the gradient. If we assume for the moment that the currents flow along the isotherms then the major current off Cape Hatteras, without becoming wider or branching, simply becomes weaker as it flows toward the east. On both sides of this current there are weak countercurrents. A second easterly current forms just off the continental shelf north of Cape Hatteras, increases in strength as it flows toward the Grand Banks area and then in its turn gradually weakens in the same manner as the first current. Finally a third stream is depicted forming in the Grand Banks area and moving toward the northeast.

In order to check on the above interpretation of data obtained from various sources a survey was made of part of the area by the ALBATROSS III in June 1951. The data collected on this cruise consisted of half-hourly bathythermograph observations to a depth of 250 meters and (over many sections) hourly surface current measurements with the GEK (VON ARX 1950). As was the case with the multiple ship survey of 1950 the majority of surface current vectors showed the same current directions as would be deduced from a plot of the 200-meter isotherms. A plot of these isotherms and the track of the ALBATROSS III are shown in figure 2. The entire area of interest could not be covered in the 26 days the research vessel was at sea but the results obtained strongly support the multiple current hypothesis. In fact the data indicated the existence of four major easterly currents separated by countercurrents of varying magnitudes.

Aside from the extravagant amount of extrapolation used in both fig. 1 and fig. 2 the most serious criticism of the multiple current hypothesis as presented here may be that the temperature structure at 200 meters does not reflect the pressure field. It may be considered as representing only a relatively shallow surface layer. Actually a similar picture of the current regime in this area could

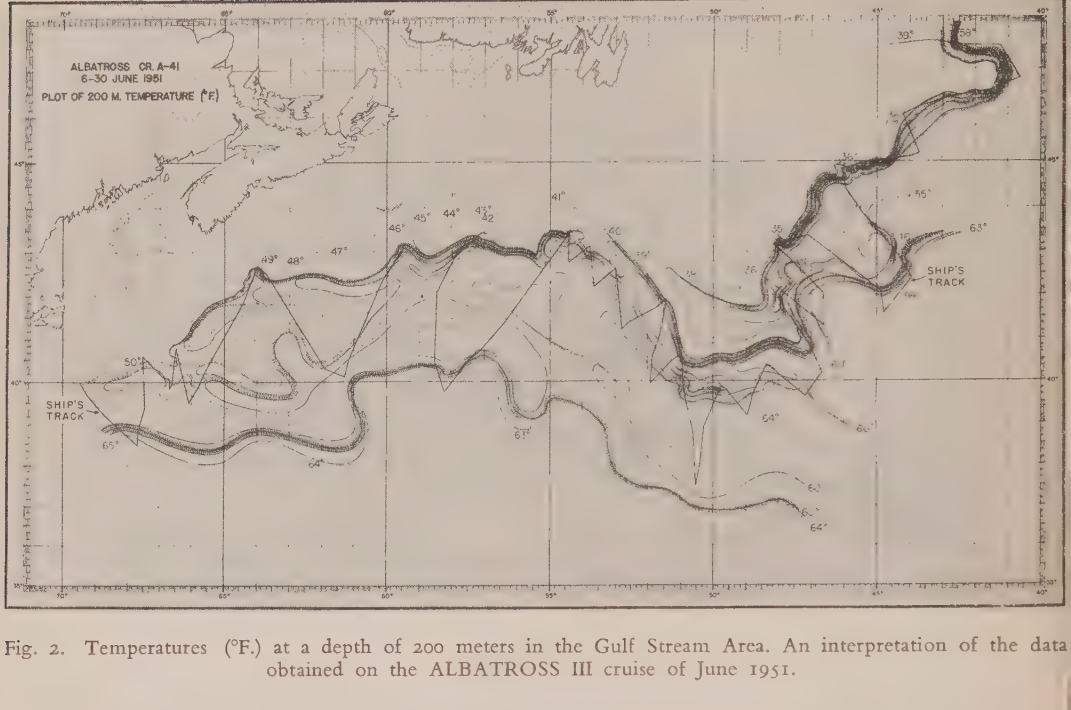

Fig. 2. Temperatures (°F.) at a depth of 200 meters in the Gulf Stream Area. An interpretation of the data obtained on the ALBATROSS III cruise of June 1951.

be obtained by using surface dynamic height anomalies referred to the 2000 decibar surface. The difficulty would be that observations taken over a period of more than 10 years would have to be used and even more extrapolation would be required.

However, an examination of all the available deep temperature and salinity sections normal to the coast between Cape Hatteras and the Grand Banks gives the following interesting results. Out of fifteen sections between Montauk, Long Island, and Bermuda, variations in the depth of the sigma-t 27.2 surface show:

- 7 sections with a slight westerly current very close in by the continental shelf;
- 13 sections with a stronger easterly current just off the shelf;
- 13 sections with a countercurrent to the left of the Gulf Stream.
- 12 sections with a countercurrent to the right of the Gulf Stream.

The average depth in meters of the 27.2 sigma-t surface at each maximum and minimum point from the shelf outward is as follows:

average	255	231	336	214	949	833
difference	—24	+105	—122	+735	—116	

Of the available sections to the east of the Montauk—Bermuda line and west of the 50th meridian only 7 reach from the continental shelf out to the Gulf Stream. These 7 all show an easterly current off the continental shelf and a countercurrent between it and the Gulf Stream. None of these sections reached far enough south to check on the existence of a countercurrent to the right of the Stream. When the data from the three most easterly sections are averaged, the depth of the sigma-t 27.2 surface at each maximum and minimum point from the shelf outward is:

average	190	132	387	383	890
difference	—58	+355	—104	+507	

Assuming that the differences in depth of the sigma-t surface between these points indicate the relative strength of the currents then it appears that the easterly current off the continental shelf increases and the Gulf Stream decreases in strength as they move toward the Grand Banks area.

If this multiple current system is accepted then there is a problem of nomenclature. As a group the currents discussed here form a

portion of the Gulf Stream System. This portion of the System fits the description of the North Atlantic Current, as given in THE OCEANS (SVERDRUP et al. 1942), except that now the name should apply to the group of currents as far west as Cape Hatteras instead of only to those currents to the east of the Grand Banks. If the term Gulf Stream is to be retained it should be understood that it applies only to the direct continuation of the Florida Current and it does not include all easterly-flowing currents between Cape Hatteras and the Grand Banks. Whether or not any of the other currents in the group should be specifically named is a question that might wait until more is known about their permanency.

Since June of this year the ALBATROSS III has been engaged in surveying the area to the east of Flemish Cap. Aboard ship the various currents are referred to as No. 1 (for the Gulf Stream), No. 2, No. 3, etc., for each successive current encountered. No. 4, the current off Flemish Cap, has been followed as far east as the 23rd meridian and the possible existence of a No. 5 has been indicated.

REFERENCES

FUGLISTER, F. C., 1947: Average Monthly Sea Surface Temperatures of the Western North Atlantic Ocean. *Papers in Physical Oceanography and Meteorology*, **10**, 2, pp. 1—25.

FUGLISTER, F. C., and L. V. WORTHINGTON, 1951: Some Results of a Multiple Ship Survey of the Gulf Stream. *Tellus*, **3**, 1, pp. 1—14.

ISELIN, C. O'D., 1936: A Study of the Circulation of the Western North Atlantic. *Papers in Physical Oceanography and Meteorology*, **4**, 4, pp. 1—101.

— 1940: Preliminary Report on Long-Period Variations in the Transport of the Gulf Stream System, *Papers in Physical Oceanography and Meteorology*, **8**, 1, pp. 1—40.

ROSSBY, C.-G., 1936: Dynamics of Steady Ocean Currents in the Light of Experimental Fluid Mechanics. *Papers in Physical Oceanography and Meteorology*, **5**, 1, pp. 1—26.

SVERDRUP, H. U., M. W. JOHNSON and R. H. FLEMING, 1942: *The Oceans: Their Physics, Chemistry, and General Biology*. New York, Prentice-Hall.

VON ARX, WILLIAM S., 1950: An Electromagnetic Method for Measuring the Velocities of Ocean Currents from a Ship Under Way. *Papers in Physical Oceanography and Meteorology*, **9**, 3, pp. 1—26.

WÜST, GEORG, and ALBERT DEFANT, 1936: Atlas zur Schichtung und Zirkulation des Atlantischen Ozeans. Deutsche Atlantische Expedition Meteor 1925—1927, Wiss. Erg., Bd. VI—Atlas, Berlin.

Height Variations in the Concentration of Ions Near the Ground During Quiet Summer Nights at Uppsala

By HARALD NORINDER and REINHARDS SIKSNA
Institute for High Tension Research, University of Uppsala

(Manuscript received 25 Juni 1951)

Abstract

Results of measurements of the concentration of small- and large-ions at different heights near the ground during quiet summer nights at Uppsala are given. Characteristic shapes for the variation of the concentration of ions are illustrated. At the ground the concentration of small ions increases more than at higher levels, where also an enhanced content of small ions can be observed during the stated weather conditions. The number of large ions descreases after sunset reaching a minimum at sunrise, after sunrise a comparatively rapid increase follows. It seems that the concentration of large ions near the ground is actually a little below that at the higher levels. Preliminary explanations of the variations are outlined.

Introduction

We have developed the concept that some of the variations of the ionic density observed by us in the summer of 1949 (17) were caused by the accumulation near the ground of emanation exhaled from the soil, and consequently also by its decay products, under certain meteorological conditions in which a minimal mixing of air takes place (18), (19). A detailed investigation of the variations of the ionic density, under meteorological conditions which might favour the accumulation of emanation near the ground, was carried out at the Institute for High Tension Research at Uppsala in the summer of 1950; the ionic density was measured at different levels above the ground in order to obtain an insight into the mixing conditions prevailing. Measurements of elements characteristic of the electrical properties of atmospheric air at different levels are not very numerous, though they may be of great importance. Investigations of the potential-gradient at three different levels have been carried out by DAUNDERER (6) and by NORINDER (15). BROWN (4) has measured the space-charge in atmospheric air at different levels near the ground. BECKER (1) and DEIJ (7) have measured the content of emanation at two levels. Conductivity of the air, mainly due to small ions, in the lowest levels of the atmosphere has been measured at different heights by HOGG (10). The vertical distribution of atmospheric condensation nuclei has been measured by YUNKER (24) at two levels.

We have further investigated the electrical elements of atmospheric air near the ground at different levels by measurements of the ionic density. In this manner we hope to gain an insight into the matter of ionization processes near the ground and their correlation with the conditions of mixing of air there.

Arrangement of the measurements

To be able to measure the ionic density at different levels above the ground a special device was built by which air was sucked from three levels above the ground ($h_1 = 0.1$, 0.05 m, $h_2 = 0.5$, 0.25 m, $h_3 = 2.1$ m). The ionic density of the air sucked from these different levels was measured with the ion-counters used during the preceding measurements at the Institute (16), (17), (23). Small ions of both polarities were measured with two reconstructed EBERT ion-counters (16) and the positive large ions with an ISRAËL large-ion counter (23). Some difficulties arose during the measurements. At sunset insects were sucked into the EBERT counters and remained on the insulators of the electrometers. The apparatus could be cleaned by compressed air or by dissembly. Another kind of difficulty was encountered with the large-ion counter during this series of measurements; the insulation losses of the counter were variable, increasing abnormally during the night and diminishing again during the early morning hours. It seemed at first that measurements of the large ions were impossible because of the above mentioned abnormal irregularity in the deterioration of the insulation. It may be supposed that the most probable cause for the observed diminution of the insulation was a radioactive deposit, precipitated on the condensers of the counter during the aspiration of air through it. If the number of large ions must be measured with a large-ion counter in the manner used by us during selected summer nights when an enhanced quantity of active deposit may be expected, especial attention must be paid to the determination of the fictive insulation "losses" of the apparatus as a function of the time of aspiration and of the time lapse after the interruption of aspiration.

Results of measurements

The measurements of the ionic density were carried out during selected nights when conditions could be expected to be favourable for the accumulation of emanation because of stratification of the air near the ground. The nights selected were without clouds and windless. Variations of the measured concentration of small and large ions during some of

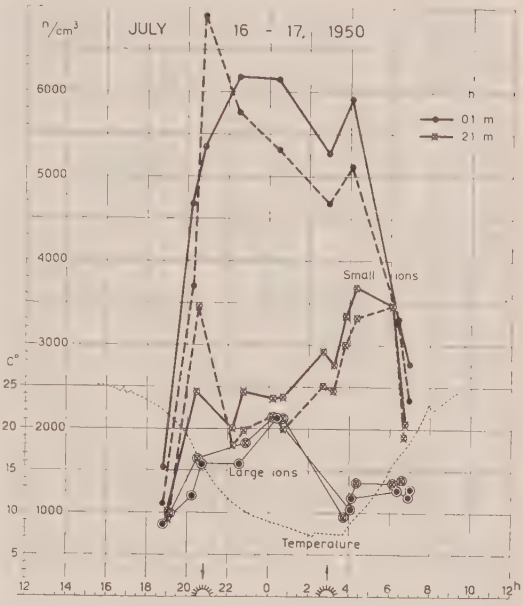

Fig. 1. Variation of concentration of ions at two levels on July 16—17, 1950; ——— positive small ions, - - - - - negative small ions, ——— positive large ions.

the nights selected are shown in figs. 1, 2, 3, 4, and 5. The positive ionic density is denoted by the full line (———) and the negative ionic density by the dashed line (- - - - -). Values corresponding to different levels are denoted by different designations as shown in the figures. The noted time is Central-European. The temperature given in the figures may be regarded as a factor, characteristic of the meteorological conditions prevailing during the observation periods.

Small ions. From an examination of the variations shown in figs. 1, 2, and 4 two superposed kinds of variation of the concentration of small ions can be identified:

(1) Variations of a longer time scale which extend over the entire observation period, and (2) variations of a shorter time scale with a duration of one to several hours. Variations of still shorter period may exist, but are not detected with the arrangement of measurements used. For a general insight into the basic effect variations of the first kind are of fundamental interest. The variations of a shorter time scale can be regarded as the result of variations in the environmental conditions. The increase of the ionic density at

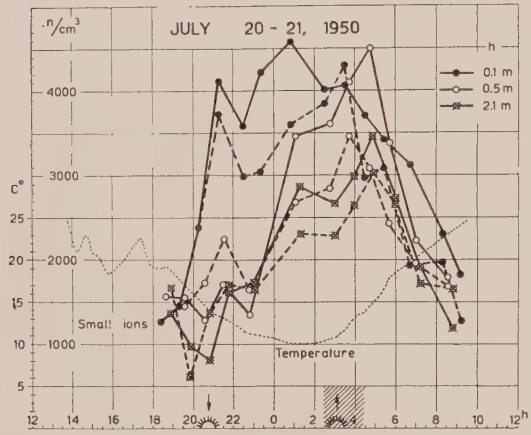

Fig. 2. Variation of concentration of small ions at three levels on July 20—21, 1950; ——— positive small ions, - - - - - negative small ions, ||||||| fog.

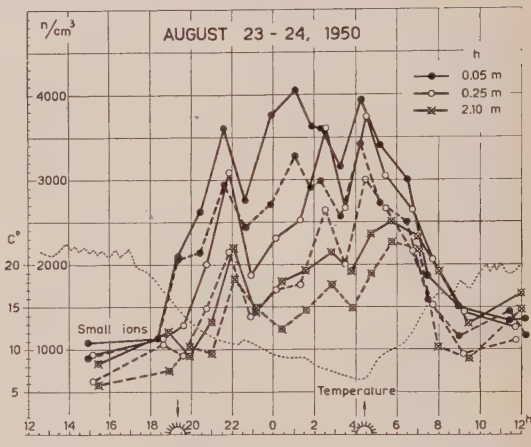

Fig. 4. Variation of concentration of small ions at three levels on August 23—24, 1950; ——— positive small ions, - - - - - negative small ions.

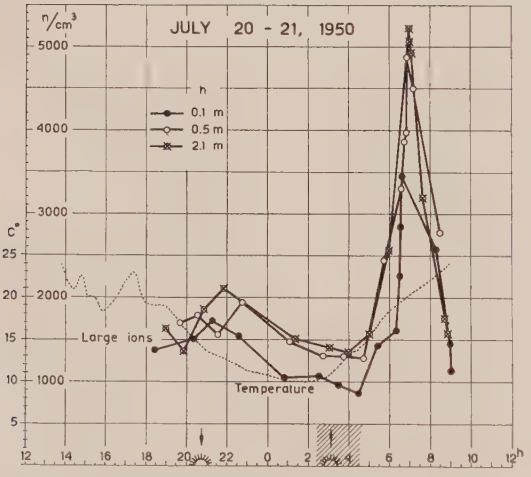

Fig. 3. Variation of concentration of positive large ions at three levels on July 20—21, 1950; ||||| fog.

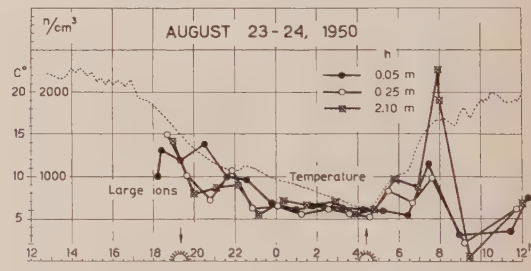

Fig. 5. Variation of concentration of positive large ions at three levels on August 23—24, 1950.

the two higher levels ($h_2 = 0.25$ m and $h_3 = 2.10$ m) at 22^h in fig. 4 can be regarded as an extreme example of such short-period variations. This increase was perhaps caused by air, with a higher content of ions or ion producers, rising locally from the ground. A stronger decrease can be observed at all three levels following the increase of ionic density at the higher levels h_2 and h_3. A similar effect can be observed during the same night between $2^h\ 30^m$ and $3^h\ 40^m$. In this way the shorter-period variations may be regarded as local disturbances which deform the general course of the effect, and from the study of which it may be possible to determine finer variations of the conditions which favour the basic effect.

Smoothed curves. In order to obtain the undisturbed course of the effect an attempt is made to smooth the curves of the measured trend of the small ions detected, neglecting variations of a shorter time scale. These smoothed curves which may be regarded as idealized trends of the effect are shown in fig. 6.

The shape of the variations of the small ion concentration. The following features of the variation in concentration of small ions during the effect may be pointed out:

(1) At the ground an increase is observed which proceeds very rapidly at sunset; during the night the ionic density remains comparatively high with only a slow decrease until 1—2 hours after sunrise when it decreases rapidly.

(2) At the higher levels an increase also begins at sunset and continues until 2—3 hours after sunrise; after that time a rapid decrease follows.

(3) At higher levels the number of small ions is smaller.

(4) The concentration of positive ions is higher than that of negative ions.

(5) The sudden increase in the concentration of negative ions over the positive ions at the beginning of the increase at sunset (fig. 1) deserves attention. A similar phenomenon was observed also during other series of measurements, especially at higher levels (for example see fig. 2).

(6) In addition to variations of a relatively long time-scale (extending over the entire observation period), variations of a shorter time scale (with a duration of one to several hours) may be observed.

Large ions. As mentioned before, it seemed impossible at first to obtain measurements of the large ions because of the abnormal deterioration of the insulation of the apparatus during the measurements. For the same reason we were unable to determine the spectral composition of large ions with the method used earlier (23). The measurements of large ions during these series were carried out at an adjusted limit mobility $k_* = 2.14 \times 10^{-4}$ cm sec^{-1}: V cm^{-1}. Taking into account the trend of the insulation it was attempted to calculate the variations of the concentration of large ions during the effect. Surprisingly, the trends obtained for the variation of the concentration of large ions were of a characteristic type. Two families of smoothed curves of these variations are shown in fig. 1 using different combinations of the observed curves. The general features of the variations of large ions during the effect are as follows:

(1) A decrease may be noted from sunset to sunrise, when a minimum is reached; after sunrise a comparatively rapid increase follows.

(2) It appears that the concentration of large ions near the ground is really a little lower than that at the higher levels.

The trend of the concentration of large ions is given in fig. 7 unexpectedly exactly; only the height of the maximum after sunrise could not be determined exactly with the data at hand. It must be noted here that by evaluating the trend of the variations of large ions during individual nights and also by the smoothing of the curves shown in fig. 7 every effort was made to suppress the variations; nevertheless a characteristic trend remained.

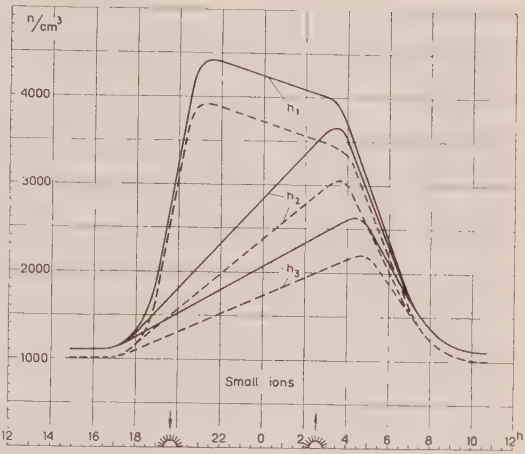

Fig. 6. Idealized trend of the variations of the concentration of small ions at the ground (h_1), and at two higher levels ($h_2 < h_3$) during quiet summer nights at Uppsala; ——— positive small ions, - - - - - negative small ions.

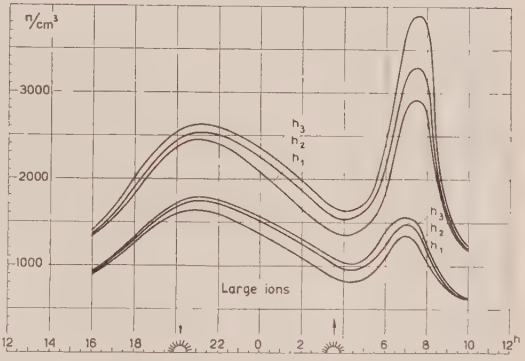

Fig. 7. Idealized trend of the variations of the concentration of positive large ions at the ground (h_1), and at two higher levels ($h_2 < h_3$) during quiet summer nights at Uppsala.

Points to be kept in mind in explaining the variations

We have previously given a preliminary general explanation of the observed variations of the concentration of ions during certain specified weather condition (18), (19). Indications will be given here, of a way by which a

more detailed explanation of the whole effect may be obtained. A survey of these subjects will be given later on.

Accumulation of emanation near the ground. The additional ions or the producers of ions necessary to produce the increase of the ionic density could not have been conveyed to the place of observation from another region because the horizontal motion of the air was feeble (in some cases calm prevailed). At the same time the vertical air motion must have been negligibly small, since with a minimum temperature at the ground turbulence must have been almost completely suppressed. The cause of the increased ionic density must be found at the place of observation itself. In our case the most probable prime cause of the increased ionic density might be expected to be the accumulation of emanation exhaled from the soil into the air layers nearest the ground, as shown more detailed in (18), (19). This effect may occur only under certain meteorological conditions under which mixing of the air is suppressed.

Austausch-processes and electrical phenomena in the atmospheric air. The mixing processes in atmospheric air may be considered as *Austausch*-processes — an idea introduced by SCHMIDT (21). Therefore the process of the accumulation of emanation in the layers of air near the ground must be considered as a process stipulated by *Austausch*. Attempts have been made to apply the theory of Austausch to several problems of atmospheric electricity. The distribution of radioactive substances in the free atmosphere has been considered in terms of Austausch by HESS and SCHMIDT (9), SCHMIDT (22), PRIEBSCH (20), and LETTAU (13). Variations of the potential-gradient have been considered in terms of Austausch-theory by BROWN (5), FRANKE (8), ISRAËL (11), and of the electrode-effect by LETTAU (13).

Our problem of the increase of the concentration of small ions near the ground under weather conditions, during which the accumulation of emanation exhaled from the soil and stratification of ions near the ground may be expected, is more complicated, but it is evident that this problem must be considered as one stipulated by *Austausch*. Consideration of the individual processes which may be of importance to the whole problem could not give us results of full certainty because of the lack of several data necessary for the calculations (for example, the combination processes between small- and large ions and nuclei, the recombination processes in the track of an α-particle etc.). Even so, conclusions of interest could be obtained by such considerations.

Some considerations concerning the trend of the number of large ions. In order to show the perspectives which may appear through a more detailed consideration of the phenomena described in this article we will here mention some events which may have a connection with the observed variations of large ions.

The minimum prior to sunrise and the enormous increase of the concentration of large ions after sunrise was at first a surprise to us. But we have taken into consideration facts known about the diurnal variation of condensation nuclei; large ions may be considered as a fraction of the condensation nuclei. Unfortunately, "in spite of the numerous observations of nuclei, there is not yet a definite relationship established between time of day and number of nuclei" as stated LANDSBERG (12). BRADBURY and MEURON (3) have stated that "The diurnal variation in nuclei-density shows a definite maximum in the forenoon and in the evening with a *pronounced minimum prior to sunrise* and a midday minimum of lesser extent. *Such a variation might be expected in the normal daily convective cycle.*" (Underlined by us.) Characteristics similar to those found by BRADBURY and MEURON for the ground level have been established by YUNKER (24) for a level 50 cm and another 20 m above the ground. It is seen that the nuclei-density at the 20-metre level is on the whole higher than that at the ground. That the concentration of nuclei at night may be much smaller than the day average is also shown by NOLAN and TEDDE (14). A theoretical consideration of the trend of the concentration of nuclei is given by FRANKE (8) in terms of Austauschprocesses. The course of the concentration of nuclei during night-hours calculated by FRANKE with a minimum and a higher maximum shows a similarity to the trend of large ions observed by us. We cannot accept in whole the mechanism used by FRANKE, but it appears that a description of the effect observed by us could be given with some modification.

It seems that a detailed investigation of

the associate phenomena may give us important information about the events considered here. In addition it could be mentioned here that also variations of sight may contribute to the understanding of our problems. BIELICH and RITSCHL (2) have considered the diminution of sight after sunset and a probable explanation of this effect is given in terms similar to those by which the observed marked diminution of sight 1—2 hours after sunrise during radiation nights is explained.

A more detailed account of the investigation presented here will appear in *Arkiv för Geofysik* published by Kungl. Svenska Vetenskapsakademien, Stockholm.

Acknowledgments

The Swedish Natural Science Research Council deserves to receive thanks for placing means at the disposal of the Institute for the performance of this investigation. Thanks must be expressed also to Professor R. MUEGGE, Director of the Institute of Meteorology and Geophysics of the University of Frankfurt a. Main, for his kindness in placing an ISRAËL large-ion counter at the disposal of the Institute. Mr. A. METNIEKS (of this Institute) and Mr. R. A. SCHOTLAND (of Massachusetts Institute of Technology) who assisted in the observations and calculations deserve appreciation.

REFERENCES

(1) BECKER, F., 1934: Messungen des Emanationsgehaltes der Luft in Frankfurt a. M. und am Taunus-Observatorium. *Gerl. Beitr. z. Geophys.* **42**, 365—384.

(2) BIELICH, F., und RITSCHL, R., 1940: Sichtrückgang nach Sonnenuntergang. *Meteor. ZS.* **57**, 122.

(3) BRADBURY, N. E., and MEURON, H. I., 1938: The Diurnal Variation of Atmospheric Condensation-Nuclei. *Terr. Magn.* **43**, 231—239.

(4) BROWN, J. G., 1933: The rôle of the space-charge in atmospheric electricity. *Terr. Magn.* **38**, 161—173.

(5) BROWN, J. G., 1935: The local variation of the earth's electric field. *Terr.Magn.* **40**, 413—424.

(6) DAUNDERER, A., 1907: Luftelektrische Messungen. *Phys. ZS.* **8**, 281—286.

(7) DEIJ, L. J. L., 1939: Metingen van het radongehalte in de atmosfeer. *Dissertation Amsterdam.*

(8) FRANKE, M., 1949: Der doppelperiodische Tagesgang des luftelektrischen Potentialgefälles als Folge des Austausches. *Geofisica pura e applicata* **14**, 1—12.

(9) HESS, V. F., und SCHMIDT, W., 1918: Über die Verteilung radioaktiver Gase in der freien Atmosphäre. *Phys. ZS* **19**, 109.

(10) HOGG, A. R., 1939: The conduction of electricity in the lowest levels of the atmosphere. *Memoirs of Commonwealth Solar Observatory* Nr 7, Mount Stromlo, Canberra, Australia.

(11) ISRAËL, H., 1950: Austauschuntersuchungen mittels luftelektrischen Messungen. *Archiv für Meteor., Geophys. u. Bioklim.* (A) **2**, 367—373.

(12) LANDSBERG, H., 1938: Atmospheric Condensation Nuclei. *Ergebnisse der Kosm. Phys.* **3**, 155—252.

(13) LETTAU, L., 1941: Anwendung neuerer Ergebnisse der Austauschlehre auf zwei luftelektrische Fragen. *Gerl. Beitr. Geophys.* **57**, 365—384.

(14) NOLAN, P. J., and TEDDE, P. G., 1950: Condensation Nuclei and Meteorological Elements in Dublin. *Archiv für Meteor., Geophys. u. Bioklim.* (A) **2**, 374—385.

(15) NORINDER, H., 1921: Research on the height variation of the atmospheric electric potential gradient in the lowest layers of the air. *Geografiska Annaler*, Stockholm, **3**, 1—96.

(16) NORINDER, H., and SIKSNA, R., 1949: The measurements of the variation characteristics of the density of small-ions. *Arkiv för Geofysik*, **1**, 1, 1—32.

(17) NORINDER, H., and SIKSNA, R., 1950: Continued measurements of the variation characteristics of the density of small-ions. *Arkiv för Geofysik*, **1**, 7, 149—158.

(18) NORINDER, H., and SIKSNA, R., 1950: Variations of the density of small-ions caused by accumulation of emanation exhaled from the soil. *Tellus*, **2**, 168—172.

(19) NORINDER, H., and SIKSNA, R., 1950; Variationen des Ionengehaltes in der bodennaher Luftschicht. *Archiv für Meteor., Geophys. u. Bioklim.* (A) **3**, 29—39.

(20) PRIEBSCH, J., 1931: Zur Verteilung radioaktiver Stoffe in der freien Luft. *Phys. ZS.* **32**, 622—629.

(21) SCHMIDT, W., 1925: Der Massenaustausch in freier Luft. *Probleme der Kosmischen Physik*, **7**.

(22) SCHMIDT, W., 1926: Zur Verteilung radioaktiver Stoffe in freier Luft. *Phys. ZS.* **27**, 371—379.

(23) SIKSNA, R., 1951: Measurements of large ions in the atmospheric air at Uppsala. *Arkiv för Geofysik*, **1**, in press.

(24) YUNKER, E. A., 1940: The diurnal variation and vertical distribution of atmospheric nuclei. *Terr. Magn.* **45**, 121—126.

Die Feldkomponentenmühle

Ein Gerät zur Messung der drei Komponenten des luftelektrischen Feldes und der Flugzeugeigenladung bei Flugzeugaufstiegen

Von H.-W. KASEMIR,
Luftelektrische Forschungsstelle Buchau a. F. des Observatoriums Friedrichshafen

(Manuscript received 1 October 1951)

Abstract

Recording the atmosperic-electric potential gradient from an aeroplane it is very useful to get all the three field-components. This is the case especially in investigations in greater altitudes and in thunderclouds. In this paper an apparatus is described working on the principle of the 'Feldmühle' (field strength meter) and giving simultaneous recording of the atmospheric-electric potential gradient separated in the three rectangular components of the field. Furthermore a method is pointed out to separate the field of the own charge of the aeroplane and to record this one separately. This enables the 'Feldkomponentenmühle' (field component meter) to be used in motor driven aeroplanes.

1. Einleitung

Alle bisher durchgeführten Messungen des luftelektrischen Feldes in der freien Atmosphäre angefangen von den Freiballonaufstiegen bis zu den modernen Messungen im Segel- oder Motorflugzeug (1, 2, 3, 4, 5, 9) beschränken sich auf die Messung oder Registrierung der vertikalen Feldkomponente. Solange man bei luftelektrisch ungestörtem Wetter nur bis zu Höhen von einigen Kilometern über dem Erdboden vordringt, kann man erwarten, daß das luftelektrische Feld vertikal gerichtet ist, und somit die Horizontalkomponenten fehlen. Bei Untersuchungen von Wolken und insbesondere von Gewitterfeldern aber treten neben der Vertikalkomponente auch erhebliche Horizontalkomponenten auf. So ist man z. B. bei der Registrierung der Vertikalkomponente in Gewitterfeldern gezwungen, über die geometrische Verteilung der Wolkenladungen gewisse Annahmen zu machen, um diese Messungen überhaupt auswerten zu können. Simpson und Robinson (3) nehmen deshalb eine Ladungsverteilung in übereinanderliegenden Kugeln an, während E. Wall (6) die Ladungsanordnung in Schichten vorzieht, um für die Auswertung der Messungen einfach zu übersehende theoretische Potential- und Feldverhältnisse zu haben. H. Wichmann (7) leitet auf Grund der meteorologischen Verhältnisse in der Gewitterwolke gekoppelt mit den elektrizitätsbildenden Vorgängen eine andere Ladungsverteilung ab, die sich nicht mehr in so einfache geometrische Formen pressen läßt. Es verbleibt also bei der Auswertung der Messungen ein gewisser Grad von Unsicherheit, der sich durch die gleichzeitige Registrierung aller drei Feldkomponenten beseitigen lassen würde.

Auch bei Schönwetterflügen wird die Horizontalkomponente des luftelektrischen Feldes dann von wesentlicher Bedeutung sein, wenn man mit dem Registriergerät Höhen erreicht,

die größer sind als die Gipfelhöhe der Gewitterwolken. Hier muß sich die Elektrizitätsströmung nach den Seiten ausbreiten und somit auch eine horizontale Feldkomponente vorherrschen. Dieser seitliche Ausgleich wird nicht erst in der Ionosphäre stattfinden (8), sondern bereits in tiefer gelegenen Luftschichten, so daß man etwa in dem Raum zwischen 15 und 50 km Höhe mit dem Auftreten von horizontalen Feldkomponenten rechnen darf.

Aus diesen und anderen Gründen wurde vom Verfasser bereits 1944 mit der Entwicklung eines Meßgerätes für Flugzeugaufstiege begonnen, das die drei Komponenten des luftelektrischen Feldes gleichzeitig registriert. Durch dieses Instrument sollte außerdem die Möglichkeit gegeben werden, das von der Eigenladung des Flugzeuges herrührende Feld von dem luftelektrischen Feld abzutrennen und gesondert zu registrieren. Denn es ist bekannt, daß Motorflugzeuge durch die Auspuffgase auf Spannungen von 5—10 000 V aufgeladen werden, so daß das Eigenfeld des Flugzeuges die schwachen luftelektrischen Felder in der Höhe überdeckt.

Die praktische Erprobung der Anlage im Flugzeug konnte leider nicht mehr durchgeführt werden. Wenn hier trotzdem dieses Gerät beschrieben werden soll, so geschieht es aus dem Grunde, weil auch heute noch die praktische Flugerprobung in absehbarer Zeit in Deutschland nicht gesichert erscheint.

2. Theoretische Überlegungen zur Feldkomponentenmühle

Das Meßgerät wurde nach dem Prinzip der automatisch rotierenden Wilsonplatte gebaut, das unter dem Namen Feldmeßmaschine oder speziell in der Luftelektrizität als Feldmühle bekannt ist. In Verbindung mit der modernen Verstärkertechnik hat sich dieses Meßverfahren wegen seiner Unempfindlichkeit gegen mechanische Beanspruchungen und wegen der geringen Isolationsanforderung zur Registrierung luftelektrischer Felder im Flugzeug ausgezeichnet bewährt.

Das Gerät mißt letzthin die durch das äußere Feld influenzierte Ladung auf einem Teilstück der Flugzeugoberfläche, bzw. die dieser Ladungsdichte proportionale Feldstärke. Zum Verständnis der 3 Komponentenmessung

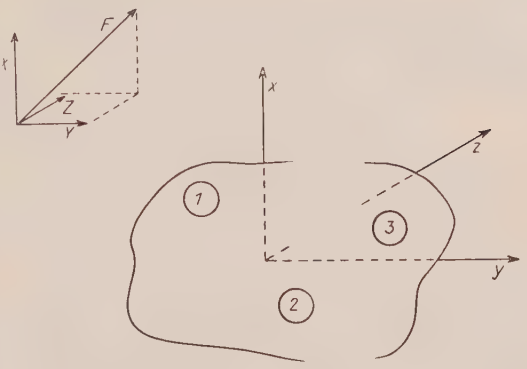

Abb. 1. Leitender Körper im elektrischen Feld beliebiger Richtung.

soll eine kurze theoretische Überlegung eingeschaltet werden.

Wir setzen einen beliebig geformten leitenden Körper in ein beliebig gerichtetes elektrisches Feld. Dieses Feld mit der Feldstärke F zerlegen wir entsprechend unserem kartesischen Koordinatensystem x, y, z in seine Komponenten X, Z, Z. (Abb. 1.)

Weiterhin schneiden wir uns 3 beliebige Oberflächenstücke 1, 2, 3 aus dem Körper aus, die aber durch einen Draht mit der übrigen Oberfläche des Körpers leitend verbunden bleiben sollen. Auf jedem Oberflächenstück wird von jeder Komponente des äußeren Feldes eine Ladung q influenziert, die der jeweils betrachteten Feldkomponente proportional ist. Die den einzelnen Oberflächenstücken zugehörigen Ladungen kennzeichnen wir durch die Indizees 1, 2, 3 und unterteilen die Gesamtladung in jedem Oberflächensegment in die Anteile, die durch die Feldkomponenten X, Y, Z induziert werden. Diese Teilladungen kennzeichnen wir durch weitere Indizees X, Y, Z. Es setzt sich also die Gesamtladung q_1 auf dem Oberflächenstück 1 zusammen aus den Teilladungen q_{1X}, q_{1Y}, q_{1Z}. Dasselbe gilt entsprechend für die Oberflächenstücke 2 und 3. Damit erhalten wir folgendes Gleichungssystem.

$$\begin{aligned} q_1 &= q_{1X} + q_{1Y} + q_{1Z} \\ q_2 &= q_{2X} + q_{2Y} + q_{2Z} \\ q_3 &= q_{3X} + q_{3Y} + q_{3Z}. \end{aligned} \qquad (1)$$

Die Teilladungen q_{1X}, q_{1Y}, ... sind nun proportional den Feldkomponenten X,

Y, Z. Diese führen wir mit Hilfe der Proportionalitätsfaktoren a_1, b_1, c_1, ... ein und erhalten aus Gl. (1.)

$$\begin{aligned} q_1 &= a_1X + b_1Y + c_1Z \\ q_2 &= a_2X + b_2Y + c_2Z \\ q_3 &= a_3X + b_3Y + c_3Z. \end{aligned} \qquad (2)$$

Da die a_1, b_1, c_1, ... konstante Faktoren darstellen, die wir etwa als Teilkapazitätskoeffizienten für die entsprechende Feldrichtung definieren und messen können, dürfen wir Gl. (2) nach den Feldkomponenten X, Y, Z auflösen und erhalten mit neuen Konstanten A_1, B_1, C_1, ...

$$\begin{aligned} X &= A_1q_1 + B_1q_2 + C_1q_3 \\ Y &= A_2q_1 + B_2q_2 + C_2q_3 \\ Z &= A_3q_1 + B_3q_2 + C_3q_3. \end{aligned} \qquad (3)$$

Die Konstanten A_1, B_1, C_1,..... können wir nach bekanntem Rechenverfahren aus den a_1, b_1, c_1, ... gewinnen. Wir wollen jedoch diese Gleichungen übergehen, da diese Konstanten bei der praktischen Ausführung des Gerätes zweckmäßig durch Eichung gewonnen werden.

Als Ergebnis halten wir fest, daß es nach Gl. 3 theoretisch möglich ist, durch Messung der Oberflächenladung an drei verschiedenen Stellen der Oberfläche des Körpers, der sich in einem beliebig gerichteten homogenen Feld befindet, die Komponenten des äußeren Feldes zu bestimmen. Die praktische Ausführung zeigt darüber hinaus, daß es keine Schwierigkeiten bereitet, die erforderliche Rechenoperation durch das Gerät automatisch ausführen zu lassen.

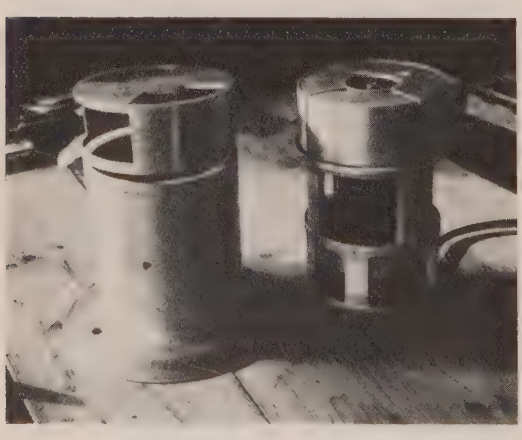

Abb. 2. Photographie der Feldkomponentenmühle.

3. Praktische Ausführung der Feldkomponentenmühle

Die Messung der Oberflächenladung bzw. der Feldstärke nach dem Feldmühlenprinzip soll hier als bekannt vorausgesetzt werden. Wir wenden uns gleich der technischen Konstruktion der Feldkomponentenmühle zu. Abb. 2 zeigt eine Photographie solch eines Gerätes. Die Feldmühle besteht also aus einem kurzen Zylinder, dessen Kopf in 8 voneinander isolierte Segmente aufgespalten ist. Hierbei entfallen auf den Zylinderdeckel 4 Segmente, während das obere Stück des Zylindermantels ebenfalls in 4 symmetrische Teilstücke unterteilt ist. Über diesen Segmenten rotiert ein etwas größerer geerdeter zylindrischer Flügel, in dem Ausschnitte derart angebracht sind, daß bei der Rotation je 2 gegenüberliegende Segmente im gleichen Rythmus frei gegeben und abgeschirmt werden. Jedes Segmentepaar des Zylindermantels ist durch einen Widerstand miteinander verbunden, der durch einen Mittelabgriff mit der Flugzeugoberfläche verbunden ist. Die Wirkungsweise dieser Anordnung wollen wir uns an der Schemafigur Abb. 3 a—3 d klar machen.

Es sind hier die 4 Segmente 1, 3 und 2, 4 des Zylindermantels im Schnitt aufgezeichnet. Sie werden von einem horizontalen Feld influenziert, dessen Richtung parallel zur Verbindungslinie der Segmente 1, 3 gegeben ist, und das senkrecht zur Zylinderachse steht. Wir sehen aus Abb. 3 b, daß das Segment 1 nur negative und das Segment 3 nur positive Influenzladung trägt. Die Segmente 2 und 4 dagegen tragen nach Abb. 3 a auf ihrer linken Hälfte negative und auf der rechten Hälfte positive Ladung.

Wir wollen nun den Ladungsfluß zwischen den Segmenten 1 und 3 bei einer Rotation des Flügels verfolgen. Als Ausgangsstellung wählen wir die in Abb. 3 a abgebildete Lage des Flügels, in der die Segmente 1 und 3 von dem äußeren Feld vollkommen abgeschirmt

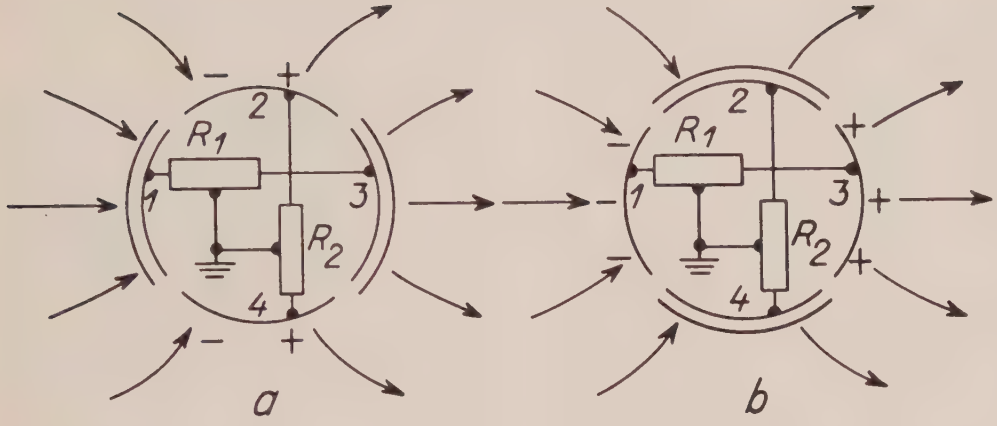

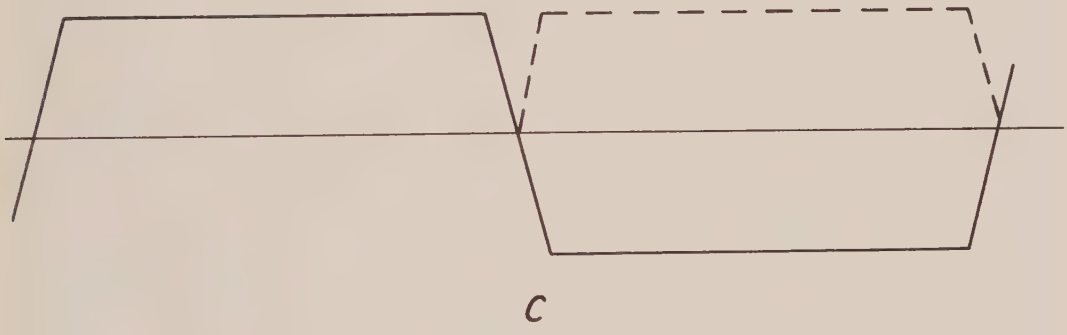

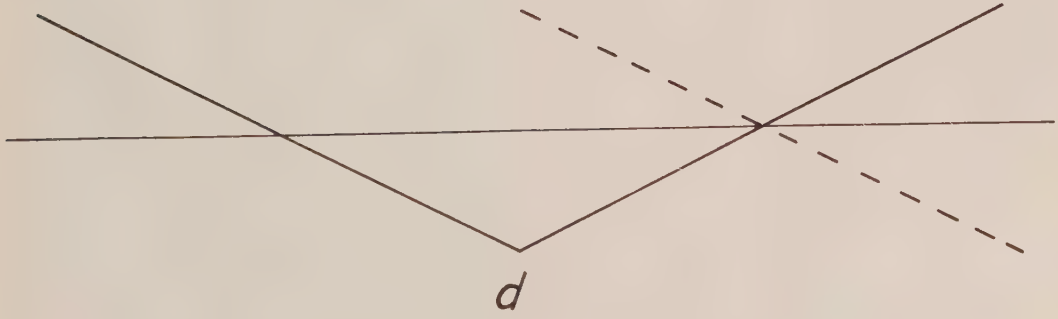

Abb. 3 a und 3 b. Mantelsegmente unter dem Einfluss eines horizontalen Feldes.
Abb. 3 c. Von den Segmenten 1 und 3 gelieferte Spannung.
Abb. 3 d. Von den Segmenten 2 und 4 gelieferte Spannung.

sind. Dreht sich der Flügel im Uhrzeigersinn bis in die Stellung 3b, so fließen unter der Einwirkung des äußeren Feldes Elektronen über den Widerstand R_1 von Segment 3 auf Segment 1. Dreht sich der Flügel weiter, bis er wieder die Stellung 3a erreicht, so gleichen sich die Influenzladungen über den Widerstand R_1 aus, es fließen also Elektronen von Segment 1 auf Segment 3. Bei weiterer Drehung wiederholt sich das Spiel von neuem. Dieser dauernde Ladungsfluß durch den Widerstand R_1 erzeugt über diesem eine Spannung, deren Verlauf in Abb. 3c schematisch dargestellt ist. Diese Wechselspannung wird dann wie üblich durch einen Verstärker verstärkt und durch einen zwangsgesteuerten Gleichrichter gleichgerichtet dem Schreiber zugeführt. Die Amplitude dieser Spannung ist der einfallenden Feldstärke proportional. Der zwangsgesteuerte Gleichrichter sorgt außerdem dafür, daß auch das Vorzeichen des Feldes nicht verloren geht.

Wir betrachten nun die Wirkung des Feldes auf die Segmente 2 und 4. Gehen wir ebenfalls von der Stellung 3a aus, so werden sich beim Drehen des Flügels in die Stellung 3b in der ersten Halbzeit die negativen Ladungen von Segment 2 mit den positiven von Segment 4 ausgleichen, während in der zweiten Halbzeit sich die positiven Ladungen von Segment 2 mit den negativen von 4 ausgleichen. Dreht sich der Flügel weiter in Stellung 3a, so ergibt sich derselbe Ladungsfluß nur mit umgekehrtem Vorzeichen. Die Kurve 3d zeigt ungefähr den resultierenden Spannungsverlauf über dem Widerstand R_2. Dieser ist gegenüber dem Spannungsverlauf über dem Widerstand R_1 so in der Phase verschoben, daß durch eine mit dem ersten Stromkreis synchrone Zwangsgleichrichtung die resultierende Gleichspannung gleich 0 wird. (Die gleichgerichtete Spannung ist in Abb. 3c und 3d gestrichelt eingezeichnet.)

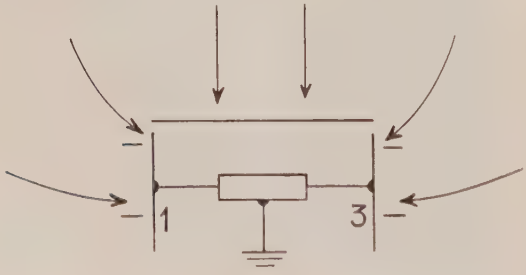

Abb. 4. Influenz des Segmentepaares 1 und 3 durch ein senkrecht einfallendes Feld.

Drehen wir jetzt die Feldrichtung so, daß sie mit der Verbindungslinie der Segmente 2 und 4 zusammenfällt, dann liefern sinngemäß diese die Spannung, die wir eben für die Segmente 1 und 3 abgeleitet haben, während letztere die gleichgerichtete Spannung 0 geben. Durch den Kunstgriff der zwangsgesteuerten Gleichrichtung sprechen also sowohl die Segmente 1 und 3 als auch die Segmente 2 und 4 nur auf die Feldkomponente an, die parallel zu der Verbindungslinie der entsprechenden Segmente gerichtet ist.

Wir müssen uns jetzt noch davon überzeugen, daß diese Segmentpaare auch unempfindlich sind gegenüber der Feldkomponente, die in Richtung der Zylinderachse einfällt. Zu diesem Zweck betrachten wir Abb. 4. In dieser sind die beiden Segmente 1 und 3 im Aufriß dargestellt.

Durch das in Achsrichtung einfallende Feld wird auf beiden Segmenten die gleich große negative Ladung influenziert. Diese Ladung fließt dem Segment 1 über den linken halben Widerstand zu und dem Segment 3 über den rechten halben Widerstand. Da in den beiden Widerstandshälften die Stromrichtung gegensinnig ist, kompensiert sich der dadurch entstehende Spannungsabfall über dem ganzen Widerstand zu 0. Dasselbe gilt für das Segmentepaar 2 und 4.

Voraussetzung für diese Kompensation ist die Symmetrie des Feldlinienbildes. Montiert man die Feldmühle z. B. auf der Oberseite des Flugzeuges, so ist diese Symmetrie für das in Richtung der Flugzeugflügel weisende Segmentepaar immer dann gegeben, wenn man die Mühle über der Mittellinie des Flugzeugs anbringt. Für das nach Kopf- und Schwanzende zeigende Segmentenpaar müßte die elektrisch neutrale Linie erst bestimmt werden. Läßt sich diese Linie aus irgend einem Grund für die Montage nicht verwenden, so kann man durch einen anderen Erdungsabgriff am Widerstand die vollständige Kompensation erzwingen.

Abschließend können wir feststellen. Die Segmentepaare des Zylindermantels geben jedes nur für jeweils eine Komponente eines äußeren Feldes eine gleichgerichtete Spannung.

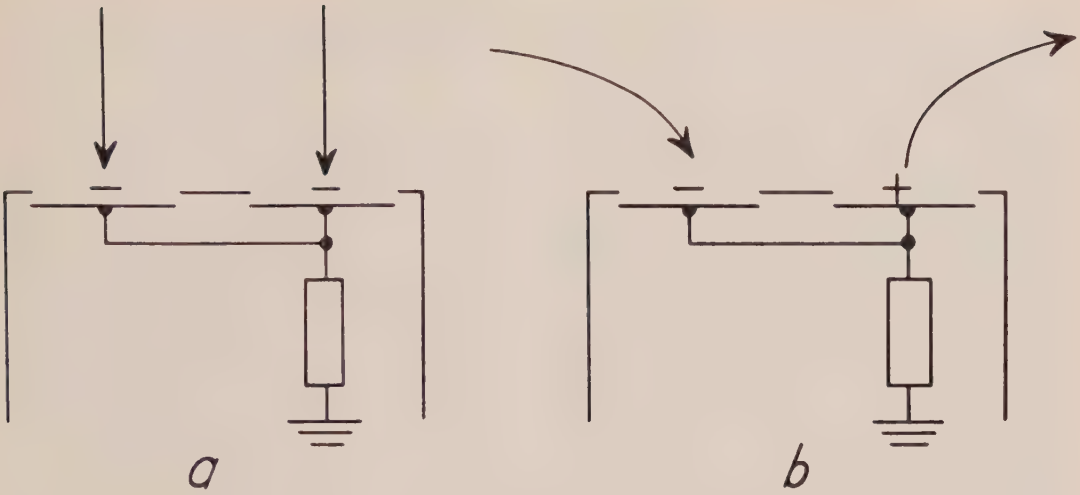

Abb. 5 a. Deckelsegmente unter der Einwirkung eines senkrecht einfallenden Feldes.
Abb. 5 b. Deckelsegmente unter der Einwirkung eines horizontal einfallenden Feldes.

Gegen die jeweils anderen beiden Feldkomponenten ist das Segmentenpaar unempfindlich, teils durch die zwangsgesteuerte Gleichrichtung, teils durch eine entsprechende Erdung des überbrückenden Widerstandes.

Etwas einfacher zu übersehen sind die Verhältnisse für die Segmente im Zylinderdeckel. Hier genügt es, wenn von den zwei Segmentpaaren überhaupt nur eines benutzt wird. Dieses wird nach Abb. 5a kurzgeschlossen und über einen Widerstand mit dem Flugzeug verbunden.

Die Wirkung für parallel zur Zylinderachse einfallende Felder ist dieselbe, wie bei der normalen Einkomponenten-Mühle. Bei senkrecht zur Zylinderachse einfallenden Feldern hebt sich die Wirkung entweder schon innerhalb ein und desselben Segments oder durch das Kurzschließen beider Segment auf, wie aus Abb. 5b ohne weiteres ersichtlich ist.

Wenn man nicht Wert darauf legt, daß man für jeden Komponentenkanal des Verstärkers einen getrennten Eingangswiderstand erhält, könnte man auf die Segmente im Zylinderdeckel überhaupt verzichten. Denn parallel zur Zylinderachse einfallende Felder kann man auch mit einer Schaltung nach Abb. 6 durch die Zylindermantelsegmente registrieren.

Hier fließt über den eingeführten Widerstand R_3 die Influenzladung auf die Segmente 1 und 3. Die Spannung für die senkrecht einfallende Feldkomponente wird über dem Widerstand R_3 abgenommen. Der Querwiderstand bleibt dabei ohne Wirkung. Die Ähnlichkeit dieser Schaltung mit den Ausführungen nach Abb. 5a und 5b ist so evident, daß nach den oben gemachten Ausführungen eine eingehende Diskussion nur eine Widerholung bedeuten würde.

Mit den bisherigen Ausführungen ist gezeigt, daß bei einer der angegebenen Konstruktionen der Feldkomponentenmühle jeweils ein Segmentepaar immer nur auf eine Feldkomponente anspricht, während es durch die anderen beiden Komponenten nicht beeinflußt wird.

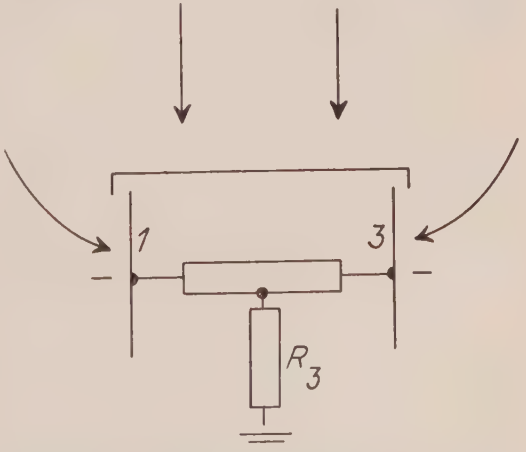

Abb. 6. Registrierung vertikaler Felder mit Hilfe der Zylindermantelsegmente.

4. Die Registrierung der Flugzeugeigenladung

Eine Komplikation entsteht bei der Feldregistrierung im Flugzeug dadurch, daß Motorflugzeuge durch die Auspuffgase so hoch aufgeladen werden, daß ihre Eigenfelder die schwachen luftelektrischen Felder in der Höhe überdecken. Man kann diese Schwierigkeit natürlich dadurch umgehen, daß man ein Segelflugzeug verwendet, von dem man eine etwa vorhandene Eigenladung mit Hilfe eines in der neutralen Linie angebrachten Ausgleichers wegbringt. Andererseits wird grade bei Messungen in Regen- und Gewitterwolken auch das Segelflugzeug durch Einfangen von geladenem Niederschlag eine derartige Eigenladung annehmen, die durch einen Ausgleicher nicht restlos beseitigt werden kann.

Bei der Komponentenmühle bietet sich zur Abtrennung dieser Eigenladungsfelder folgender Weg. Es wird hierzu für die Zylindermantelsegmente eine Schaltung nach Abb. 6 und für die Zylinderdeckelsegmente eine Schaltung nach Abb. 5a verwendet. Wir bezeichnen die parallel zur Mühlenachse einfallene Komponente des äußeren Feldes mit F_X und die von der Eigenladung herrührende Feldstärke mit E. Für das Eigenladungsfeld gelten bei den einzelnen Segmenten andere Teilkapazitätskoeffizienten als für das äußere Feld. Die ersteren bezeichnen wir mit b_1, b_2 und die letzteren mit a_1, a_2.

Mit der Schaltung nach Abb. 7 können wir jetzt das Eigenladungsfeld von dem äußeren Feld auf folgende Weise separieren.

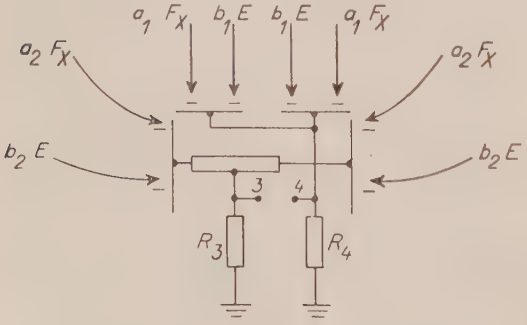

Abb. 7. Schaltung zur Trennung der Wirkung des Eigenladungsfeldes von der des äusseren luftelektrischen Feldes.

Die über dem Widerstand R_4 entstehende Spannung U_4 ist gegeben durch

$$U_4 = a_1 F_X + b_1 E, \tag{4}$$

während für die über R_3 entstehende Spannung U_3 gilt

$$U_3 = a_2 F_X + b_2 E. \tag{5}$$

Durch passende Wahl der Widerstände R_3 und R_4 können wir erreichen, daß $a_1 = a_2$ wird. Dann erhalten wir durch Gegeneinanderschalten der Widerstände R_3 und R_4 an der Punkten 3 und 4 die Eingangsspannung U_e für den Verstärkerkanal der Eigenladung. Denn es ist

$$U_e = U_3 - U_4 = (b_1 - b_2) E. \tag{6}$$

Es ist also U_e nur proportional der Eigenladungsfeldstärke E. Dasselbe Schaltbild verwenden wir für die andere Kombination der Zylindermantel- und Deckelsegmente. Hier gleichen wir die R_3 und R_4 entsprechenden Widerstände aber so ab, daß in den Gleichungen (4) und (5) $b_1 = b_2$ wird. Dann fällt der Eigenladungsanteil heraus, und wir erhalten

$$U_X = U_3 - U_4 = (a_1 - a_2) F_X. \tag{7}$$

U_X ist also eine Spannung, die nur proportional der parallel zur Mühlenachse einfallenden Feldkomponente F_X ist.

Eine Störung der Anzeige der horizontalen Feldkomponenten durch die Eigenladungsfeldstärke erfolgt nicht, wenn die Mantelsegmente nach Abb. 3a bzw. 7 geschaltet werden. Es gilt dann für das Eigenladungsfeld dasselbe, was an Hand der Abb. 4 für die vertikale Feldkomponente dargelegt wurde. Durch den Mittelabgriff des Querwiderstandes fällt die Wirkung des Eigenladungsfeldes heraus.

Eine praktische Schwierigkeit könnte aber dadurch entstehen, daß sowohl die Werte für a_1 und a_2 als auch für b_1 und b_2 fast gleich groß sein werden. Durch die Differenzbildung in den Klammern von Gl. 6 und 7 erhalten wir also für U_e und U_X kleine Werte. Nach dem Stand der heutigen Verstärkertechnik bereitet es zwar keine Schwierigkeit auch kleine Wechselspannungen genügend hoch zu verstärken. Aber schwerer wird es sein, den genauen Abgleich der Widerstände zu erreichen. Außerdem muß die von der Kontaktspannung und die von der mehr oder minder

guten Erdung des rotierenden Flügels herrührende Störspannung der Mühle klein gehalten werden.

Sollte sich also herausstellen, daß dieser Weg nur mit großem Aufwand beschritten werden kann, so bleibt immer noch die Möglichkeit offen eine einfache Hilfsmühle mit hinzuzuziehen. Diese kann dann an einem geeigneten Ort und zwar an der Unterseite des Flugzeuges montiert werden. Dadurch erhalten die entsprechenden Koeffizienten a_1, a_2 und b_1, b_2 verschiedenes Vorzeichen, verstärken also einander. Für die Konstruktion der Komponentenmühle gelten sonst sinngemäß dieselben Erfahrungen, die man beim Bau der einfachen Feldmühle gesammelt hat, auf die aber hier nicht mehr eingegangen werden soll.

Zusammenfassung

Bei der Registrierung des Luftelektrischen Feldes im Flugzeug ist es äusserst wünschenswert, alle drei Feldkomponenten aufzunehmen. Dies gilt besonders bei Untersuchungen in grossen Höhen und bei Gewitterfeldern. In dieser Arbeit wird eine Apparatur beschrieben, die nach dem Feldmühlenprinzip arbeitet und die gleichzeitige Registrierung der nach kartesischen Koordinaten zerlegten Komponenten des luftelektrischen Feldes gestattet. Ferner wird ein Weg aufgezeigt mit dieser Apparatur das Feld der Eigenladung des Flugzeuges von dem luftelektrischen Feld abzutrennen und für sich gesondert zu registrieren. Dadurch ist es möglich die Feldkomponentenmühle auch im Motorflugzeug zu verwenden.

LITERATUR

(1) Everling, E., u. A. Wigand, 1921: Spannungsgefülle und vertikaler Leitungsstrom in der freien Atmosphäre nach Messungen bei Hochfahrten im Freiballon. *An. d. Phys.* **4**, 66, 261 — 288.

(2) Simpson G. C., F. J. Scrase, 1937: The Distribution of Electricity in Thunderclouds I. *Proc. R. Soc.* A. **161**, 309—352.

(3) Simpson G. C., G. D. Robinson, 1941: The Distribution of Electricity in Thunderclouds II. *Proc. R. Soc.* A. **177**, 281—329, 1941.

(4) Kasemir, H.-W., I. v. Wittich, 1943: Feld- und Eigenladungsregistrierungen bei Flugzeugaufstiegen. *ZWB Forschungsbericht* Nr. 1886,

(5) Ross Gunn, 1948: Electric Field Intensity Inside Natural Clouds. *J. Applied Physics* **19**, 481—484.

(6) Wall, E.: Das Gewitter I. Wetter u. Klima 1/2, 7—21, 1948.
— Das Gewitter II. Wetter u. Klima 3/4, 65—74, 1948.
— Das Gewitter III. Wetter u. Klima 7/8, 193—204, 1948.
— Das Gewitter IV. Wetter u. Klima 11/12, 321—326, 1948.

(7) Wichmann, W.: Grundprobleme der Physik des Gewitters. Wolfenbüttler Verlagsanstalt. Wolfenbüttel u. Hannover 1948.

(8) Israel, H., u. H.-W. Kasemir, 1949: In welcher Höhe geht der weltweite luftelektrische Ausgleich vor sich. *Ann. d. Geophysique* **5**, 313—324.

(9) R. Lecolazet, 1948: Étude Expérimentale de l'état éleqtrique des cumulus de beau temps, interprétation des résultates.» *Ann. de Géoph.*, **4**, 81 — 95.

Numerical Tendency Computations from the Barotropic Vorticity Equation

B. BOLIN[1] and J. CHARNEY, Institute for Advanced Study, Princeton

(Manuscript received 10 October 1951)

Abstract

As a preliminary test of the usefulness of the barotropic vorticity equation for numerical forecasting a series of tendency computations have been made for a period of ten days in February 1951. Despite the difficulty of comparing instantaneous tendencies with observed changes over a finite time interval (12 hours) some positive information was obtained concerning computational errors as well as errors in the atmospheric model. The computations support the conclusion reached by CHARNEY and ELIASSEN (1949) that the Rocky Mountains are of importance in their influence on the large scale upper level flow pattern over the United States.

1. Introduction

In a recent article by CHARNEY, FJØRTOFT and VON NEUMANN (1950)[2] a series of numerical forecasts for the 500 mb surface was made using the barotropic vorticity equation. Unfortunately, the number of forecasts was too small to permit general conclusions about the accuracy of the computations, nor was it possible to separate truncation errors from errors due to defects in the model. Final conclusions of this kind cannot be drawn until a large number of complete 24-hour forecasts have been made. Such computations are planned for the high-speed electronic computer being built at the Institute for Advanced Study.

In the four complete forecasts that were described in (I), it was found that the initially computed tendency gives a fairly good idea of the 24-hour change obtained by a complete integration. This is obviously still more true for a 12-hour forecast. Thus one might expect to obtain some useful results from a comparison between initial tendencies and the subsequent observed 12-hour change provided some proper way of comparison can be devised. With this idea in mind a series of tendency computations was carried through for a period in February 1951. It was possible to obtain some information from these computations regarding computational errors as well as defects in the model. It was also instructive to study the computed tendencies in some detail in that they furnish direct illustrations of the quasi-barotropic behaviour of the atmosphere.

It should be stressed that a series of complete forecasts has to be made as a final test of the computational scheme as well as of the model. We can obviously not obtain any information from these computations about errors due to the finite extrapolation in time and the extent to which computational errors put a limit on the time over which a forecast can be made.

[1] Now at University of Stockholm.

[2] In the following we shall refer to this article by (I).

This study should rather be looked upon as a series of experiments intended to serve as a guide for further work.

2. The solution of the vorticity equation

The reader is referred to (I) for a detailed discussion of the problems that arise when trying to solve the barotropic vorticity equation for a certain initial set of data. Here only a general outline is given of the procedure followed.

Both from empirical and theoretical investigations we know that there exists a level in the mid-troposphere which is approximately non-divergent. As in (I) we shall assume that the 500 mb level coincides with this level. (It will be seen that some of the major errors in the tendency computations are introduced by this assumption.) Thus the vorticity equation may be written

$$\frac{\partial \zeta}{\partial t} = - \mathbf{v} \cdot \nabla (\zeta + f). \tag{1}$$

ζ is the relative vorticity, $\mathbf{v}$ is the horizontal wind velocity and f the Coriolis parameter. It was shown in (I) how this equation may be transformed into

$$\nabla^2 \frac{\partial z}{\partial t} = J\left(\frac{g m^2}{f} \nabla^2 z + f, z\right) = J(\eta, z), \tag{2}$$

where the geostrophic wind equation has been used for the evaluation of the vorticity. Here z denotes the height of the 500 mb surface, m is the scale factor in the transformation from spherical coordinates to the particular map used in the computations, η is the absolute vorticity and $J(\alpha_1, \alpha_2)$ is defined as $J(\alpha_1, \alpha_2) = \partial\alpha_1/\partial x \cdot \partial\alpha_2/\partial y - \partial\alpha_2/\partial x \cdot \partial\alpha_1/\partial y$. It is our intention to solve this Poisson equation in order to obtain the initial value of $\partial z/\partial t$ and compare that tendency with the observed 12-hour change of z. For hand computation equation (2) is most rapidly solved by the relaxation method described by SOUTHWELL (1946). However, it is necessary to specify $\partial z/\partial t$ on the boundary. Since these quantities are not known, we are forced to introduce artificial boundary conditions. When carrying out a complete 24-hour forecast, this question deserves special attention, but as we only are going to compute the initial tendency we may assume that $\partial z/\partial t = 0$ on the boundary. This will undoubtedly introduce errors close to the boundary, but the magnitude of these errors decreases rapidly in going away from the boundary. The reason is that the effect of the correct boundary conditions at a fairly small distance from the boundary becomes equivalent to $\partial z/\partial t = 0$ on the boundary because of the interference of positive and negative boundary values. In the verification, no points have been used at a distance less than $2\,\Delta S$ from the boundary, ΔS being the grid interval used in solving the finite difference equation corresponding to (2).

For the solution of equation (2) we choose a rectangular area on the map with sides $p \cdot \Delta S$ and $q \cdot \Delta S$, where ΔS is the distance between the gridpoints in a square grid and p and q are integers. The coordinates of the grid points are given by $i \cdot \Delta S$ and $j \cdot \Delta S$ $(i = 0, 1, 2 \ldots p; j = 0, 1, 2 \ldots q)$. $\nabla^2 z$ is computed for every other point $(i + j = 2n)$ according to the formula

$$(\nabla^2 z)_{ij} = \frac{1}{(\Delta S)^2} [z_{i-1,j} + z_{i,j-1} + z_{i,j+1} + z_{i+1,j} - 4 z_{ij}] \tag{3}$$

$$i + j = 2n, \qquad 1 \leq i \leq p - 1, \qquad 1 \leq j \leq q - 1$$

J_{ij} is then obtained for points where $i + j = 2n + 1$ according to

$$J_{ij}(\eta, z) = \frac{1}{4(\Delta S)^2} [(\eta_{i+1,j} - \eta_{i-1,j}) \times (z_{i,j+1} - z_{i,j-1}) - (\eta_{i,j+1} - \eta_{i,j-1}) \times (z_{i+1,j} - z_{i-1,j})] \tag{4}$$

$$i + j = 2n + 1, \qquad 2 \leq i \leq p - 2, \qquad 2 \leq j \leq q - 2$$

and where $\eta_{ij} = \frac{g m^2}{f_{ij}} (\nabla^2 z)_{ij} + f_{ij}$. Thus the non-homogeneous term of equation (2) is obtained for points on the map forming a square grid with the grid interval $\Delta S \sqrt{2}$. The equation is solved by relaxation methods.

This procedure differs from (I) in that the vorticity is computed using a gridsize of ΔS, while equation (2) is solved using a grid interval of $\Delta S\sqrt{2}$. The scheme outlined here was chosen for the following reasons: In (I) it was found that the value $\Delta S \approx 736$ km was too large, in particular for the evaluation of the vorticity. Here ΔS was chosen considerably smaller for the computation of the vorticity ($\Delta S = 4°$ long. at lat. $45° = 315$ km). However, the time required for solving equation (2) by relaxation methods increases very rapidly with increasing number of grid points. In order to keep this time within reasonable limits, the relaxation was carried out for the larger grid size ($\Delta S\sqrt{2}$). The method cannot be used for a complete forecast, because tendencies are only obtained for every other point and new vorticities cannot be computed over the smaller grid after the first time extrapolation has been carried out. Finally it might be of some interest to mention that a complete calculation of $\partial z/\partial t$ takes four to five hours for an experienced computer for a grid with $p = 18$ and $q = 15$. This includes the evaluation of the initial field of z from the map.

3. Period under investigation and methods of verification

In all about forty computations were made in which tendencies were computed for every twelve hours for the period February 3, 03 GMT—February 13, 03 GMT over an area covering the United States, the major part of Canada and the western part of the Atlantic Ocean. For these computations the conventional analysis from the Weather Bureau —Air Force—Navy Analysis Center (WBAN) was used. It was pointed out in (I) that an objective analysis would have been preferable and the same conclusion may be drawn from the present computations. It was also realized that the data coverage over the oceans is too poor to permit an analysis that is accurate enough for this type of computation. For this reason it was decided only to verify the computations over the United States and southern Canada. In order to see to what extent the analysis may have influenced the results over these areas, the maps February 4, 15 GMT—February 12, 15 GMT were re-analysed without reference to the WBAN analyses using smoothness in the vorticity field as a basic guiding principle. The same computations then were carried out for these re-analysed maps.

Some simple statistical methods have been used for the estimation of the errors in the computations. From the two independent analyses the probable error, due to uncertainties in the analysis and the replacement of the differential equation (2) by a finite difference equation was computed. This involved the assumption of a Gaussian distribution of errors. For the comparison of the computed tendencies with actual observed changes over twelve hours several methods can be used. For the present study the computed value of $1/2\,[(\partial z/\partial t)_{t=t_0} + (\partial z/\partial t)_{t=t_0+\Delta t}] \cdot \Delta t = x_1$, was compared with the observed value of $(z_{t=t_0+\Delta t} - z_{t=t_0}) = x_2$ (Δt being 12 hours). This method has the advantage that no assumptions concerning the movement of the fall and rise areas have to be made, such estimates being always more or less subjective. On the other hand, it has the disadvantage that two computations are involved in each verification. Furthermore, this verification scheme cannot be used if the changes are quasi-periodic with a period less than 36 to 48 hours. In such cases all changes will be underestimated. During the period under consideration, this has not affected the computations to any considerable extent.

The comparison between x_1 and x_2 was made in a few different ways. The following quantities were computed:

1) The correlation coefficient r
2) The regression equation $x_1 = a\,x_2 + b$
3) A quantity K defined by

$$K = \frac{\sqrt{\Sigma (x_1 - x_2)^2}}{\sqrt{\Sigma x_1^2} + \sqrt{\Sigma x_2^2}}$$

K has the advantage of being a function both of r and a. $K = 0$ if $x_{1i} \equiv x_{2i}$ for all i, and is approximately 0.7 if $r = 0$, the exact value depending upon σ_1 and σ_2. (σ_1 and σ_2 being the root mean square of x_1 and x_2 respectively.) Quite generally $K \leq 1$.

It should be stressed that this study is not intended to be a complete statistical treatment

of the computed data. It contains merely some order of magnitude estimates of errors in order to permit the discussion of physical aspects of the problem.

4. Computational errors

Apart from errors due to defects in the barotropic model the following errors arise in the computations:

1) Errors due to uncertainties in the analysis of the initial data.

2) Truncation errors, e.g. errors due to the replacement of the differential equation by a difference equation.

3) Errors depending upon the particular method of verification in replacing $\int_{t_0}^{t_0+\Delta t} (\partial z/\partial t)\, dt$ by x_1. Furthermore, there are inaccuracies in the determination of the observed change, x_2.

By comparing the tendencies that were obtained from the two analyses of the same synoptic situations we can obtain an estimate of the combined effect of 1) and 2). It was found that the probable error of the tendency computation introduced by these two factors was 100 feet/12 hours compared with a root-mean-square of the tendencies themselves of 370 feet/12 hours during this period. These errors may be considered to be distributed at random, thus giving rise to a probable error of 70 feet in the determination of x_1. From the same two sets of maps we find that the probable error in x_2 is 30 feet. We cannot obtain a direct estimate of the errors that are introduced by replacing $\int_{t_0}^{t_0+\Delta t} (\partial z/\partial t)\, dt$ by x_1. In spite of this it seems safe to conclude that the observed probable difference of 160 feet between x_1 and x_2 cannot be explained by computational errors. This is supported by other evidence as shown below.

It is now of some interest to examine the agreement between x_1 and x_2 somewhat more closely. The quantities r and K were computed for an area covering the United States and southern Canada for every tendency calculation that was made. In fig. 1 these values are given as functions of time. The solid curve represents the results that were obtained by using WBAN-analysis, the dashed curve is based on computations from the re-analysed maps. The two curves follow each other fairly closely except for the last few points of the diagram. This again indicates that factors other than analysis and the method of finite differences influence the results, which after all is very likely as we know that the atmosphere is not barotropic. The differences that are observed at the end of the period are mainly due to changes in the analysis on Feb. 11, 15 GMT and Feb. 12, 03 GMT. These were con-

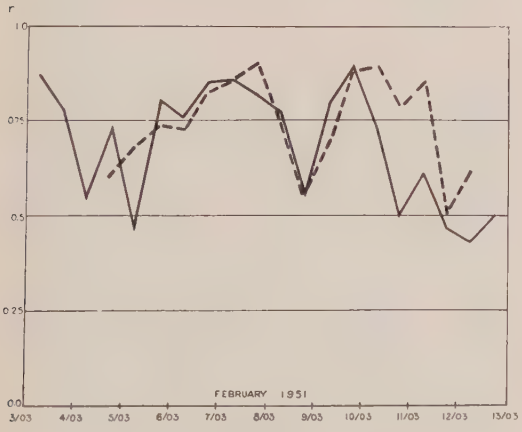

Fig. 1 a.

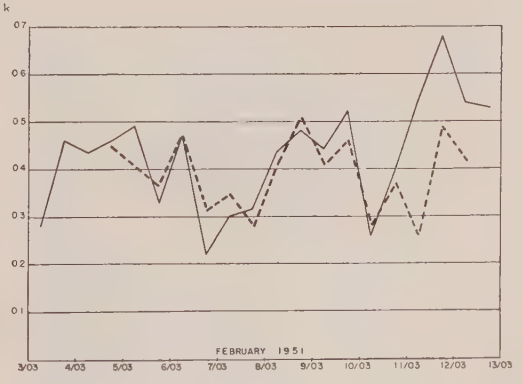

Fig. 1 b.

Fig. 1: Graphical representation of the variation of the correlation coefficient, r (a), and the verification coefficient, K (b). The solid lines represent the results obtained from the WBAN-analyses, the dashed lines those obtained from the reanalysed maps.

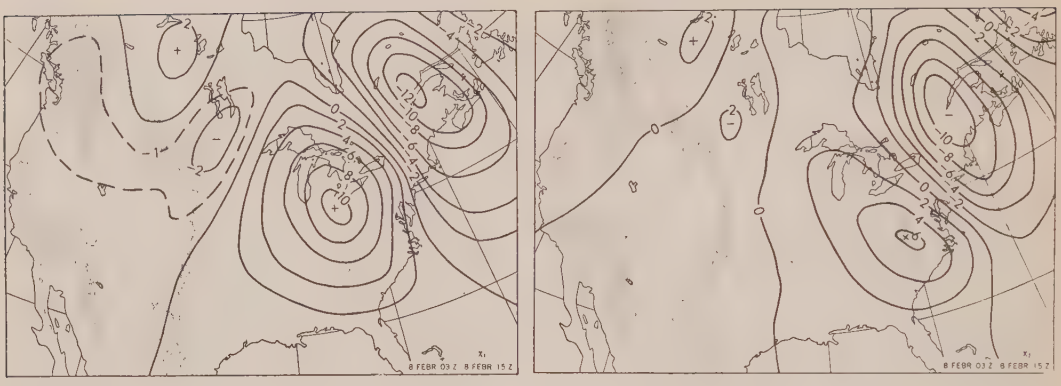

Fig. 2 a. Fig. 2 b.

Fig. 2: Computed mean tendency, x_1, in tens of feet/12 hours, for the period 8 Feb. 03 GMT—15 GMT, 1951 (a), and the corresponding observed change, x_2 (b). The situation was chosen to picture an average case ($r = 0.73$, $K = 0.41$).

siderable, in particular on the later occasion. It should be pointed out that when the number of observations is as large as it is over the United States, changes of the analysis to such an extent can be made only if some observations are neglected in one analysis but not in the other.

The mean values of r and K for the whole period are 0.74 and 0.43 for the WBAN-maps and 0.77 and 0.41 for the re-analysed maps, a scarcely significant difference. It is not immediately clear what these values mean, and we can not say what r and K would be for complete 24-hour forecasts. The iterative method used for that computation certainly introduces errors. Tentatively we may say that the values of r and K obtained here are fairly close to the values that would be obtained in a 12-hour forecast but somewhat larger than one might expect for a 24-hour integration. In order to give an idea of what the values of r and K mean the result of a computation is shown in fig. 2. The situation was chosen to picture an average case ($r = 0.73$, $K = 0.41$).

Returing to the curves in fig. 1 we next ask ourselves for the reason for the systematic variation in time of r and K that we observe. A closer analysis quite clearly shows that the relative errors of the computed tendencies decrease when the tendencies themselves become larger, in other words the results are better when well-defined rise and fall areas exist. Thus the computations were most successful on Feb. 6 and 7 when waves in the westerlies moved along the jet in a regular way. Besides this effect certain physical factors probably have given rise to these variations. The material is, however, insufficient for a closer examination of these aspects.

5. The barotropic model

In this whole approach to the problem of forecasting large-scale atmospheric flow patterns the two most important questions are:

1) To what extent does the atmosphere behave as a two-dimensional barotropic fluid?

2) How is the theory for a barotropic atmosphere best applied to the real atmosphere?

These questions have been discussed intensively during the last ten years since Rossby and collaborators presented the first ideas on long waves in the atmosphere (1939). From the results obtained in (I) and in the computations carried out here we can make some further comments on the importance of barotropic processes in the atmosphere.

It is well-known that the rotation of a fluid has a pronounced influence upon its motion. This was already noticed by Taylor (1921) who was able to demonstrate this effect in simple model experiments. The stronger the rate of rotation the more pronounced is the tendency for the motion to become quasi-similar in planes perpendicular to the axis of rotation. It seems reasonable to assume that an analogous effect is present in the atmosphere.

Here the motion is already kinematically restricted to take place in a hemispherical shell and for large-scale flow patterns we may thus expect that it is the vertical component of the rotation of the earth that is of importance. Consequently this tendency for similarity from level to level should be found at high and middle latitudes but not in equatorial regions. By and large this agrees with what is observed in the atmosphere. In middle latitudes the similarity from layer to layer is a striking feature of the flow (above the friction layer), while recent investigations of the tropics show large differences between the lower and upper troposphere (RIEHL, 1950). This gives some justification for treating the motion of the atmosphere in the middle latitudes as two-dimensional.

The atmosphere is a thermally active fluid and at first it may seem strange that worthwhile results can be obtained by treating it as a barotropic fluid. However, we know that it would take approximately one week for friction to reduce the kinetic energy of the atmosphere by 50 per cent if this loss were not replaced by baroclinic processes. The total kinetic energy is approximately constant, thus the baroclinic processes in the atmosphere do not replace more than about 10 per cent of the total kinetic energy in twenty-four hours. There are several reasons to believe that this change of potential energy into kinetic energy does not take place simultaneously all over the hemisphere but mainly in connection with what is known as real deepening or intensification of atmospheric systems. Thus outside such restricted areas the change in the atmospheric flow patterns are primarily the result of a *redistribution of kinetic energy*. Such a redistribution essentially is a barotropic process.

Even if the total kinetic energy of a barotropic fluid is conserved (apart from frictional dissipation) local intensifications of the flow may occur in a barotropic fluid. It has been shown (KUO, 1949; FJØRTOFT, 1950) that waves in parallel flow are unstable if certain criteria are fulfilled and YEH (1949) has pointed out that dispersion of kinetic energy may give rise to intensification of disturbances in the flow. Some examples have also been given indicating that these processes are of importance in the atmosphere. In most cases, however, it is difficult to tell whether baroclinic processes have not also affected the development. Having been able to compute the changes in the fluid that would take place if the atmosphere were barotropic, we may obtain an idea of where and when the baroclinicity plays a significant role. From this point of view it is of some interest to study the series of computations from Feb. 6, 03 GMT, to Feb. 8, 15 GMT. During this period a wave developed from a fairly small disturbance in the westerlies to a very intense trough. The 500 mb maps for Feb. 6, 03 GMT, Feb. 7, 03 GMT and Feb. 8, 15 GMT are shown in figs. 3a to 5a. The heavy lines give the distribution of absolute vorticity. The com-

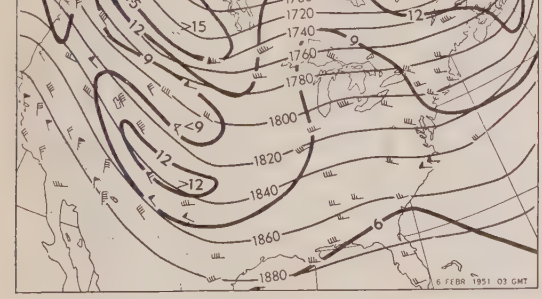

Fig. 3a.

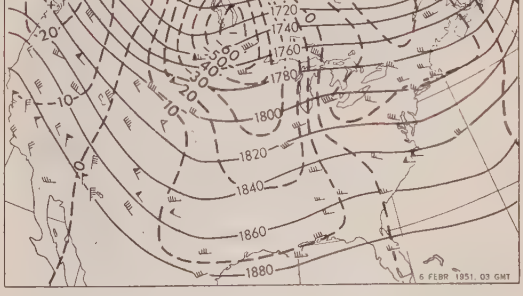

Fig. 3b.

Fig. 3: 500-mb chart at 03 GMT, 6 Feb. 1951. Thin lines are the contours labelled in tens of feet. The heavy lines in fig. a give the distribution of absolute vorticity in units of 10^{-5} sec^{-1} and the dashed lines in fig. b show the computed tendency in tens of feet/12 hours.

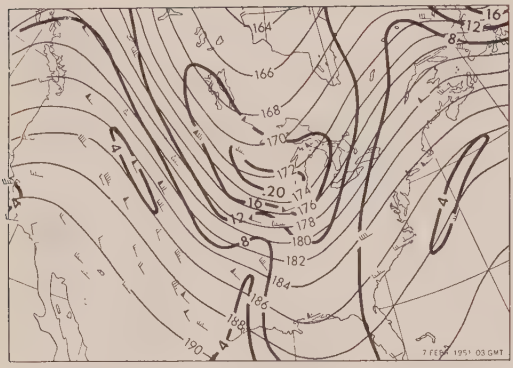

Fig. 4 a.

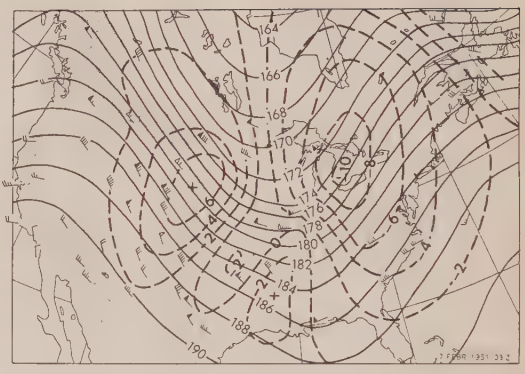

Fig. 4 b.

Fig. 4: 500-mb chart at 03 GMT, 7 Feb. 1951. Legend as in fig. 3.

puted tendencies are given in figs. 3 b—5 b (dashed lines). We observe that the changes during the first 24 hours seem mainly to be the result of a redistribution of the vortex lines, and there is only a slight increase of the intensity of the vorticity maximum in spite of the fact that the wave is amplifying. This indicates that the changes are quasi-barotropic (the diagram in fig. 1 shows that the most successful tendency computations for the whole 10-day period were made during these 24 hours). It is now interesting to see that the development of the wave, at least qualitatively, is indicated by the barotropic tendencies. Both on Feb. 6, 03 GMT and Feb. 7, 03 GMT (in fact also on Feb. 6, 15 GMT, not shown here) the zero-line of the tendency field is located well to the west of the trough line as computed barotropically and the fall area in front of the trough is more intense than the rise area behind (figs. 3 b, 4 b). On Feb. 8, on the other hand, we observe a pronounced increase of the vorticity in the trough. It is also seen from fig. 1 that the tendency computations become worse during this period and a complete 24-hour forecast probably would give still larger discrepancies between the computed and observed changes of the flow pattern. Here baroclinic effects seem to have played an important role in the development. From this qualitative discussion one therefore gets the impression that the initiation of the development of the trough was barotropic while baroclinic effects became more and more important for the further intensification.

In fig. 3 another illustration of the quasi-

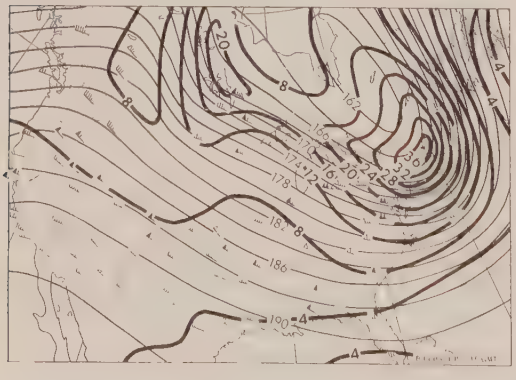

Fig. 5 a.

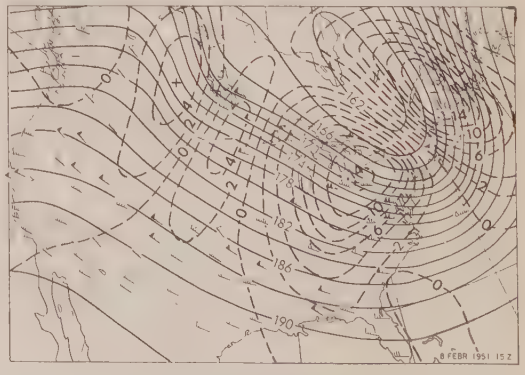

Fig. 5 b.

Fig. 5: 500-mb chart at 15 GMT, 8 Feb. 1951. Legend as in fig. 3.

barotropic behaviour of the atmosphere is shown (northern US around long. 100° W). We see clearly how the contour lines of the 500 mb surface are ajusted when a strong jet pushes into a region where the flow is less intense. The intensification of the gradient is clearly indicated in the tendency computations and agrees by and large with the observed changes.

By inspecting a series of barotropic tendency computations of this kind it is possible to formulate qualitative rules for the changes that may be expected from different flow patterns. This is not the place for a detailed discussion of such rules; it should merely be stated that many of them are in accordance with empirical rules that have proven to be useful for the daily prognosis of the flow pattern at upper levels.

Up to this point very little has been said about the best methods for applying these barotropic tendency computations to the real atmosphere. We have simply assumed that the flow at 500 mb is governed by the barotropic vorticity equation, in other words that the 500 mb surface is the level of non-divergence. This is not in accordance with reality, and considerable errors are introduced by the assumption. Some idea of these errors were obtained in the following way: For each gridpoint in the area of verification the regression coefficient a was computed using all tendency computations that were made. Systematic variations of a were found as shown in fig. 6. During this period a had a maximum value of approx. 1.4 in the Great Lake Region and was less than 0.6 over parts of the Rocky Mountains. This indicates that the changes as computed for an equivalent barotropic atmosphere were stronger than the observed changes at 500 mb in the Middle West, while the reverse was true over the mountains. To some extent this may have been caused by the use of the geostrophic assumption which results in an overestimate of the vorticity advection in troughs and an underestimate in ridges. During this period a mean trough was located over the middle west where the computed tendencies were too strong and a ridge is found over the Rocky Mountains. However, the differences are too large to be explained merely as an effect of the geostrophic approximation. Instead we may look upon them as indications of a systematic variation in the height of the level of non-divergence, the level lying below the 500 mb surface where $a > 1$ and above where $a < 1$. Thus the lines of constant a as a first approximation may be considered as contour lines of the level of non-divergence. It has been pointed out by CHARNEY (1947) and others that such variations of the height of that level may be expected in the long waves in the westerlies. In this particular area the influence of the Rocky Mountains also seems very important. As the level of non-divergence is located approximately in the middle of the atmosphere (with respect to pressure) one might expect to find it at higher elevation over the mountains. As the computations were fairly restricted both in time and space we were not able to examine more closely the cause of the varation of the height of the level of non-divergence. The values of a as computed here, however, strongly indicate that the assumption of the 500 mb level as the level of non-divergence introduces considerable errors. In (I) it was indicated that integrating through the vertical and thus treating some kind of a mean atmosphere tends to remove this difficulty. However, the interpretation of the flow pattern with respect to weather then becomes more difficult.

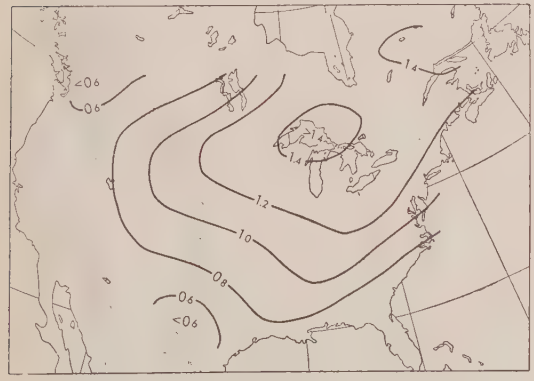

Fig. 6: Geographical distribution of the regression coefficient, a, computed from the whole material.

Another possible effect of the mountains is indicated in these computations. It was found that the constant factor b in the regression equation has a very characteristic distribution over the area under consideration. (cf. fig. 7). This may be explained as a result of neglecting the divergence and convergence

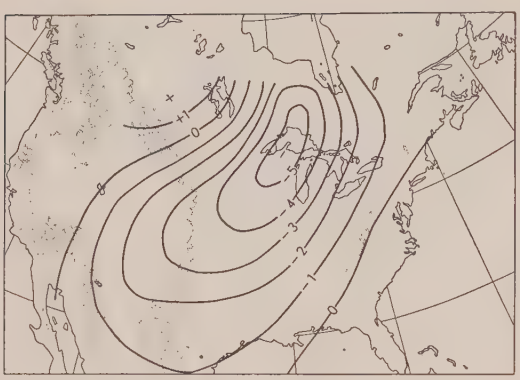

Fig. 7: Geographical distribution of the constant factor, b, in the regression equation, computed from the whole material (tens of feet/12 hours).

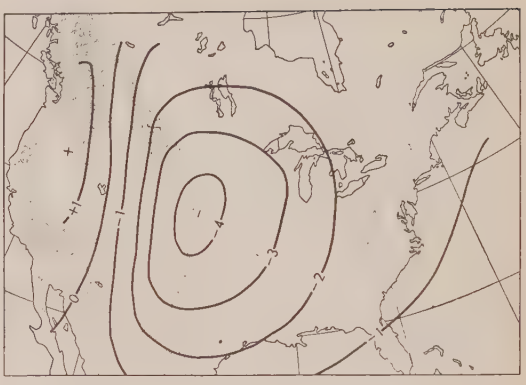

Fig. 8: Computed tendency field (in tens of feet/12 hours) as a result of horizontal divergence and convergence caused by the mountain using $^1/_2\ \bar{\mathbf{v}}$ as representative for the mean surface wind during the period.

that is caused by the mountains when the flow is forced over them. We have made an estimate of the mean 12 hour change of the 500 mb surface caused by this effect during the period by assuming that the divergence term in the vorticity equation may be computed by putting $\mathrm{div}_2\,\mathbf{v} = \mathbf{v}_0 \cdot \nabla h$, where $\mathbf{v}_0$ is the surface wind and h is the height of the mountains. It was assumed that $\mathbf{v}_0 = {}^1/_2\,\mathbf{v}$ and the tendencies thus obtained are shown in fig. 8 expressed in 10 feet/12 hours. The resemblance between fig. 7 and fig. 8 is quite good both with respect to the structure of the pattern and the magnitude of the changes, in particular as the assumption that $\mathbf{v}_0 = {}^1/_2\,\mathbf{v}$ is a fairly crude approximation. By and large the computations support an idea already put forward by CHARNEY and ELIASSEN (1949).

The disagreement between the observed changes of the flow pattern and those derived from the tendency calculations here have been interpreted as a result of the variation of the level of non-divergence and as an effect of the mountains.

A few attempts were made to correct the barotropic computations in a manner indicated in (I) and in CHARNEY (1951) by assuming that the thermal wind rather than the actual wind does not vary in direction with height and that temperature is advected horizontally. The changes in the 500 mb tendency were small and gave no systematic improvement. The surface tendencies, which were also calculated by the method, were for the most part of the right sign. We were, however, led to the conclusion that the advective hypothesis is not satisfactory as the correlation between the computed and observed patterns was poor.

Summarizing the results of these computations the following should be noticed:

1) The data coverage over the United States seems sufficient to give the initial conditions with the accuracy that is required for the present type of computation. Over the oceans a much denser net of upper observations must be established before successful forecasts can be made by the present methods.

2) A severe defect of the model used in these computations seems to be the assumption that the 500 mb level coincides with the level of non-divergence.

3) Computations of this kind are important in that they give us a method of *separating* purely barotropic effects from baroclinic processes. This will be of great help when trying to extend the present model of the atmosphere to incorporate the baroclinicity.

Acknowledgments: The writers wish to acknowledge the benefit they have received from many stimulating discussions about these computations with Dr M. Neiburger, Mr T. V. Davies and Mr J. Smagorinsky.

REFERENCES

Charney, J., 1947: Dynamics of long waves in a baroclinic westerly current. *J. Meteor.* **5**, pp 135—162.

Charney, J. and Eliassen A., 1949: A numerical method for predicting the perturbations of the middle latitudes. *Tellus* **1**, 2, pp 38—54.

Charney, J., Fjørtoft, R. and von Neumann, J., 1950: Numerical integration of the barotropic vorticity equation. *Tellus*, **2**, pp 237—254.

Charney, J., 1951: Dynamic forecasting by numerical process. Compendium of Meteorology, *Am. Met. Soc.* pp. 470—482.

Fjortoft, R., 1950: Application of integral theorems in deriving criteria of stability for laminar flows and for the baroclinic circular vortex. *Geof. Publ.* **17**, 6, 52 pp.

Kuo, H .L., 1949: Dynamic instability of two-dimensional non-divergent flow in a barotropic atmosphere. *J. Meteor.* **6**, pp 105—122.

Riehl, H., 1950: On the role of the tropics in the general circulation of the atmosphere. *Tellus*, **2**, 1, pp 1—17.

Rossby, C.-G. and collab., 1939: Relation between variations in the intensity of the zonal circulation of the atmosphere and the displacements of the semi-permanent centers of action. *J. Marine Res.* **2**, pp 38—55.

Southwell, R. V., 1946: *Relaxation methods in theoretical physics.* Oxford Clarendon Press. 248 pp.

Taylor, G. I., 1921: Experiments with rotating fluids, *Proc. Roy. Soc. London* (A) 100, pp 114—121.

Yeh, T. C., 1949: On energy dispersion in the atmosphere. *J. Meteor.* **6**, pp 1—16.

The Structure of Mean Circulations

By R. W. JAMES, Edinburgh

(Manuscript received 10 August 1951)

Abstract

A discussion of the best mode of expressing the facts of the mean westerly flow in temperate latitudes parametrically leads to the result that over North America the shape of the vertical geostrophic westerly wind profile is nearly invariant with respect to time and place. The vertical wind profile can be expressed in terms either of the change pressure-gradient with height, or of contour-height gradient with pressure-level. In either case the profile shape is characteristic, and varies little with season, longitude or latitude over North America.

The intensity of the mean circulation varies rythmically with season, but that for any one month may vary markedly from year to year.

The profile shape for an oceanic region differs from that of a land region such as eastern North America in exibiting a lower ratio of high-level to surface wind, and in being much more variable from month to month.

It is shown that the pressure-difference at 7 km between two latitudes, or the difference in mean height of the 200 mb surface gives a measure of the total geostrophic momentum between those latitudes. The square of these quantities also gives a measure of the total kinetic energy of the westerlies between these two latitudes.

1. Introduction

The accumulating mass of aerological material over the past ten years has permitted the construction of mean meridional cross-sections of geostrophic westerly winds. This is a graphic method of conveying the salient characteristics of the mean circulation pattern in some areas of the globe, but it should not be regarded as the ultimate in descriptive aerology because it happens to be the mode best adapted for textbook presentation.

The present paper will be devoted to an alternative, parametric representation of general geostrophic westerly flow in selected areas. The scientific advantage of parametric representation is that it describes mean flow in quantitative terms. This is obviously necessary if we are ever to have a quantitative theory of the general circulation, for a quantitative theory requires quantitative facts to fit it.

The two methods are essentially alternative presentations of the same facts. From a complete parametric presentations, one may readily derive a corresponding cross-section, and alternatively, a complete set of parameters can be inferred from an accurate cross-section.

We shall find, in passing, that an investigation of parameters apt for describing mean flows leads to considerably simplified techniques which may be employed in deriving cross-sections.

2. Mean geostrophic circulation as a function of latitude

If we plot the mean pressure at a fixed height at points along a meridian against the cosine of the latitude, we get a curve the slope

of which is at each point proportional to the Westerly geostrophic momentum per unit volume, for, if

$$p = f(\cos \varphi),$$

$$\varrho U_g = \frac{-1}{2\Omega a \sin\varphi} \frac{\partial p}{\partial \varphi} = \frac{1}{2\Omega a} \frac{\partial p}{\partial \cos \varphi}$$

where Ω is the earth's rotational speed, a the earth's radius, ϱU_g the density of westerly geostrophic momentum.

When ϱ, the density, is known, the value of U_g, the geostrophic wind-speed may be inferred.

Hess (1948) has published summer and winter mean ascents for stations close to meridian 80° W, ranging from Arctic Bay, latitude 73° 16′ N, to Salinas, 2° 12′ S. From these data the winter pressure-profiles at heights 3 km (lower, curve) and 10 km, are plotted as a function of cos φ in fig. 1.

It will be noticed that along much of their length, say between the latitudes of Detroit and Monsonee (42° and 56° respectively), the two curves are almost parallel. We find the same shape of curve at other levels between 3 and 10 km. Below 3 km the profile slope falls off. We infer from this parallelism between about 40° and 50° that *momentum is approximately invariant with height in the middle and upper troposphere in winter over Eastern America.*

At latitudes lower than about 40° the two curves begin to diverge, the slope of the upper curve being the greater. Hence below about latitude 40° in winter momentum *increases* with height in the troposphere.

We remark that the slope of the 3 km curve increases steadily with decreasing latitude up to between Huntingdon and Charleston, say in latitude 36°. This constitutes a latitude of maximum momentum and is termed the *jet latitude*. For lower latitudes still the momentum decreases, and becomes zero at the maximum of the pressure profile curve, in latitude 20° approximately. This point we shall term the *doldrum latitude*.

Examining the 10 km profile we find a main jet latitude, again at 36°, and a subsidiary, weak one between Monsonee and Port Harrison, say at latitude 55°. The doldrum latitude of this level is 14°.

The locus of the doldrum latitudes at all

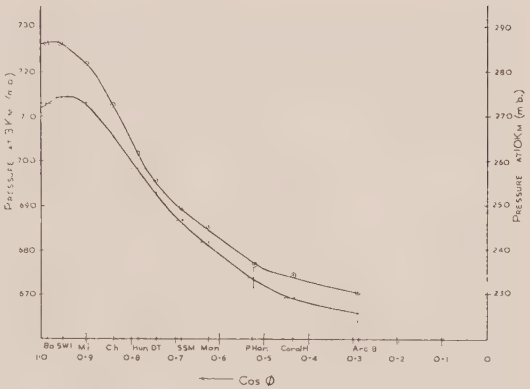

Fig. 1. Pressure at 3 k. m. (starred points) and at 10 km (circles) as a function of Cos φ, meridian 80° W. approx., winter.

levels is termed the *doldrum axis*. It will be observed that the doldrum axis slopes equatorward with height, being in latitude 30° at the surface, 20° at 3 km, and 14° at 10 km.

The *jet axis* is the locus of the jet latitudes at all levels. The main jet axis is practically vertical in latitude 36°. The secondary jet, in latitude 55° does not reach down to the 3 km level.

As we shall see in the next section there is a tendency for momentum to increase with height up to a certain level, and then to decrease. The height of maximum momentum is termed the *momentum jet height*, and the locus of momentum jet heights for all latitudes may be called the *momentum jet profile*. The momentum jet height is found to be approximatly 7 km. The intersection of the jet axis with the momentum jet profile gives the point at which momentum is a maximum. It is termed the *momentum jet centre*. The coordinates of the main momentum jet centre are $\varphi = 36°$, $z = 7$ km. For the subsidiary jet we have, $\varphi = 55°$, $z = 7$ km.

The momentum jet height is not the same as the *velocity jet height;* on account of the variation of density with height the maximum of velocity is found on the jet axis at a height of about 12 km. In describing the velocity field we define a *velocity jet profile* and a *velocity jet centre* in a way exactly analogous to the corresponding momentum parameters.

In order to characterize the westerly geostrophic flow completely we must finally specify an intensity factor. A number of

possibilities exist. We could take the momentum at the main momentum jet centre (or velocity at the velocity jet centre). Alternatively a mean momentum between specified latitudes might be used, the best level to take being the height of the momentum jet profile, 7 km approximately. This second alternative is more in accord with current usage, which accords a unique position to the *zonal index* or pressure difference at fixed level (usually the surface) between latitudes 30° and 60°.

The zonal index at the jet level, 7 km, will be shown later to represent the mean momentum of the westerlies at all levels between the assigned latitudes.

Once the zonal index at 7 km (or the momentum at the momentum jet centre), the momentum jet profile, the jet axes and the doldrum axis have all been specified, together with the variation of momentum with height, the structure of the momentum field is completely specified.

Fig. 2 shows the corresponding profiles at 3 and 10 km for Hess' summer data. The salient feature is the reduction of the zonal index as compared with winter. The pressure-drop between Charleston and Port Harrison at 7 km is 23.5 mb in summer, as compared with 42.1 mb in winter. Mean westerly summer momentum is just over one-half the mean winter momentum.

The doldrum axis has migrated to about 28° latitude, and is almost vertical, while the momentum jet centre is now at latitude 55°.

3. The vertical profile of momentum

It has been shown (JAMES unpublished) that the latitudinal pressure-difference between

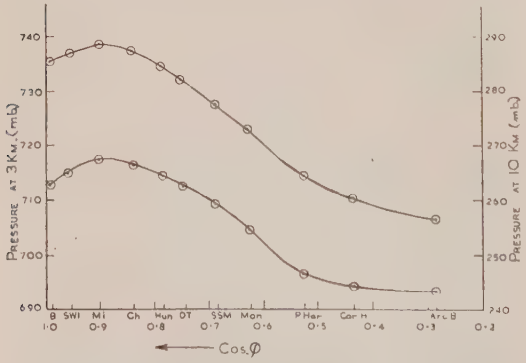

Fig. 2. Meridional summer profiles of pressure at 3 km and 10 km.

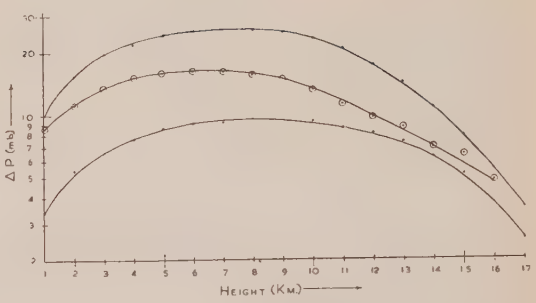

Fig. 3. Pressure at a fixed height between different latitudes. Top curve, Charleston—Sault-Ste. Marie, intermediate curve, Sault-Ste. Marie—Port Harrison, lowest curve, Charleston—Miami.

two points in nearly the same longitude varies with height according to the relation

$$\Delta p = (\Delta p)_m \exp\left[-k(z - Z_m)^2\right] \quad (1)$$

where Z_m is the momentum jet height, and $(\Delta p)_m$ is the pressure difference at this height. We may term $(\Delta p)_m$ the *jet intensity* between the pair of stations concerned.

Fig. 3 shows the relation between Δp and height plotted on a logarithmic scale for station pairs in the Hess winter data. The upper curve gives the pressure difference between Charleston and Sault-Ste-Marie, latitudes 33° and 46½° respectively. The flat maximum occurs at about 7.3 km, the mean momentum jet height for this latitude range, and is practically symmetrical for a range of 5—6 km on either side of this central point. The profile is almost identical with one for Charleston-Caribou as yet unpublished, being closly represented by a profile of the form (1), as may be verified by plotting the cumulated value of Δp against z on probability paper.

The middle curve represents the mean vertical profile of westerly momentum for the latitude range 46½°—58½° (Sault-Ste-Marie and Port Harrison). The mean momentum jet level is at 6.6 km.

The lowest curve, Miami, latitude 26°, and Charleston, is again of the form (1). The momentum jet level is at 8.4 km. The same type of profile is found for the pressure-difference between Port Harrison and Arctic Bay (latitude 73°), the momentum jet height being 6.3 km.

We see, therefore, that the shape of the vertical momentum profile is characteristic

over a latitude range, 25° N—73° N of eastern North America. It can be shown that the profile shape (1) holds for West and Central U. S., and in different seasons. It is thus a quasi-invariant of the mean westerly flow over the U.S.

Since the momentum profile shows a very flat maximum the Clayton-Egnell rule, momentum constant with height, gives a good approximation over quite a considerable range of height. For about 2 km on either side of the jet level the reduction in momentum is only about 6 %, while for a range of 8 km centred at the jet level the maximum departure is 20 %.

A parameter specifying the properties of the vertical profile is the *equivalent thickness*, Z_T, defined by

$$Z_T \Delta p_m = \int_0^\infty \Delta p \, dz$$

Z_T is the thickness of an equivalent stratum of air having everywhere a momentum equal to the momentum at jet level, with the same total momentum as the actual atmosphere.

The average winter equivalent thickness is 12.5 km between latitudes 26° and 33°, 11.4 km between 33° and 46½°, 11.5 km between 46½° and 58½°, and 10.0 km for latitudes 58½° to 73°. These are actually underestimates, for the momentum below 1 km and above 16 km. has been disregarded. It can be shown that the equivalent thickness does not vary significantly with season; it is, in fact, a quasi-invariant of the mean circulation.

The total westerly momentum between latitudes φ_1 and φ_2 in a meridional slab of unit thickness extending vertically to infinity is

$$a \int_{\varphi_1}^{\varphi_2} d\varphi \int_0^\infty \varrho U \, dz$$

When one of the latitudes lies in the region of low level easterlies, the lower limit of the z integral becomes the height of the doldrum axis in that latitude.

For the total momentum between, say, latitudes 30° and 60° we may thus write

$$U = \frac{1}{2\Omega} \int_{30°}^{60°} \frac{Z_T}{\sin \varphi} \left(\frac{\partial p}{\partial \varphi}\right)_m d\varphi$$

where $\left(\frac{\partial p}{\partial \varphi}\right)_m$ is the pressure gradient along the jet profile. Hence to an approximation, since the equivalent thickness varies only slightly with latitude,

$$U \approx \frac{Z_T (\Delta p)_m}{2\Omega \sin \bar{\varphi}} \qquad (2)$$

where $\bar{\varphi}$ is some mean latitude.

The total mean westerly momentum between two latitudes is thus proportional to the pressure-difference between 30° and 60° at the height Z_T, or 7 km.

The total momentum over the whole westerlies belt is given by

$$U' = \pi a \, Z_T \operatorname{Cot} \bar{\varphi} \, (\Delta p)_m / \Omega \qquad (3)$$

where $(\Delta p)_m$ must now be interpreted at the zonal index at 7 km between latitudes 30° and 60°.

The zonal index at other levels gives a (more approximate) measure of the total atmospheric momentum, because of the quasi-invariance of the vertical profile-shape. However, the 7 km level is to be preferred as the momentum changes with height least here, and is less subject to random fluctuations. The worst level to take is the surface, as here the profile is subject to fluctuations connected with the boundary conditions which may not be appreciably reflected in the mean flow at height.

4. The use of contours

Hess' data are given in terms of pressure at a fixed level. It is now standard practice in most weather services to quote contour heights of standard pressure surfaces rather than pressures at fixed height levels. Fig. 4 shows the mean contour heights for the year 1946—49, inclusive, as a function of cos φ for U.S. stations around 80° W longitude for the 300 and 700 mb levels.

These profiles show the same salient features as those drawn for pressure at fixed height levels. They have the advantage that the slope determines velocity directly, and not momentum. By reading off the slopes of the contour profiles for a number of different pressure-

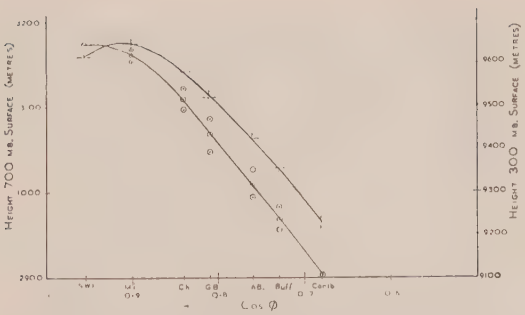

Fig. 4. 700 mb contours (starred) and 300 mb contours (circles) as a function of latitude for meridian 80° W. approx, for 1946—49. The upper circles indicate 300 mb, contour height in the year of greatest height (1949) and the lower circles apply to 1947, the year of least profiles. The intermediate points, through which the smooth curve has been drawn, refer to the mean four year values.

levels, it is possible to compute cross-sections with much greater facility and speed.

Three points (circled) are shown for each station in the 300 mb profile in fig. 4. The middle point is the four year mean contour height, and through these points the smooth curve of the mean profile is drawn. The upper set of points gives the mean contour heights in the year of greatest general contour height (1949), while the lowest set corresponds to 1947, the year of least general contour height. It will be seen that the annual mean height of the 300 mb surface may change by more than 50 metres from year to year, but that the surface rises or falls by much the same amount in all latitudes. If the fall or rise were uniform in all latitudes the slope relations would remain unchanged and the West-wind pattern would be unaltered from year to year.

However, we should expect a greater variability of mean contour height in high than in low latitudes. This is borne out in fig. 4, where it will be seen that the '49 and '47 mean contours differ by 30 m at Miami and by 80 m at Greensboro. We should consequently expect years of high average contour height to be weak jet years, and years of low average height to display strong jets.

The main jet latitude is approximately 36° for both 1947 and 1949, but the westerly speed at the 300 mb level is 33 % higher in 1947 than in 1949. There is a subsidiary maximum between the latitudes of Pittsburg and Buffalo in 1949, and between Buffalo and Caribou, or in higher latitude, in 1947, this subsidiary jet being stronger in 1949. Fig. 4 thus reveals appreciable variations in the strength and structure of the annual mean westerlies from year to year, although the overall pattern is not radically altered. It should be borne in mind, also, that systematic errors, changing from year to year cannot be completely excluded from the estimates of mean 300 mb contour heights.

5. The vertical wind profile

The difference in the mean contour height of a given pressure-surface between two stations is a measure of the mean geostrophic wind component between the stations in a direction transverse to the line joining them. If one station is due North of the other the westerly component of mean wind is measured.

The way in which this height-difference varies with the pressure-surface gives a measure of the change in geostrophic wind-speed with height. In an application such as this it is natural to take pressure as the measure of height. Whether we take as our argument the actual pressure, or its logarithm, as being more nearly proportional to height is purely a matter of convenience. In fig. 5 we plot mean contour height difference between Charleston and Caribou against pressure for the four-year period, 1946—49. The curve shown is the *reduced* profile, normalized so that $(\Delta Z)_{max} = 1$.

It will be noticed that the points lie evenly on a smooth curve which is almost a linear

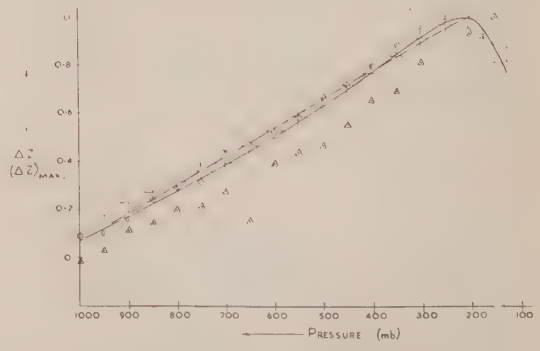

Fig. 5. Mean vertical westerly wind profile between two latitudes. The full curve is drawn through the four year mean contour-differences, Charleston—Caribou. The circled points represent the same relationship for Pittsburg—Caribou, and the starred points are for Greensboro—Pittsburg. The triangles apply to Charleston—Miami.

function of pressure up to jet level. The linear relationship

$$U = U_0 (p - p_m) / (p_0 - p_m) + \\ + U_{max} (p_0 - p) / (p_0 - p_m) \qquad (4)$$

where p_0 is the surface pressure and p_m the pressure at jet level, U_0 and U_m being the corresponding westerly geostrophic speeds, is indicated by the dotted line in fig. 5. If a closer relationship is desired a parabolic curve could be fitted, but for many purposes the linear relation will be found quite accurate enough. The jet level is estimated to be 220 mb.

The profile shown is that of mean westerlies over a considerable latitude range. It is therefore of interest to see whether the shape is substantially unchanged for a narrower range of latitude. The starred points in fig. 5 give the vertical profile between Greensboro and Pittsburg, while the circled points show the relationship for Pittsburg-Caribou. The points lie very close to the curve drawn for Charleston-Caribou, so that the profile shape is very nearly independent of the latitude between 33° and 47°. Above 200 mb there is some considerable scatter indicating that observations at the highest levels may not be absolutely representative.

Even below latitude 33° the vertical profile shape is very similar to that for higher latitudes. The points enclosed in triangles give the profile-shape for Miami-Charleston. The scatter is more noticeable, probably due to the small difference in contour height between these stations, but the linear relationship is still a reasonable approximation. The jet level is somewhat higher than in higher latitudes, at 190 mb.

It is also possible to show that the vertical profile-shape does not change significantly with season. In fig. 6 the mean reduced vertical profile, Charleston-Caribou, 1946—49 is again drawn, together with points for the months January, April, July and October, 1949, for the same pair of stations. The points for the first three months cluster very closely around the four-year mean profile, with no significant seasonal change. The most discordant month, October 1949, is indicated by the lower line. The jet level is higher, and the curve more concave than for the annual mean. Even so, the similarity between the two curves is striking.

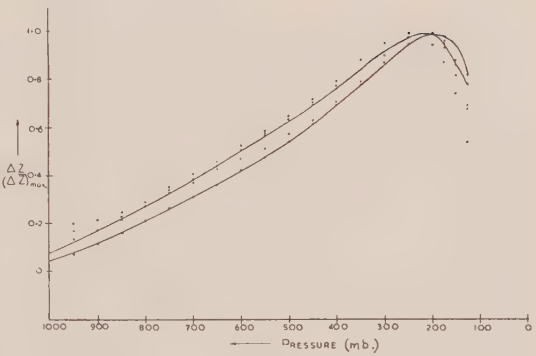

Fig. 6. The four year mean westerly wind profile for Charleston—Caribou — full curve, with indications of seasonal variation. The points refer to the different seasons, but it is apparent that the seasonal scatter of profile shape is slight.

The scatter of monthly values from the four-year mean profile is most pronounced below 850 mb. This is perhaps not unexpected; the wind-field at low levels is most likely to be influenced by surface boundary conditions which may have nothing to do with the general westerly flow-invariance of the wind-speed profile. That it does not vary appreciably with longitude over the U. S. can be inferred from the invariance of its counterpart, the momentum profile.

6. The annual variation of geostrophic wind

We have remarked that the vertical profile of geostrophic mean wind is a quasi-invariant of the atmospheric circulation over the U.S.; it does not change appreciably with season. Hence the seasonal variation of wind at any one pressure-level may be taken as typical

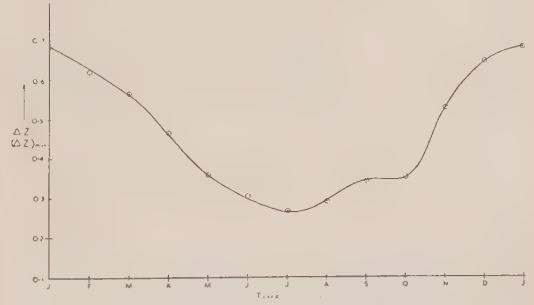

Fig. 7. The seasonal variation of mean westerly wind between Charleston—Caribou.

of the variation at all levels, except, possibly, near the surface.

In fig. 7 we show the mean annual variation of contour-height difference between Charleston and Caribou, 1946—49 at the 200 mb. level.

The geostrophic Westerly speed of the mean circulation reaches a maximum in January and a minimum in July. The curve is approximately sinoidal in shape.

The curve shown is based on four years of data; the periodic curve in any one year may depart markedly from this pattern. Thus the maximum in a given year may well occur in December or February, or even March; the minimum might be displaced to June or August. The strength of the mean monthly circulation in any month may be displaced a month or two from the seasonal mean. In the most variable month, the departure from the seasonal mean will be 25 % or more above or below normal in 30 % of months. Nevertheless, in spite of large 'casual' variations in the strength of the circulation, there is a strong underlying seasonal rhythm. The October plateau, showing up in fig. 7, may be a real effect, or may be due simply to the inclusion of a run of abnormally sluggish Octobers. Such points can only be settled by a longer series of data than that used here.

7. The kinetic energy of middle latitudes

The mean westerly wind-speed at a given pressure level between two stations on the same meridian separated by a latitude distance Δy is

$$U = \frac{g \Delta Z}{2 \Omega \sin \bar{\varphi} \, \Delta y}$$

where ΔZ is the contour-height difference, and $\bar{\varphi}$ is a mean latitude. The total momentum over the latitude distance Δy of a meridional slab of unit thickness is, then

$$\Delta y \int_0^\infty \varrho \, U \, dz = \frac{1}{2 \Omega \sin \bar{\varphi}} \int_0^{p_0} \Delta Z \, dp$$

Now we have seen that ΔZ as a function of pressure (height) is a quasi-invariant of the mean circulation

$$\Delta Z = (\Delta Z)_m f(p), \quad f(p_m) = 1$$

We may thus write for the total momentum of the slab

$$U = \frac{(\Delta Z)_m}{2 \Omega \sin \bar{\varphi}} \int_0^{p_0} f(p) \, dp,$$

and for the total momentum of an entire latitude belt, assuming the functional form of $f(p)$ to be the same in all longitudes,

$$\frac{\pi a (\Delta Z)_m}{\Omega} \cot \bar{\varphi} \int_0^{p_0} f \, dp$$

We see, therefore, that the total westerly momentum in a given latitude range is proportional to the difference in the mean contour heights at the level of maximum geostrophic wind-speed. The integral

$$\int_0^{p_0} f \, dp$$

has the dimensions of pressure. We term it p_T the *pressure-thickness*. It represents the weight, in pressure units of atmosphere, which, possessing everywhere the maximum wind-speed, has the same total momentum as the actual atmosphere.

From the vertical profile of geostrophic speed, already determined, we find,

$$p_T = 540 \text{ mb.}$$

Since f is a quasi-invariant of the westerly circulation, so is p_T. Hence a convenient overall index of the strength of the westerly circulation is the mean contour height difference at a level of approximately 200 mb.

This formulation is in every way equivalent to that in terms of the zonal index, for which we have the equivalent thickness as the quasi-invariant. Whether the pressure thickness or the equivalent thickness is used to characterize the mean vertical profile depends entirely on whether we are dealing with contours or fixed level charts.

The total kinetic energy in a vertical longitudinal slab of unit thickness between two latitudes is

$$K = \frac{1}{2} \int_{\varphi_1}^{\varphi_2} a \, d\varphi \int_0^\infty \varrho \, v^2 \, dz$$

Hence

$$K = \frac{g(\Delta Z)_m^2}{4\,\Omega^2 \sin^2 \bar{\varphi}} \int_0^{p_0} f^2\, dp \qquad (5)$$

We may thus define a *kinetic pressure-thickness*,

$$p_K = \int_0^{p_0} f^2\, dp$$

Since f is quasi-invariant, so is p_K. From the 4-year mean vertical profile between Charleston and Caribou, we find

$$p_K = 385 \text{ mb.}$$

We see from the expression (5) that the total atmospheric geostrophic kinetic energy between two latitudes is proportional to the square of the contour height difference at about 200 mb between the two latitudes.

8. Other longitudes

It is important to know whether the relationships found apply to the N. American continent only, or generally characterize the entire Westerly belt. YEH (1950) has published a winter cross-section along 76° E, using actual rawin data rather than geostrophic speeds. The general structure is strikingly similar to that found by Hess for Eastern America. Two jets occur around latitudes 28° and 42°. Both these positions are further south than the corresponding jets over America, and jet speeds are about 20 % higher. In latitude 40° the speed of jet level is some 6—8 times that at 900 mb, in agreement with what is found over N. America. From the appearance of the cross-section it would seem that wind-speed is a nearly linear function of decreasing pressure, as over N. America. A profile published by CHAUDHURY (1950) shows approximately the same characteristics.

From this it might appear that the structure of the westerlies is approximately the same in all longitudes. At the moment there are no cross-sections available for Western Europe, a circumstance which might call for some surprise, considering the wealth of data available.[1]

[1] Since completing this paper the author has drawn a geostrophic cross-section down the Greenwich meridian (Met. Mag. Dec. 1951). This cross-section is in substantial agreement with the conclusions advanced here.

Indications point to the structure of the mean circulation near the zero meridian differing appreciably from that found over N. America, or Asia. Fig. 8 shows the mean contour difference (normalized) between Larkhill (latitude 52°) and Lerwick (60°) for the two year period 1948—49. While in a general way the vertical profile for the meridian of Greenwich resembles that found over N. America in corresponding latitudes, there are perceptible differences. The relation between geostrophic speed and decreasing pressure does not show such a close approach to linearity. Moreover, the jet height is closer to the 300 mb surface than to the 200 mb surface The jet speed for Larkhill-Lerwick is only about three times the 950 mb speed, the corresponding ratio over similar latitudes ni N. America being 6 or more.

Perhaps the most striking feature of the westerly circulation near the Greenwich meridian is its great *variability*, as constrasted with the relative steadiness of the flow over N. America. Monthly mean normalized contour height differences are plotted in fig. 8. They show a very wide scatter about the long-term average profile shape, with no significant seasonal variation. In fig. 6 we indicated the monthly 'scatter' of profile shape over the eastern U. S., and comparing the two figures it will be at once apparent that the scatter is altogether greater in the case of the British figures. The two dotted lines in fig. 8 indicate the envelopes of extreme scatter

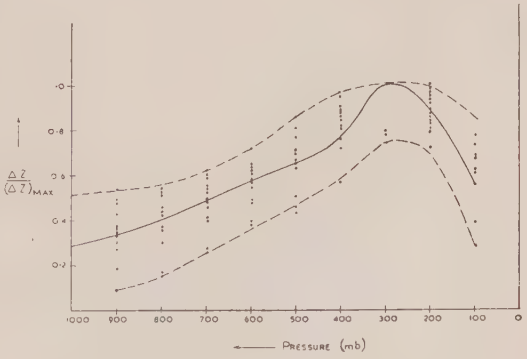

Fig. 8. The mean annual vertical wind profile for the Greenwich meridian (Larkhill—Lerwick). The points indicate the monthly scatter, the dotted lines, the extremes within which the profile-shape may lie.

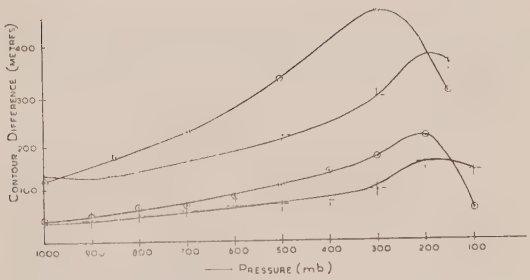

Fig. 9. S. Hemispheric mean vertical west wind profiles. Circles summer, stars winter. Upper set of curves, Macquarie Is.-Laverton, lower set Auckland—Taieri.

about the mean vertical profile of geostrophic wind. It is evident that in any 'extreme' month the profile shape may bear very little resemblance to its long-term mean. We may contrast the profile steadiness over N. America and over U.K. by saying that for 4 months of the year the mean monthly wind at, say, 500 mb will depart by more than 6½ % of the value predicted from the long-term mean profile-shape over N. America, but will depart by 25 % or more from the long-term value in the region of the U.K. In the U. S. it is possible to take the long-term mean profile as a good approximation to the actual monthly profile, but over U. K. this is no longer possible; the profile-shape is not quasi-invariant.

These facts demand further factual investigation. Why is the stability of mean westerly flow so strikingly different in different regions of the earth?

Riehl (1949) has conjectured that the observed stability in the structure of the Westerlies is due to lee effects of high geographical barriers. The westerly flow is notably uniform in geographical barriers. The westerly flow is notably uniform in lee of the Andes (Riehl) and of the Himalayas (Jeh). The quasi-invariance of the westerly flow-pattern over eastern N. America may similarly be attributed to the effects of the Rockies. This explanation would attribute the instability of the flow near the Greenwich meridian to the absence of a high barrier to westward, with a resulting absence of a quasi-stationary lee flow-pattern.

If this explanation were the correct one vertical profiles in the Southern Hemisphere, except in lee of the Andes, may be expected to display a structure similar to that found for the British Stations. In fig. 9 four southern hemisphere profiles are plotted. The top pair relate to summer and winter for the station-pair, Laverton (38° S, 145° E) and Macquarie Island (54° S, 159° E) (Loewe and Radok, 1950). The summer profile is indicated by the circled points. These profiles are more reminiscent of the U. K. than the U.S. profiles. The jet height is nearer the 300 mb level in summer, and the 200 mb level in winter. The ratio of jet speed to 950 mb speed is over 3 in summer and under 3 in winter, in agreement with the value of this ratio observed for Larkhill-Lerwick. One feature not observed in Northern Hemisphere data is that the geostrophic speed at jet level is higher in summer than in winter. This feature is reproduced also in the profiles for Auckland (37° S, 175° E) and Taieri (46° S, 170° E) (Hutchings 1950). The jet height for these two stations is closer to the 200 mb level both in summer and in winter. It will be borne in mind that the Southern profiles are based on very limited data — only one month of Macquarie Island data, and two months from Taieri. However, the profiles shows the same characteristics, although the data are limited, and refer to different times. There is a strong presumption for supposing the mean southern profiles to resemble closely those found in corresponding regions of the Northern Hemisphere.

On the Riehl hypothesis one would attribute the N. American type of vertical wind profile to the presence of an orographic barrier, and the U.K. type of profile to the absence of any barrier to westward. The facts presented here are certainly not inconsistent with such a presumption.

On the other hand, an alternative conjecture equally fits the facts. It might be postulated that the pattern of flow observed over N. America is typical of a continental region, while the U. K. type of profile is equally typical of an oceanic area.

Over a continent there is a considerable surface frictional drag, with a resultant conversion of westerly angular-momentum. I. this loss of A. M. is to be made good by high-level advection, it is reasonable to anticipate strong mean westerlies aloft, and a marked gradient of wind with height.

On the other hand, over an oceanic region the A. M. depletion at the surface is less for a given pressure gradient, and a smaller turn-round of westerly momentum at height will be required to make good the losses. Hence a smaller increase in westerly wind with height will suffice to maintain a steady state.

Of great interest is the apparent unsteadiness of the oceanic circulation, as manifested by the variability of the monthly mean profiles near the Greenwich meridian. A more intensive study of oceanic profiles is necessary if we are to establish the nature of this instability, and its implications for the global balance.

The unsteadiness of the mean profile over Oceanic regions may be a reflection of the actual variability of wind, associated with the frequency of migrating disturbances. BROOKS and CO-WORKERS (1950) have published world maps of standard vector wind deviation for levels between 700 mb and 130 mb. In these charts the global pattern is clear, a maximum variability over the oceans in middle latitudes, and minima over the continents.

Minima are found, at all levels throughout the year, to be associated with the Himalayas, Andes and Rockies. The African minimum shows a decided preference for the highest ground from Tanganyika to Abyssinia. A trough connected with the European Alps is also in evidence up to 500 mb.

This might be taken as evidence favouring Riehl's hypothesis, although it may be difficult to show why the presence of perturbations in the mean flow should affect the stability of the flow itself. Nevertheless, there seems to be a distinct association between wind variability and the year to year variability in mean flow.

REFERENCES

BROOKS, C. E. P., DURST, C. S., CARRUTHERS, N., DEWAR, D., SAWYER, J. S., (1950): Upper Winds over the World. *Geophys. Mems.*, **85**, M. O. London.

CHAUDHURY, A. M., 1950: On the vertical distribution of wind and temperature over Indo-Pakistan along meridian 76° E. in winter. *Tellus* **2**, 1, 56—62.

HESS, S. L., 1948: Some new mean meridional cross-sections through the atmosphere. *J. Met.* **5**, 293—400.

HUTCHINGS, J. W., 1950: A meridional atmospheric cross-section for an oceanic region. *J. Met.* **7**, 94—100.

JAMES, R. W The vertical Structure of Wind and Pressure Fields. Hitherto unpublished.

LOEWE, F. and RADOK, U., 1950: A meridional aerological cross-section in the southwest Pacific. *J. Met.* **7**, 58—65.

RIEHL, H., 1949: Effect of Andes Mountains. *Bull. Am. Met. Soc.* **30**, 9, p. 330.

YEH, T-C., 1950: The circulation of the high troposphere over China in the winter of 1945—46. *Tellus* **2**, 3, 173—183.

Dynamical Aspects of the General Circulation and the Stability of Zonal Flow

By HSIAO-LAN KUO, Massachusetts Institute of Technology[1]

(Manuscript received 4 Sept. 1951)

Abstract

From solutions of the linearized vorticity equation applied to systems with a variable basic zonal current, it is shown that the effect of damped disturbances is to feed energy into the zonal flow and transfer angular momentum from zones of easterlies into zones of westerlies, thereby strengthening the zonal circulation of the atmosphere. Amplifying disturbances withdraw energy from the zonal flow and transfer angular momentum from zones of westerlies into zones of easterlies, thereby weakening the strong zonal circulation and transforming it into cellular vortex motions. Thus the migratory cyclones and anticyclones are necessary elements for developing and maintaining the zonal circulation, while, on the other hand, they also act occasionally as brakes on the general circulation, keeping it from growing indefinitely.

The neutral disturbance corresponding to a typical zonal wind profile in winter is investigated by numerical integration. The stream line pattern is found to be rather similar to a typical flow pattern in the upper troposphere during a period of little change, indicating that this flow pattern is associated with the nearly neutral or slightly damped oscillations.

1. Introduction

When the motions of the atmosphere have been smoothed by taking averages along the latitude circles and over longer periods to eliminate the transient irregularities, we obtain systems of zonal currents, the so called prevailing westerlies and easterlies, which represent the more prominent overall pattern of the general circulation. This zonal wind system is interrupted from time to time by the presence of disturbances, both in the westerlies and easterlies, the number of which is much greater at lower levels than at upper levels. One of the fundamental problems that has always confronted meteorologists is the explanation of the nature of the physical processes that take place in the general circulation and also in the secondary circulations associated with it. It is evident that a complete answer to this problem can be achieved only through many different approaches which take into account physical processes in the atmosphere, among which those maintaining the global balance of energy and of momentum for the zonal wind systems are fundamental.

The concept of the balance of angular momentum in the general circulation was used first by JEFFREYS (1926), who pointed out that the maintenance of the prevailing winds in a steady state against surface friction necessitates a transfer of westerly angular momentum from the zone of surface easterlies into the zone of westerlies. However, the prevailing zonal winds are by no means steady. They go through cycles of decay and rebuilding, in addition to the mean seasonal changes in

[1] The research resulting in this work has been sponsored in part by the Geophysical Research Directorate of the Air Force Cambridge Research Laboratories.

intensity and location. Statistical investigations have shown that the general circulation in middle latitudes tends to oscillate between extremes of strong and weak zonal motions, the time interval between consecutive maxima being of the order of magnitude of 4—6 weeks (ALLEN, 1940; WILLETT, 1947) Thus the study of the general circulation should not be restricted to the problem of maintaining the steady zonal winds against ground friction, but should also include the mechanisms for their growth and decay. However, it is most probable that the process that maintains the zonal winds is also responsible for their growth and decay and therefore the two problems can be studied simultaneously. But in view of the complexities of the natural process, we cannot expect to obtain a complete solution of the problem from any single set of equations; the physical processes themselves probably work through many different stages, so that a reasonable solution can only be achieved through many different steps. The purpose of this paper is to investigate some essential mechanisms pertaining to the overall atmospheric circulations, that are directly connected with the development of the zonal winds.

In the past, the mechanism of the general circulation which maintains the energy and momentum balances, has by and large been looked upon as consisting of a large-scale convective process, with ascending motions in lower latitudes and descending motions in higher latitudes, the development of a large zonal velocity being attributed to the action of the deflecting force of the earth's rotation. Recently the importance of the mean vertical motion for the maintenance of the zonal wind systems has been questioned by STARR (1948 a, 1949), who suggests that the horizontal energy and momentum transfer can be accounted for by the horizontal components of the general circulation and of the lesser circulations, or by the eddies with quasi-vertical axes. This idea has also been suggested by Rossby in his theory of horizontal mixing (1947, 1949). The investigations of WIDGER (1949), MINTZ (1949) and WHITE (1950) have substantially confirmed this point of view; therefore the possibility of the existence of mean meridional circulations will be disregarded in this study.

In the atmosphere the zonal wind systems are most clearly defined above about 5 kms. Above this level, especially around the level of the tropopause where the maximum of the meridional momentum transfer occurs, the transfer of heat (WHITE, 1950) is relatively of little importance and the motion of the air is controlled largely by the equation of vorticity about the vertical and the continuity equation. Below this level, the heat supply and heat transfer must play an important role and the instability of this layer, which can be inferred from the presence of the large number of disturbances there, is probably associated with these factors, although the exact nature of this instability is still not very clear to us. This type of instability has been discussed by CHARNEY (1947) EADY (1949) JAW (1946) and BERSON (1949). On the other hand, in the upper troposphere and lower stratosphere, the atmosphere generally moves with a persistent flow pattern, indicating that it is in a relatively stable state, while very unstable conditions happen only occasionally (for example, the formation of cut-off lows and highs). Since in this study we are mainly concerned with the processes which govern the maintenance and development of the zonal wind system, it is sufficient if we restrict the investigation to those processes which are prominent in the upper part of the troposphere, assuming the existence and not concerning ourselves with the origin of disturbances in this field. We shall thus divide the atmosphere roughly into two layers and study the motions within the upper layer only. However, this partition into two layers is taken only as a convenient means of analysis rather than a real barrier for transfer from one region to the other. Energy can be received from the lower layer through irregular disturbances, and can also be given by the upper to the lower layer on some occasions. Thus there is a mechanism in replenishing the kinetic energy of the upper system, even though we treat it as barotropic. In this way, we consider the lower layer merely as a source or sink of disturbances for the upper layer, and the divergence and vertical motion as a means of communication between these two layers.

In order to separate the divergence effect from the overall processes, we shall assume that it takes place intermittently within some

specific time intervals, so that after some disturbances have been produced in the upper layer, the subsequent motions are horizontal nondivergent and therefore governed by the simple vorticity equation without divergence. In this way, the most important problems concerning the dynamics of the upper atmosphere can be discussed by the solutions of the simple vorticity equation. It can be shown by integrating the equations with respect to the mass distribution along the vertical that the mean motion of the whole atmosphere can also be approximately described by this two-dimensional barotropic model. Therefore the results obtained may also be considered to represent the mean motion.

Since there is no other energy source in this simplified model, the total kinetic energy must remain constant during the time under consideration. Thus any change of the kinetic energy of the mean zonal flow must come from the kinetic energy of the disturbances, and the study amounts to an investigation of the interactions between the lesser circulations and the zonal wind systems. In the following, the method of harmonic perturbations (both in x and in time t) will be adopted. The problem is therefore reduced to the discussion of the stability of the zonal wind profiles with respect to the disturbances. Here the term "Stability" is defined according to the reactions of the disturbances to the zonal wind systems in the horizontal plane. In this respect three kinds of disturbances can be distinguished: the disturbances which withdraw kinetic energy from the mean zonal flow are said to be *amplified*, those which supply kinetic energy to the mean zonal flow are said to be *damped* and those which neither give nor take energy from the mean zonal flow are *neutral*. Since this study is not aimed at explaining the origin of the disturbances (although it may help to explain the development of some large disturbances), these disturbances are taken to have been added to the upper layer from below. It then becomes physically feasible to discuss the different effects produced by damped as well as amplified disturbances. We shall demonstrate later that one of the effects is to transfer westerly angular momentum from the belts of slower zonal flow into belts of stronger zonal flow, therefore to strengthen the prevailing zonal winds and to overcome the frictional effects, although the disturbances themselves carry no resultant momentum. On the other hand, the amplified disturbances take kinetic energy from the main flow and transfer zonal momentum away from the zone of strong westerlies. Thus it appears that the zonal mean motion is not merely a statistical result of these irregular disturbances, as is frequently stated in descriptive studies of the general circulation. Rather the general circulation is built up and regulated by the disturbances (migratory cyclones and anticyclones). Its growth and decay are closely connected with the activity and development of the disturbances and these in return are connected with the stability of the zonal flow.

2. The rates of change of the mean zonal velocity and kinetic energy

The equations of motion over a spherical earth for horizontal and frictionless flow may be written

$$\frac{\partial u}{\partial t} - Zv = -\frac{1}{\varrho}\frac{\partial p}{a\cos\Phi\partial\lambda} - \frac{1}{2}\frac{\partial v_h^2}{a\cos\Phi\partial\lambda} \tag{1a}$$

$$\frac{\partial v}{\partial t} + Zu = -\frac{1}{\varrho}\frac{\partial p}{a\partial\Phi} - \frac{1}{2}\frac{\partial v_h^2}{a\partial\Phi} \tag{1b}$$

where $Z = f + \zeta = 2\omega \sin \Phi + \frac{1}{a\cos\Phi}\left[\frac{\partial v}{\partial\lambda} - \frac{\partial u\cos\Phi}{\partial\Phi}\right]$ is the vertical component of the absolute vorticity, hereafter referred to simply as the absolute vorticity, ζ the relative vorticity, u and v the zonal and meridional components of the horizontal velocity, $v_h^2 = u^2 + v^2$, ϱ the density, p the pressure, a the mean radius of the earth, and λ and Φ are the longitude and latitude respectively.

As only large-scale motions connected with the general circulation will be discussed, all quantities may be averaged along latitude circles. Thus the velocity components and vorticity can be written as $u = \bar{u} + u'$, $v = \bar{v} + v'$, and $Z = \bar{Z} + \zeta'$. Here the bars denote average values defined as $\bar{u} = (2\pi)^{-1}\int_0^{2\pi} u d\lambda$, and u', v', ζ' are the departures from the average values, which can also be taken as representing a perturbation. The motion is assumed to be

purely horizontal and nondivergent within the time interval under consideration. This implies $\int_0^{2\pi} v\,d\lambda = 2\pi\bar{v} = 0$. In this respect the motion is similar to a geostrophic velocity field. Since the effect of the variation of the density ϱ in x-direction is small, ϱ will be taken as constant unless otherwise stated. The above condition then means that there is no net mass transport across the latitude circle at that level. If the motion at this level is representative of the mean atmospheric flow, this is equivalent to the condition

$$\int_0^{\infty}\int_0^{2\pi} \varrho v \cos\Phi\, d\lambda\, dz = 0.$$

When equation (1a) is integrated along the latitude circle and use is made of the nondivergent assumption, we find that the rate of change of the mean zonal velocity is given by

$$\frac{\partial u}{\partial t} = \frac{1}{2\pi}\int_0^{2\pi} v\zeta\, d\lambda = -\int_0^{2\pi} \frac{\partial(uv\cos^2\Phi)}{2\pi a\cos^2\Phi\partial\Phi}\, d\lambda =$$

$$= \frac{1}{a\cos^2\Phi\,\varrho}\,\frac{\partial\tau}{\partial\Phi} \qquad (2)$$

where $-2\pi a^2\tau = \int_0^{2\pi} a^2\cos^2\Phi\varrho uv\,d\lambda =$ $= 2\pi a^2\overline{\varrho uv}\cos^2\Phi$ represents the total northward transfer of angular momentum across the latitude circle. When the convergence of meridians is neglected, linear momentum can be used and $\tau = -\overline{\varrho uv}$. Thus the time rate of change of the mean zonal momentum in the narrow zone contained between the latitudes Φ and $\Phi + \delta\Phi$ is proportional to the net inward transport of angular momentum into this zone, namely $\partial\tau/a\cos^2\Phi\partial\Phi$, or alternatively to the northward transport of vorticity.

In discussing the development of the general circulation it is useful to consider also the time rate of change of the kinetic energy of the mean zonal flow. This may be dealt with quite generally as follows. Multiplying the general momentum equation in the zonal direction (obtained by combining the first equation of motion and the continuity equation, both in three-dimensional forms) by the mean zonal velocity $\bar{u}$ and integrating over the whole volume Σ of air contained between the two latitude surfaces $\Phi = \Phi_1$, and $\Phi = \Phi_2$, we get

$$\frac{\partial\bar{E}_x}{\partial t} = \frac{1}{2}\int_\Sigma \frac{\partial\varrho\bar{u}^2}{\partial t}\, d\Sigma = -$$

$$-2\pi a^2\iint\left[\bar{\dot{\lambda}}\,\frac{\partial(\overline{\varrho uv}\cos^2\Phi)}{\partial\Phi} + \right.$$

$$\left. + \bar{u}\cos\Phi\,\frac{\partial(\overline{\varrho uw})}{\partial z} - f\bar{u}\overline{\varrho v}\cos\Phi\right] d\Phi\, dz =$$

$$= \int_\Sigma\left[\overline{\varrho u'v'}\cos\Phi\,\frac{\partial\bar{\lambda}}{\partial\Phi} + \overline{\varrho u'w'}\,\frac{\partial\bar{u}}{\partial z}\right] d\Sigma +$$

$$+ \int_\Sigma\left[\left(f + \cos\Phi\,\frac{\partial\bar{\dot{\lambda}}}{\partial\Phi}\right)\overline{\varrho v}\bar{u} + \right.$$

$$\left. + \overline{\varrho w}\bar{u}\,\frac{\partial\bar{u}}{\partial z}\right] d\Sigma + \int\overline{\varrho uv}_n\bar{u}\,dS \qquad (3)$$

Here it is assumed that the variation of ϱ with longitude and with time are both small and have been neglected. Equation (3) shows that the kinetic energy of the mean zonal flow can change by a conversion from the kinetic energy of the eddy motions, an inflow of this energy through the boundaries, and possibly by the presence of a mean meridional cell. The pressure force does not occur in this equation, therefore this energy cannot be produced directly by the pressure force.

The significance of this equation for the study of the maintenance and development of the mean zonal winds has been discussed by the writer elsewhere (Kuo, 1951). It has been shown that only the horizontal eddy stress $\overline{u'v'}$ and the mean meridional motion can serve as sources of kinetic energy of the mean zonal flow, and that the term $\overline{\varrho u'v'}\cos\Phi\,\frac{\partial\bar{\dot{\lambda}}}{\partial\Phi}$ in the last member of this equation is of the right order of magnitude and sign to account for the total frictional loss. We shall therefore restrict our investigations merely to this effect, which can be discussed adequately by using our simplified model.

Since the production of the total kinetic energy is also of paramount importance in understanding the physical processes, we may also write down the equation for the time

rate of change of the total kinetic energy of the horizontal motion:

$$\frac{1}{2}\frac{\partial \varrho v_h^2}{\partial t} = -\nabla\cdot\left[p\vec{v}_h + \frac{1}{2}\varrho v_h^2\vec{v}_h\right] + p\nabla\cdot\vec{v}_h - \frac{\partial}{\partial z}\left(\frac{\varrho}{2}v_h^2 w\right) \qquad (4)$$

where $\nabla\cdot$ denotes the horizontal divergence. The significances of the different terms have been discussed by Starr (1948 b). It may be noted that the pressure force is certainly a source for the total kinetic energy although not for the mean zonal kinetic energy, hence it may be concluded that its effect is to produce eddy and meridional motions.

Suppose we now integrate equation (4) over the whole region Σ bounded by two latitude surfaces along which $v = 0$, the earth's surface where $w = 0$ and the top of the atmosphere where $\varrho v_h^2 w = 0$ and the motion is assumed to be nondivergent, then all the terms on the right disappear. The equation then expresses the constancy of the total kinetic energy for the entire region. Suppose now the complete motion is divided into a mean zonal flow $\bar{u} = (2\pi)^{-1}\int_0^{2\pi} u\,d\lambda$ and a perturbation u', v' and denote the kinetic energy of the horizontal perturbation in Σ by E' then we find by making use of (2) and (4) that

$$\frac{\partial E'}{\partial t} = \frac{1}{2}\iint\frac{\partial}{\partial t}[\varrho(u'^2+v'^2)]\,a^2\cos\Phi\,d\lambda\,d\Phi =$$

$$= -\frac{\partial \bar{E}_x}{\partial t} = -a^2\iint\varrho\bar{u}\frac{\partial\bar{u}}{\partial t}\cos\Phi\,d\lambda\,d\Phi =$$

$$= 2\pi a^2\int_{\Phi_1}^{\Phi_2}\tau\frac{\partial\dot{\lambda}_0}{\partial\Phi}\,d\Phi \qquad (5)$$

where the integration along z has been omitted and where $\dot{\lambda}_0$ denotes the initial value of $\bar{u}/a\cos\varphi$. The same equation can be obtained from (3). It should be pointed out that equation (5) is applicable only when the entire region is considered. For any particular region or a small belt, the transport of kinetic energy through the boundaries must be taken into consideration and therefore we must use equation (4).

3. The perturbation equations and boundary conditions

In the upper troposphere and lower stratosphere, the large-scale motions are to a large extent horizontal, nondivergent and barotropic, we therefore assume that this motion may be described by the vorticity equation and the equation of continuity. Because of the difficulty of finding general solution of non-linear partial differential equation, the vorticity equation will be linearised and it then becomes

$$\left(\frac{\partial}{\partial t} + \dot{\lambda}_0\frac{\partial}{\partial\lambda}\right)\zeta' + \frac{v'}{a}\frac{dZ_0}{d\Phi} = \nu\nabla^2\zeta' \qquad (6)$$

where u_0 is the basic current depending upon Φ only, Z_0 is the absolute vorticity of the basic current, ν is the kinematic viscosity. The suffix zero occuring in $\dot{\lambda}_0$ and z_0 denotes initial values of $\dot{\lambda} = \bar{u}/a\cos\Phi$ and $\bar{Z}$. This equation will be used to investigate the changes from the initial state. The frictional term on the right is generally small and can be neglected except as discussed below. Since the motion is assumed nondivergent, the continuity equation takes the form

$$\nabla\cdot\vec{v}_h = \frac{1}{a\cos\Phi}\left[\frac{\partial u'}{\partial\lambda} + \frac{\partial(v'\cos\Phi)}{\partial\Phi}\right] = 0 \qquad (7)$$

and a stream function Ψ for the perturbation velocities may be introduced, defined by

$$\frac{v'}{a}\cos\Phi = \frac{\partial\Psi}{\partial\lambda},\quad \frac{u'}{a} = \dot{\lambda}\cos\Phi = -\frac{\partial\Psi}{\partial\Phi} \qquad (8)$$

where the dots indicate time derivatives. In terms of this stream function, the relative vorticity ζ' of the perturbation is given by

$$\cos^2\Phi\,\zeta' = \frac{\partial^2\Psi}{\partial\lambda^2} + \frac{\partial^2\Psi}{\partial\gamma^2} \quad \text{where} \quad \gamma = \log(\tan\Phi + \sec\Phi).$$

The perturbation stream function can be represented by the sum of a number of elementary independent harmonics of the form

$$\Psi = \Psi(\gamma)\,e^{in(\lambda-\mu t)} \qquad (9)$$

where n is the wave number around the globe and μ may be complex, $\mu = \mu_r + i\mu_i$; μ_r represents the angular phase velocity and $n\mu_i$ the amplifying factor of the particular harmonic disturbance. When (9) is substituted in the linearised vorticity equation (6) we find

$$(\dot{\lambda}_0 - \mu)(\Psi'' - n^2\Psi) + \frac{dZ_0}{dy}\Psi = \\ = -i\nu n^{-1}[\Psi^{iv} - 2n^2\Psi'' + n^4\Psi] \quad (10)$$

where the primes denote differentiation with respect to y. This equation must be satisfied by all the component harmonic perturbations. Since ν is extremely small in the atmosphere, the terms on the right-hand side of (10) can generally be neglected. In this case we get the nonviscous differential equation

$$(\dot{\lambda}_0 - \mu)\left(\frac{d^2\Psi}{dy^2} - n^2\Psi\right) - \frac{dZ_0}{dy}\Psi = 0 \quad (11)$$

However, it should be pointed out that if the frictional term is neglected entirely in the vorticity equation (6), then no distinction can be drawn between amplified and damped disturbances, since either the harmonic factor $e^{in(\lambda-\mu t)}$ or $e^{-in(\lambda-\mu t)}$ will give the same differential equation (11). Therefore we must take (11) as the limit of (10) with ν extremely small, with the necessary corrections for its solutions in the vicinity of the singular points where $\mu_r = \dot{\lambda}_0$.

The general solution of (11) for each harmonic contains two arbitrary constants. No specific information can be obtained without imposing some restrictions on their values. The necessary restrictions are the boundary conditions that must be satisfied by each harmonic. In the atmosphere, the only natural horizontal boundary conditions are those needed to make the perturbations finite at every point, therefore Ψ and $d\Psi/dy$ must be equal to zero at the two poles. However, since the motion over the southern hemisphere is generally unknown to us, our discussion is necessarily restricted to the northern hemisphere. It therefore appears best to introduce the equator as a line of symmetry, and disregard all the seasonal variations. Thus we may use the following different set of boundary conditions under different circumstances: (a) $\Psi = 0$ at the pole, which must be satisfied, and either $d\Psi/dy = 0$ (symmetric) or $\Psi = 0$ (antisymmetric) at the equator. Each of these conditions will give a zero momentum transfer ($\tau = 0$) at the equator. In addition to the study of the hemisphere as a whole, we may consider a perturbation confined to a smaller belt. For this case, we use (a) $\Psi = 0$ along two latitude circles. Although these boundaries are rather arbitrary, it might be of interest for example to examine the belt within the subtropics which separates the easterlies from the westerlies. It may be noted that τ, defined in (2), vanishes at the boundaries.

By applying one boundary condition to the general solution of the particular harmonic, one of the two arbitrary constants can be eliminated, while the other boundary condition enables us to determine the permissible value of μ for any given n or conversely. Therefore the total perturbation stream function is given by

$$\Phi(t, \lambda, y) = \Sigma c_j \Psi_j(y) e^{in_j(\lambda - \mu_j t)} \quad (12a)$$

where the arbitrary constants c_j are determined by the initial disturbances

$$\Phi(o, \lambda, y) = \Sigma c_j \Psi_j(y) e^{in_j\lambda} \quad (12b)$$

Thus, the harmonics that are present at any moment correspond to those present at the initial moment and the solution is unique. When every component disturbance is known, then (12a) can be used to forecast the velocity field. But at the present, we can only discuss the general properties of the individual harmonic components as related to the profile of the basic zonal currents.

4. The solutions of the vorticity equation and the nature of the disturbances

The solution of equation (11) has been discussed by the author in a previous study (Kuo, 1949) for the motion over an infinite plane or a cylindrical earth, in which the coriolis parameter was taken as a linear function of Φ and the profile of the basic current symmetrical. Though the results obtained there are still generally valid for the motion over spherical earth and for asymmetrical profiles, certain

modifications are unavoidable and consequently we shall now discuss the problem further.

Equation (11) shows that if the phase velocity μ lies within the range of values of $\dot{\lambda}_0$, the point $y = y_s$ where $\mu = \dot{\lambda}_0$ is a singular point of the equation.[1] The solutions show certain peculiarities around this point and require careful examination. These questions do not exist for those disturbances whose phase velocity is distinct from the velocity of the basic current. It is therefore necessary to divide the disturbances according to their velocities of propagation into three groups: (a) those propagating faster than the maximum velocity max. $\dot{\lambda}_0$ of the basic current, (b) those travelling slower than the minimum basic current min. $\dot{\lambda}_0$, and (c) those propagating with a velocity within these two limits.

The disturbances in the groups (a) and (b) will be discussed very briefly. It can be shown, by writing $\frac{dZ_0}{dy} = h - d^2\dot{\lambda}_0/dy^2$ (where $h = 2(\omega + \dot{\lambda}_0)\sec h^2 y + 2\tanh y\, d\dot{\lambda}_0/dy$ corresponding to β for motion in a plane) and employing Sturm's oscillation theorem, that under the conditions existing in the atmosphere ($h > 0$ generally) there can be no neutral disturbance in (a). That is to say, in general, no neutral disturbance that is governed by the simple vorticity equation will travel faster than the maximum velocity of the basic flow in middle latitude westerlies and equatorial easterlies. On the other hand, there always exist neutral disturbances in group (b), since $h(\mu - \dot{\lambda}_0)^{-1}$ is then negative (see KUO, 1949).

Now let us examine the possibility of having amplified or damped disturbances in these two groups. If μ is complex, Ψ must also be complex, $\Psi = \Psi_r + i\Psi_i$. Thus, when equation (11) is multiplied by the conjugate function $\Psi^\star = \Psi_r - i\Psi_i$, we get by separating the real and imaginary parts:

$$\frac{d}{dy}\left[\Psi_i \frac{d\Psi_r}{dy} - \Psi_r \frac{d\Psi_i}{dy}\right] \equiv \frac{dW}{dy} = g_2 \frac{dZ_0}{dy} |\Psi|^2 \qquad (13a)$$

[1] Suffix S will always refer to the value of a function at the singular point $y = y_s$.

$$\frac{d}{dy}\left[\Psi_r \frac{d\Psi_r}{dy} + \Psi_i \frac{d\Psi_i}{dy}\right] = \left|\frac{d\Psi}{dy}\right|^2 + \left(n^2 - g_1 \frac{dZ_0}{dy}\right)|\Psi|^2 \qquad (13b)$$

where W is the Wronskian of Ψ_r and Ψ_i, $W = \Psi_i \frac{d\Psi_r}{dy} - \Psi_r \frac{d\Psi_i}{dy}$, and $g_1 = (\dot{\lambda}_0 - \mu_r)|\dot{\lambda}_0 - \mu|^{-2}$, $g_2 = \mu_i |\dot{\lambda}_0 - \mu|^{-2}$. Equation (13b), when integrated from one boundary to the other, determines the phase velocity. When (13a) is integrated from one boundary to the other we find

$$W_2 - W_1 = \int_{y_1}^{y_2} g_2 \frac{dZ_0}{dy} |\Psi|^2 dy \qquad (14)$$

which shows that a necessary condition for having a complex μ, or $g_2 \neq 0$, is to have $\frac{dZ_0}{dy}$ change its sign somewhere within the region, since the boundary conditions require both W_1 and W_2 to be zero. This condition holds both for the amplified and damped disturbances in the groups (a) and (b), since there is no singular point for these perturbations.

In the atmosphere, the absolute vorticity Z_0 is largely determined by the coriolis parameter and therefore increases with latitude over most of the hemisphere. From (13 b) it can be seen that under this condition there is no disturbance at all in group (a) and only neutral disturbances in group (b). Rossby's long waves are examples of these neutral disturbances.

Group (c). This group includes nearly all the wave disturbances actually observed in the atmosphere, which travel with phase velocities within the range of velocities of the basic current, min. $\dot{\lambda}_0 \leqslant \mu_r <$ max. $\dot{\lambda}_0$. For these disturbances, the points y_s where $\mu = \dot{\lambda}_0$ are singular points of (11). (For the jet stream profiles, there are generally two singular points for every value of μ, one on each side of the jet). Only one solution of the equation (11) is regular at this point, while the second involves a term with the factor $\log(y - y_s)$ (KUO, 1949), and therefore is many-valued. Since the motion cannot be many-valued, the change of the value of ψ in passing from the

negative to the positive side of y_s must be determined properly, by finding the path of continuation around y_s. This is obtained by considering the solutions of (11) as the limits of the asymptotic solutions of (10) with a very small coefficient of viscosity. Is has been shown by many investigators (e.g., LIN, 1945; WASOW, 1947; KUO 1949) that this continuation must be taken along a path below the singular point $y(s_1)$ where $d\lambda_0/dy$ is positive and above the singular point $y(s_2)$ where $d\lambda_0/dy$ is negative. Therefore, the solutions should be taken as

$$\Psi_1 = \eta + a_2\eta^2 \quad \ldots \tag{15a}$$

$$\left.\begin{aligned} \Psi_2 &= 1 + b_2\eta^2 + \ldots + G_s\Psi_1 \log \eta \qquad \text{for } \eta > 0 \\ \Psi_2 &= 1 + b_2\eta^2 + \ldots + G_s\Psi_1(\log|\eta| - \pi i) \quad \text{for } \eta < 0 \end{aligned}\right\} \tag{15b}$$

where

$$\eta = y - y_s \text{ and } G_s = -\left(\frac{d\lambda_0}{dy}\right)_s^{-1}\left(\frac{dZ_0}{dy}\right)_s = 2a_2.$$

However, according to LIN (1945) and WASOW (1947), the set of solutions are not valid within a small region around the singular point for the damped disturbances. This means that although the neutral and amplified disturbances can be discussed by employing the inviscid vorticity equation (11), some other effects need be considered within the small region around the singular points in discussing the damped disturbances. This point becomes clear in the case when the absolute vorticity Z_0 is a monotone increasing function of y.

With this in mind, we can use the solutions (15). According to the two expressions of Ψ_2 on the two sides of y_s, there is a change of the value of $\dfrac{d\Psi}{dy}$ from $y_s - \varepsilon$ to $y_s + \varepsilon$, given by

$$\left(\frac{d\Psi}{dy}\right)_{y=y_s+\varepsilon} - \left(\frac{d\Psi}{dy}\right)_{y=y_s-\varepsilon} = -\Psi_s\left|\frac{d\lambda_0}{dy}\right|_s^{-1}\left(\frac{dZ_0}{dy}\right)_s \pi i \tag{16}$$

There is, therefore, a rapid change in u' across a singular point if $\left(\dfrac{dZ_0}{dy}\right)_s$ is not zero and ε very small.

Now we may proceed to discuss the stability of the zonal winds for the disturbances in group (c). Since the inviscid vorticity equation (11) is valid for all real y when $\mu_i > 0$, a necessary condition for the existence of amplifying disturbances, as can be seen from (14), is that dZ_0/dy should change its sign somewhere in the region, the same as for the disturbances in the groups (a) and (b). Unlike the disturbances in the groups (a) and (b), this condition is not necessary for damped disturbances, because equation (11) and its solution are not valid for some parts of the real y axis.

The same condition is also necessary for the existence of neutral disturbances in this group. This has been proved in the previous study by the writer (KUO, 1949) by considering the jump of the Wronskian across the singular point, given by

$$W(y_s + \varepsilon) - W(y_s - \varepsilon) = = u\left(\frac{dZ_0}{dy}\right)_s\left|\frac{d\lambda_0}{dy}\right|^{-1}|\Psi_s|^2 \tag{17}$$

Since for neutral disturbances both Ψ_r and Ψ_i must be solutions of equation (11), the variation of W is zero at all points except the singular points where there are jumps given by (17). As W is zero at the two boundaries, the sum of these jumps must be zero. For the symmetric jet profiles the values of the two jumps are the same; therefore each must be zero. Thus either $\left(\dfrac{dZ}{dy}\right)_s$ or Ψ_s must be zero. The impossibility of the latter has been proved by the writer (KUO, 1949) by the method of comparison, which can also be used for other profiles. It can also be proved by employing the expression (13b). Thus dZ_0/dy must change its sign and go to zero in the region. Also dZ_0/dy must be zero at the singular point for symmetrical jets; that is to say, this neutral disturbance travels with the velocity of the basic current $\lambda_0(c)$ at the critical point[2] (the point where $\dfrac{dZ_0}{dy} = 0$). This is also true for the unsymmetrical jets when the value of λ_0 is the same at the two critical points.

[2] Suffix c will always refer to the value of a function at the critical point $y = y(c)$.

For unsymmetrical jets in which the values of $\dot{\lambda}_0$ at the two critical points $y(c_1)$ and $y(c_2)$ are not the same, the condition that the total jump of W must vanish requires $\left(\frac{dZ_0}{dy}\right)_{s1}$ and $\left(\frac{dZ_0}{dy}\right)_{s2}$ to have opposite signs, which assumes the vanishing of dZ_0/dy somewhere in the region. This neutral disturbance travels with a phase velocity between the two values of $\dot{\lambda}_0$ at the two critical points, as has been proved by FOOTE and LIN (1950).

It has thus been shown that a necessary condition for the existence of amplifying disturbances is that dZ_0/dy should equal zero somewhere in the region and change its sign. The same condition is also necessary for the existence of neutral disturbances in group (c) and of damped disturbances in the two groups (a) and (b), but it is not necessary for damped disturbances in group (c).

5. Equations of angular momentum transfer, energy exchange and the stability of zonal flow

The relation between the meridional transport of angular momentum and the stability of the zonal flow has been discussed by the writer in a previous investigation (KUO, 1949). While the results obtained there are correct for the particular profile studied, they need some modifications and elaborations. The same problem has also been discussed by MACHTA (1949) and HASSANEIN (1949). These authors show that even with a constant basic current, some perturbations are able to produce a constant meridional transfer of momentum. However, these perturbations do not satisfy the boundary conditions of this paper, and furthermore, a constant momentum transfer without accumulation does not help the momentum budget, as can be seen from equation (2). Because of the importance of this momentum transfer and the energy exchange between the basic zonal current and the perturbations, they will be discussed in some detail in the following two sections.

The perturbation velocity components u' and v' can be expressed in terms of the stream function,

$$u' = -\left[\frac{d\Psi_r}{dy}\cos n\xi - \frac{d\Psi_i}{dy}\sin n\xi\right] e^{n\mu_i t}$$

and $v = -n[\Psi_r \sin n\xi + \Psi_i \cos n\xi] e^{n\mu_i t}$, where $\xi = \lambda - \mu_r t$ is the phase angle. From these expressions and by making use of equation (13a), the average northward angular momentum transfer across unit length of the latitude circle is found to be given by

$$\varrho\overline{u'v'}\cos^2\Phi = -\tau =$$

$$= \frac{1}{2}\varrho n\mu_i e^{2n\mu_i t}\int_{y_1}^{y}\frac{|\Psi|^2}{|\dot{\lambda}_0 - \mu|^2}\frac{dZ_0}{dy}\,dy \qquad (18)$$

This transfer can also be expressed in terms of the tilting of the troughs and ridges, defined as the curves along which the meridional velocity is zero. The location of the trough and ridge curves is determined by $\tan n\xi = -\Psi_i/\Psi_r$ and therefore the angle α which they make with the northerly direction is given by

$$|\Psi|^2 \tan\alpha = \Psi_r^2 \sec^2 n\xi \frac{d(n\xi)}{ady} = W =$$

$$= \mu_i \int_{y_1}^{y}\frac{|\Psi|^2}{|\dot{\lambda}_0 - \mu|^2}\frac{dZ_0}{dy}\,dy \qquad (19)$$

Since $|\Psi|^2$ is proportional to $\overline{v^2}$, we see that the angular momentum transfer given by equation (18) is proportional to the product of the mean kinetic energy of the perturbation and the tilting of the troughs and ridges.

The vorticity transport can either be obtained in the same way, or simply by differentiating (18) with respect to y. Thus we have

$$\overline{v'\zeta'} = \frac{1}{2\pi}\int_0^{2\pi} v'\zeta'\,d\lambda = \frac{dW}{dy} e^{2n\mu_i t} =$$

$$= -\frac{\mu_i}{|\dot{\lambda}_0 - \mu|^2}\frac{dZ_0}{dy}|\Psi|^2 \qquad (20)$$

This equation shows that the vorticity transfer produced by the damped disturbances is in the direction of increasing Z_0 while that produced by the amplifying disturbances is in the direction of decreasing Z_0, therefore it is

not always in the direction of the absolute vorticity gradient. When the zonal flow is stable, it actually is transported in the direction opposite to the gradient of vorticity, therefore has the effect of increasing this gradient; only a very unstable flow will result in a thorough mixing and a reduction of the existing vorticity gradient.

Substituting equation (18) into (2), we get the time rate of change of the mean zonal velocity:

$$\frac{\partial \bar{u}}{\partial t} = -\frac{n\mu_i}{2} e^{2n\mu_i t} \frac{dZ_0}{dy} \frac{|\Psi|^2}{|\dot{\lambda}_0 - \mu|^2} \tag{21}$$

It also follows that the effect of the damped disturbances is to produce an increase of $\bar{u}$ in the region where dZ_0/dy is positive and a decrease where dZ_0/dy is negative, thus their effect is to intensify the zonal flow. The effect of the amplifying disturbances is in the opposite direction, that is to flatten the jet-stream of westerlies and easterlies.

When the expression (18) for τ is substituted nto the energy equation (5), it becomes

$$\frac{\partial E'}{\partial t} = -a \int_{\Phi_1}^{\Phi_2} \dot{\lambda}_0 \frac{\partial \tau}{\partial \Phi} \partial \Phi =$$

$$= \frac{1}{2} \varrho n \mu_i e^{2n\mu_i t} \int_{\Phi_1}^{\Phi_2} \dot{\lambda}_0 \frac{|\Psi|^2}{|\dot{\lambda}_0 - \mu|^2} \frac{dZ_0}{d\Phi} d\Phi \tag{22}$$

From (22) it may be seen that if the perturbation kinetic energy is to increase ($\mu_i > 0$), then, besides the condititon that dZ_0/dy should change its sign somewhere in the region, we must also have positive dZ_0/dy associated with higher values of $\dot{\lambda}_0$ and negative dZ_0/dy with lower values of $\dot{\lambda}_0$. This may be considered as a second necessary condition for the occurrence of amplified disturbances and is equivalent to the condition given by FJÖRTOFT (1950). For the profile of a jet-stream of westerlies, this condition is automatically satisfied when dZ_0/dy changes its sign within the region. It is not necessarily satisfied however, for example, an easterly current around the equator can satisfy these requirements simultaneously only if the current is sufficiently strong.

It can now be shown that for the jet stream profiles, these two conditions are sufficient for the occurrence of amplified disturbances. That is to say, when they are fulfilled, equation (11) and the given boundary conditions actually permit solutions with a positive μ_i.

The existence of amplified disturbances for a symmetric jet stream velocity profile has been proved in a previous study (KUO, 1949) by applying the Sturm oscillation theorem. This is done by first establishing the existence of a neutral disturbance with $\mu_r = \dot{\lambda}_0(c)$. For the jet-type velocity profile in which the current velocities at the two critical points c_1 and c_2 are the same, and dZ_0/dy is positive in the central part and negative in the outer parts of the region, the ratio $[\dot{\lambda} - \dot{\lambda}(c)]^{-1} dZ_0/dy$ is always positive and finite. It follows that a neutral disturbance with $\mu = \lambda_0(c)$ exists, since the solutions of the equation

$$\frac{d^2\Psi_1}{dy^2} = \left[n^2 - \frac{\dfrac{dZ_0}{dy}}{\dot{\lambda}_0 - \dot{\lambda}_0(c)} \right] \Psi_1, \quad \Psi_1(0) = 0 \tag{23}$$

become oscillatory for sufficiently small values of n^2. When we investigate the eigen value $\mu = \mu_r + i\mu_i$ in the neighborhood of this eigen-value $\mu = \dot{\lambda}_0(c)$ we find that (KUO, 1949) if $\mu_r > \dot{\lambda}_0(c)$ then $\mu_i < 0$, and if $\mu_r < \dot{\lambda}_0(c)$, then $\mu_i > 0$. Hence the disturbances which are travelling with a phase velocity greater than the critical values $\dot{\lambda}_0(c)$ will be damped and those which are travelling with a phase velocity less than the critical value $\dot{\lambda}_0(c)$ will be amplified.

The existence of neutral and amplified disturbances for the profiles with $\dot{\lambda}_0(c_1)$ and $\dot{\lambda}_0(c_2)$ differing slightly from each other can be discussed by the argument used by FOOTE and LIN (1950). From the above discussions one can summarize the necessary and sufficient conditions for the existence of amplified and neutral disturbances (with $\mu_r = \dot{\lambda}_0$) as follows:

If dZ_0/dy equals zero and changes its sign somewhere in the region and if $\dfrac{dZ_0}{dy} > 0$ where $\dot{\lambda}_0$ is large and < 0 where $\dot{\lambda}_0$ is small, then amplified and neutral disturbances may exist.

A necessary and sufficient condition for the existence of damped disturbances is that $\frac{dZ_0}{dy}$ *is not identically zero in the entire region.*

In applying the equations (18) — (22) to the damped disturbances propagating with the current velocity of some point, it must be remembered however that the solution does not hold in the small region around the singular point. Since this interval is generally small, we can neglect the large fluctuations within it and just compute the change of τ across this interval from (17). Then equation (22) can also be used to discuss the damping effect. The dissipation of kinetic energy through friction within the narrow viscous strip can only increase this damping effect, and not reverse it.

6. Momentum and vorticity transfer and energy exchange for different velocity profiles

We shall next consider the meridional momentum and vorticity transfer and energy exchange between the perturbations and the mean flow for some typical profiles.

(a) *Jet-stream profile in which the values of* $\dot{\lambda}_0$ *at the two critical points are the same.*

Assume that there are two critical points $\left(\text{points where } \frac{dZ_0}{dy} = 0\right)$, $y(c_1)$ and $y(c_2)$, one

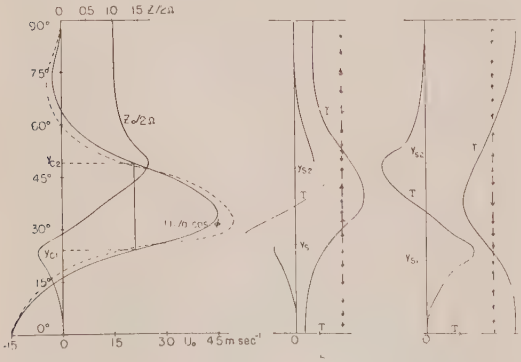

Fig. 1. (a) The mean zonal current and the mean absolute vorticity distributions. The dashed curve represents the mean zonal winds produced by damped disturbances at some later time. (b) Schematic orientation of the troughs and ridges (T) and the meridional distribution of the stress $\tau = -\overline{\varrho u' v'} \cos^2 \Phi$ for damped disturbances; the arrows indicate direction of vorticity transport. (c) Same as (b) for amplified disturbances.

to each side of the jet stream of westerlies. The profile must be such that Z_0 decreases with latitude in the outer parts of the region and increases in the central part, as is shown in fig. 1. For this profile, a neutral disturbance exists which propagates with the velocity $\dot{\lambda}_0(c)$, which has its troughs directed from north to south, which gives zero momentum transfer at all points, and which causes no energy exchange between the basic flow and the perturbation.

Now we discuss the damped disturbance which moves with a velocity only slightly greater than the critical velocity $\dot{\lambda}_0(c)$, and having singular points. The eddy stress τ (southward angular momentum transport) produced by this damped disturbance ($\mu_i < 0$) decreases slowly from zero at $y = y_1$ to a negative value up to the point $y(s_1) - \varepsilon$, according to equation (18); then it decreases rapidly across the singular point, corresponding to the change of W given by (17), up to $y(s_1) + \varepsilon$, since dZ_0/dy is positive at $y(s_1)$. Although the inviscid theory fails to be valid within the small belt 2ε around $y(s_1)$ we may approximate to the distribution of τ within this small interval by the dotted curve, as is indicated in fig. 1b. As the change of τ across this interval is known, its values at all other points where the inviscid theory holds can be computed from (18). Thus it increases from a negative value at $y(s_1) + \varepsilon$ to a positive value at $y(s_2) - \varepsilon$, where it has another rapid decrease up to $y(s_2) + \varepsilon$, and then decreases to zero as the other boundary is approached. The vorticity transfer is northward in the central region between $y(c_1)$ and $y(c_2)$ and southward in the outer regions, as denoted by the small arrows. The direction of the trough and ridge lines for these damped disturbances is represented by the curve T. It is seen that the troughs and ridges are oriented with their convex-side toward the east in the vicinity of the jet stream, and momentum is transferred from the outer parts into the central part, (from regions where the zonal current is small into the regions where it is great), therefore having the effect of intensifying the zonal currents. It is also seen that τ and the wind shear $\frac{d\dot{\lambda}_0}{dy}$ have opposite signs in most parts of the region;

therefore the damped disturbances supply their energy into the main zonal flow. The dashed curve in fig. 1a represents the zonal wind distribution produced by the damped disturbances at some later time.

For the amplifying disturbances, τ is given by (18) at every point. It increases from zero at $y=y_1$ to a positive value, has a higher rate of increase near the singular point, and attains its maximum value at $y(c_1)$, then decreases to a negative minimum value at $y(c_2)$, and increases to zero as the other boundary is approached, as is shown in fig. 1c. Thus positive τ is associated mainly with positive $d\dot{\lambda}_0/dy$ and negative τ with negative $d\dot{\lambda}_0/dy$, showing that the kinetic energy of the perturbation will increase with time. The vorticity transfer is in the opposite direction as produced by the damped disturbances. The trough lines and ridge lines are oriented with their convex side toward the west. There is a flow of angular momentum from the central part into the outer parts, with the effect of flattening the profile of the zonal motion.

For the disturbances without singular points ($\mu_r \neq \dot{\lambda}_0$), the general features of the distribution of τ and the orientation of the trough and ridge-lines are the same as have been discussed above.

The results obtained above agree with those obtained in a previous study (Kuo, 1949) for symmetric profiles and over a plane or a cylindrical earth. When the asymmetry is not great, the general conclusions obtained also hold for the profile with different values of $\dot{\lambda}_0$ at the two critical points. For this kind of profile, a constant momentum transport can be produced between the two critical points by a neutral disturbance as has been discussed by Foote and Lin (1950). However, no other effect on the mean zonal flow will be produced by this neutral disturbance except a gradual reduction of this difference of $\dot{\lambda}_0$ between the two critical points.

(b) *Jet is limited to middle latitudes while the vorticity distribution at higher and lower latitudes is dominated by the coriolis parameter.*

In the atmosphere, even when the westerlies are strong, and the absolute vorticity has a maximum to the north and a minimum to the south of the jet, the negative gradient of vorticity generally does not extend to the equator, but Z_0 attains a second weaker maximum at a lower latitude, showing the predominance of the effect of earth's rotation. This type of vorticity distribution, such as is represented in fig. 2, occurs much oftener than the case (a) and therefore deserves separate discussion.

In this case, there and four critical points in the zonal wind profile where dZ_0/dy vanishes, the two inner ones having higher values of $\dot{\lambda}_0$. If $\dot{\lambda}_0$ is the same at these two inner critical points, $y(c_2)$ and $y(c_3)$, a neutral disturbance will travel with this velocity. Another neutral disturbance corresponding to the two outer critical points may also exist.

For damped disturbances, the distribution of τ and the direction of the troughs and ridges are represented by the curves in fig. 2b. It starts from zero and increases to a maximum at $y(c_1)$, then decreases from $y(c_1)$ to $y(c_2)$. Assuming that this damped disturbance is travelling with a velocity greater than $\dot{\lambda}_0(c_2)$, so that $\left(\frac{dZ_0}{dy}\right)_{s1}$ is positive, then τ will have a sudden decrease across this singular point, and reach a large negative value at $y(s_1)+\varepsilon$. It increases from there to the point $y(s_2)-\varepsilon$, where it reaches a positive value, and then decreases rapidly across the singular point $y(s_2)$. It attains a small negative value as $y(c_4)$ is approached and increases to zero near the pole. It is seen that $\tau \dfrac{dZ_0}{dy}$ is mainly negative,

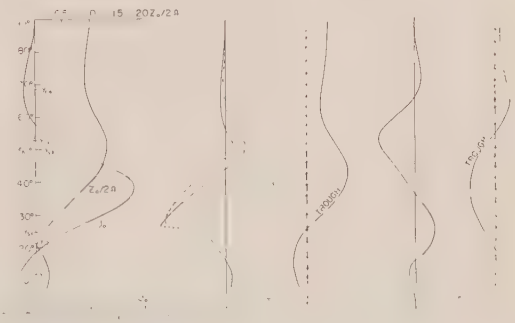

Fig. 2. Same as Fig. 1 for a weaker zonal wind profile.

therefore the total kinetic energy of the perturbation decreases with time, being fed into the zonal flow, at least in part. Also, angular momentum is transported into the central part of the zone of westerlies, strengthening the westerlies and also developing an easterly current north of the equator, thus gradually increasing the degree of instability. For this case, the troughs and ridges are tilted with their convex side toward the east in the zone of westerlies, but the direction is reversed in the equatorial belt and also near the pole.

For the amplifying disturbances, the distribution of τ is represented by the curve in fig. 2c. It is seen that $\tau\, d\dot{\lambda}_0/dy$ is mainly positive and has large values in the central part of the profile, so that the perturbation is withdrawing kinetic energy from the main flow. But in the outer parts, $\tau\, d\dot{\lambda}_0/dy$ is negative, so that the perturbation is also supplying kinetic energy into the main flow, strengthening the zonal flow in those parts, as can be seen from equation (22). Thus this case is relatively stable as compared with the case (a).

It should be pointed out that these discussions of the distribution of τ with respect to the zonal wind profile apply only to the individual situations. Because the jet-stream of westerlies fluctuate both in their latitudinal position and strength, and because different effects are produced by different kinds of disturbances, the distribution of the average values of τ for a longer period may differ considerably from that given by the corresponding mean profile.

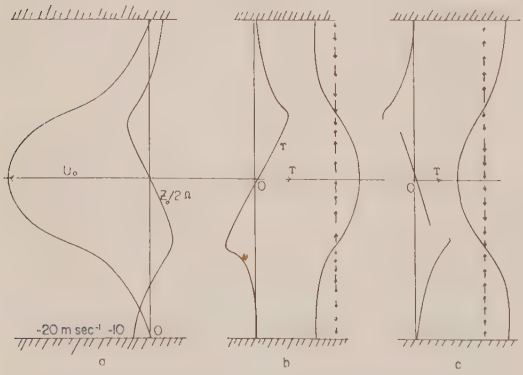

Fig. 3. Distribution of τ and vorticity transfer in the equatorial easterlies. (b) for amplified disturbances. (c) for damped disturbances.

(c) *Waves in the high level easterlies in equatorial belt*

Although there is no natural boundary between the high level westerlies in middle and higher latitudes and the high level easterlies in equatorial latitudes, different kinds of perturbations exist in these two regions. The disturbances in the westerlies move rather rapidly towards the east and are numerous, while in the easterlies there are relatively few large disturbances, and these generally move slowly towards the west or remain stationary. Therefore we may take the equatorial easterlies as a separate region.

The case when the easterly current is more concentrated in the equatorial belt and flat in the outer regions, with dZ_0/dy negative around the equator and positive in the outer parts will be discussed. According to the discussion in section 5, both damped and amplified disturbances can exist in this case. An examination of equation (18) shows that for amplified disturbances, τ is positive north of the equator and negative to the south, with the same sign as the shear of the basic current, as indicated in fig. 3b. This gives an increase of the perturbation kinetic energy. The trough and ridge lines for these amplifying disturbances are oriented with their convex side toward the east, contrary to that in the zone of westerlies. This tilting gives an equatorward flow of westerly momentum and will tend to flatten and possibly destroy the zonal flow pattern.

For damped disturbances with phase velocity within the range of $\dot{\lambda}_0$ in the belt, the distribution of τ is represented by the curve in fig. 3c, with the proper rapid change across the singular point. It is seen that τ is negative to the north and positive to the south of the equator, so that the perturbation kinetic energy will decrease. The troughs and ridges are tilted with their convex side toward the west, and momentum is transferred away from the equator, with the result that the easterly current is strengthened near the equator, increasing the degree of instability.

Besides these disturbances with μ_r within the range of $\dot{\lambda}_0$ in the belt, we might also have disturbances moving toward the west at a speed faster than the maximum easterly current.

The general features of the distribution of τ are the same as those described above.

(d) *When dZ_0/dy is positive in the entire region*

When the prevailing zonal winds are weak, the value of Z_0 is determined primarily by the coriolis parameter, therefore may increase with latitude over the entire hemisphere. According to the preceding discussions, this case is stable and cannot be disturbed spontaneously. The same conclusion may also be reached by applying the non-linearized vorticity equation $dZ_0/dt = 0$ (FJÖRTOFT, 1950; STARR, 1950; KUO, 1950). However, the linear theory also tells us that all possible neutral disturbances travel with phase velocity $\mu \leq \min. \dot{\lambda}_0$. Thus if any disturbance is added to the system and is moving with a velocity within the range of $\dot{\lambda}_0$, which is generally the case because added vorticity moves with the current, the motion cannot follow the law of conservation of absolute vorticity at every point, for some other effects necessarily enter into the problem (either viscosity or divergence), at least in some small regions. If we allow viscosity into the small region around the singular points, then damping effect will take place.

Although viscosity is important for these damped disturbances, its effect will be small outside the small strips around the singular points. Therefore the distribution of the stress τ is still given by equation (18) in these regions, and increases with latitude. Across the small strips around the singular points, τ has rapid decreases, attains a negative value at $y(s_2)+\varepsilon$, and goes to zero as the boundary $y=y_2$ is approached. Corresponding to these negative jumps of τ, the mean zonal current decreases within these strips. The mean vorticity decreases around $y(s_1)$ and increases around $y(s_2)$, indicating a tendency of creating a minimum and a maximum of $\overline{Z}$ along these latitudes respectively.

One physical explanation of this process is that high concentrations of vorticity are always present in the small-scale disturbances, which under the influence of the northward increase of Z, will result in a transport of cyclonic vorticity toward higher latitudes (KUO, 1950). The accumulative action of eddy viscosity near the singular points in spreading out the existing vorticity concentrations helps to build up extreme values of vorticity along these latitudes.

7. The neutral disturbances in the upper troposphere in winter

In order to compare the general results obtained above with actual flow patterns in the atmosphere, a solution of the perturbation equation for some normal zonal wind profile is desirable. Here the study will be restricted to the neutral disturbances which probably represent the flow pattern observed on the upper air weather charts during a period of relatively little change.

The average basic current studied in this section is given in fig. 4. It is taken to represent a mean profile of the layer from 900 mb to 100 mb, and resembles a typical profile at the 500 mb level across a section of strong westerlies. In order to simplify the integration, the profile has been greatly smoothed and adjusted to make $\dot{\lambda}_0$ have the same value at the two inner critical points.

For this neutral disturbance, the phase velocity is given by the current velocity at the inner critical points. The corresponding wave number and the eigen function can be obtained by Taylor's expansion. Thus, if Ψ and its derivatives at the starting point $y=y_1$ are known, the value of Ψ and its first derivative at the nearby point $y = y_1 + \eta$ are given by

$$\Psi(y_1 + \eta) = \Psi(y_1) + \eta\Psi'(y_1) + \frac{\eta^2}{2!}\Psi''(y_1) + \frac{\eta^3}{3!}\Psi'''(y_1) + \frac{\eta^4}{4!}\Psi^{iv}(y_1) + \ldots$$

$$\Psi'(y_1 + \eta) = \Psi'(y_1) + \eta\Psi''(y_1) + \frac{\eta^2}{2!}\Psi'''(y_1) + \frac{\eta^3}{3!}\Psi^{iv}(y_1) + \frac{\eta^4}{4!}\delta\Psi^{iv}(y_1)$$

where the primes denote differentiation with respect to y and

$$\delta\Psi^{iv}(y_1) = \Psi^{iv}(y_1) - \Psi^{iv}(y_1 - \eta)$$

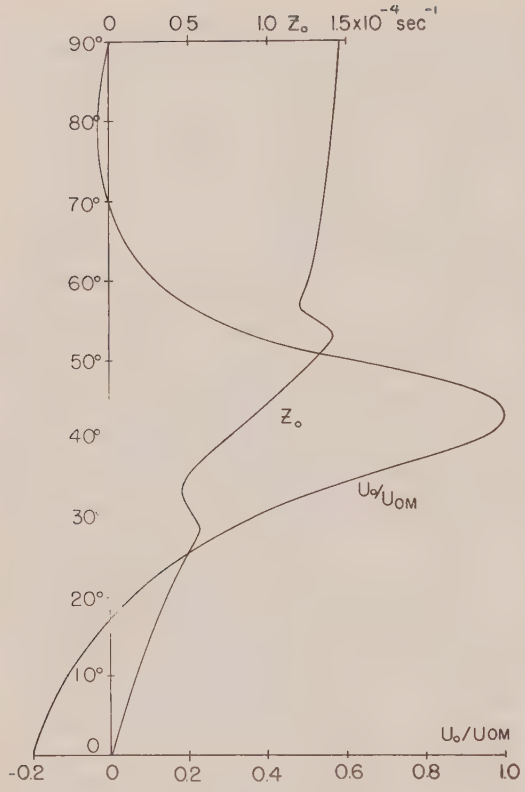

Fig. 4. The mean zonal wind profile and absolute vorticity distribution in winter, with $u_{0M} = 40$ m. sec^{-1}.

Since Ψ has to satisfy the vorticity equation at every point, the second and higher derivatives have to be computed from (11) by successive differentiation and by use of the values of the lower derivatives already obtained. Thus

$$\Psi''(y_1) = \left[n^2 - (\dot{\lambda}_0 - \mu)^{-1} \frac{dZ_0}{dy}\right]_{y_1} \Psi(y_1) \equiv$$

$$\equiv (n^2 - F)_{y_1} \Psi(y)$$

$$\Psi''' = (n^2 - F)\Psi' - F'\Psi$$

$$\Psi^{iv} = (n^2 - F)\Psi'' - 2F'\Psi' - F''\Psi$$

and so on, and Ψ can be integrated in a step-by-step manner.

To start the integration, the solutions corresponding to the distribution of F near the equator are obtained. In our case, F is equal to -23 near the equator. Thus, for $y = 0$, (11) becomes $\Psi'' = m^2\Psi$, where $m^2 = n^2 + 23$, and the solution that satisfies the boundary condition $\Psi(0) = 0$ is

$$\Psi = A \sinh my \tag{24}$$

The first and higher derivatives for the starting point can be computed from this solution and the values of Ψ and its derivatives at $y = 0 + \eta$ computed from the Taylor expansions. The value of $\delta\Psi^{iv}$ at the starting point can either be neglected or computed from the solution given above. If the condition $u' = 0 = -\partial\Psi/\partial y$ is used for $y = 0$, we get another solution. Since the difference is small, it will not be discussed.

Since the other boundary condition applies at $y = \infty$ (the pole) in our coordinate system, it is necessary to replace it by the condition

$$\Psi' + n\Psi = 0 \tag{25}$$

for a very large value of y, i.e., Ψ should decrease exponentially as the pole is approached. For the profile we are studying, the function F can be represented by $F = -2\ (y - 0.8)^{-2} = = -2x^{-2}$ for $y > 1.3$ (north of 65° N), to a high degree of approximation. Thus, for $y > 1.3$ equation (11) becomes

$$\frac{d^2\Psi}{dx^2} - \left(n^2 + \frac{2}{x^2}\right)\Psi = 0 \tag{26}$$

The solution of (26) which satisfies the condition (25) is given by

$$\Psi = C\left(n + \frac{1}{x}\right) e^{-nx} \tag{27}$$

and is valid for $y > 1.3$.

When the function Ψ with its derivatives obtained from (24) has been integrated to $y = = 1.3$, the ratio Ψ'/Ψ should agree with that given by (27). The value of n that fulfils this requirement is the eigenvalue of the problem, and the corresponding Ψ the eigenfunction. It is found that the neutral oscillation corresponding to the two inner critical points of the profile in fig. 4 has the eigenvalue $n = 9.5$. The phase velocity of this neutral disturbance is $\mu_r = 0.05\ \omega$, about 12 deg. lat per day. The 500 mb and 300 mb maps during the winter months January and February show that the wave number is generally from 8 to 10, and

the phase velocity is about 10—15 degrees of longitude per day. The eigenfunction Ψ and its first derivative are given in fig. 5. It is seen that the perturbations are much stronger on the north side of the jet than on the south side; this agrees with the statistical result obtained by RIEHL, YEH and LA SEUR (1950) that the maximum value of $\overline{v}^2$ occurs generally to the north of the jet.

In the perturbation stream function, the arbitrary constant has been chosen to give a maximum perturbation velocity $u' = 12$ m sec^{-1} while the maximum velocity of the basic current is 40 m sec^{-1}. The perturbation kinetic energy is less than 10 per cent of that of the basic flow.

Since only an integral wave number is permissible, we shall take $n = 9$ instead of 9.5. The total stream function is plotted in fig. 6. It is seen that closed cyclonic and anticyclonic centers are produced to the north and south of the jet stream of westerlies as a result of the perturbation. However, the anticyclonic centers are very weak, much weaker than the cyclones to the north. In order to produce the large semi-stationary anticyclonic centers in the subtropics, it is necessary to superpose another slowly moving disturbance, largely determined by the two outer critical points in the profile. Since this generally does not effect the flow pattern in middle and higher latitudes, it will not be discussed.

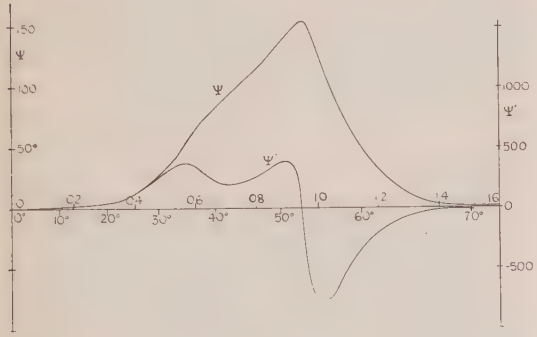

Fig. 5. The eigen function Ψ and its derivative for the neutral disturbance.

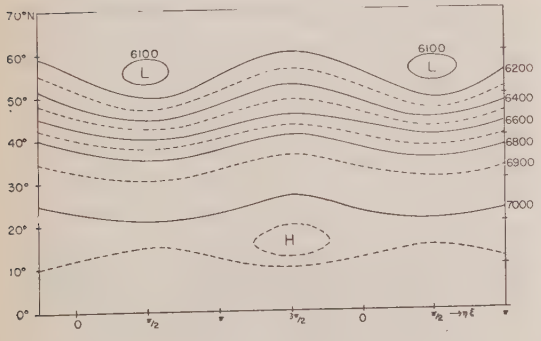

Fig. 6. Composite contour lines in meters.

8. Summary

From the discussions above, it is seen that different disturbances have quite different effects on the zonal flow, according to whether the basic flow is stable or unstable for the particular disturbance. In the upper atmosphere under normal conditions, the absolute vorticity is largely determined by the coriolis parameter, increasing toward the north in most regions. This situation is stable for most disturbances. Thus, when disturbances are added to the upper layer, most of them will undergo a damping process, transport zonal momentum from regions of weaker to regions of stronger zonal motion, and supply kinetic energy to the zonal flow. Parts of these zonal momentum and energy being transported downwards to overcome ground friction. The remainder will have the effect of strengthening and sharpening the zonal westerlies and easterlies, and thereby also increase the degree of instability.

When the process of building up of the zonal wind systems through the damping disturbances has gone on for a sufficiently long period of time, the currents become strong and sharp, and maxima and minima of absolute vorticity are produced, the zonal wind distribution becomes unstable for the more effective disturbances, with longer wave lengths and smaller phase velocities. (From the vorticity distribution in fig. 5 and the solution obtained in the previous section, it may be inferred that the wave number of maximum instability is about 4 or 5 during the periods when the jet stream is strong in the winter months.) The amplitude of these disturbances will then increase to form closed cold lows to the south and warm highs to the north of the jet. As these amplified disturbances have the effect of transferring angular momentum from

regions of higher to regions of lower zonal velocity, and withdraw kinetic energy from the zonal flow, the intensity of the mean zonal flow is greatly reduced by these disturbances, and the zonal wind profile is flattened.

After this breakdown, the absolute vorticity distribution is again dominated by the coriolis parameter, so that the situation is stable for other disturbances, and the damping effect operates once again, to rebuild the prevailing zonal winds. Thus according to this study, the general circulation will go through cycles of decay and rebuilding, due to the effect of these disturbances. It may be noted that their kinetic energy, at least in part, must be destroyed through the convergence effect, or transferred to the lower layer, so that the energy of the upper system will not continually increase.

From the foregoing discussions, it may be concluded that *the damped disturbances are really necessary parts in building up the prevailing zonal winds and overcoming the loss of kinetic energy and angular momentum through friction in the lower atmosphere. On the other hand, although large amplified disturbances occur only occasionally, they act in such a way as to prevent the prevailing winds from growing indefinitely, and therefore act as brakes for the general circulation.*

Acknowledgements

The writer wishes to express his gratitude to Professor V. P. Starr and Professor C. C. Lin for their valuable suggestions and discussions, to Dr T. V. Davies for his help in preparing the manuscript.

REFERENCES

Allen, R. A., and others, 1940: Report on an experiment in fiveday weather forecasting. *Papers in Physical Oceanography and Meteorology*, M.I.T. and Woods Hole Oceanographic Institution, 8, No. 3.

Berson, F. A., 1949: Summary of a theoretical investigation into the factors controlling the instability of long waves in zonal currents. *Tellus*, **1**, 4, pp. 44—52.

Charney, J. G., 1947: The Dynamics of Long Waves in a Baroclinic Westerly Current. *J. Meteor.* **4**, 135—163.

Eady, E. T., 1949: Long Waves and Cyclone Waves, *Tellus*, **1**, 3, 33—52.

Fjortoft, R., 1950: Application of Integral Theorems in Deriving Criteria of Stability for Laminar Flows and for the Baroclinic Circular Vortex. *Geofys. Publ.*, **16**, 5., 1—52.

Foote, J. R., and Lin, C. C., 1950: Some Recent Investigations in the Theory of Hydrodynamic Stability. *Quart. App. Math.*, **8**, 3, 265—280.

Hassanein, S. A. M., 1949: A wave pattern changing with time as a solution of the vorticity equation for non-divergent motion. *Tellus*, **1**, 4, 58—60.

aw, J. J., 1946: The Formation of the Semipermanent Centers of Action in Relation to the Horizontal Solenoidal Field. *J. Meteor.*, **3**, 103—114.

Jeffreys, H., 1926: On the Dynamics of Geostrophic Winds. *Quart. J. R. Meteor. Soc.*, **52** ,85—104.

Kuo, H. L., 1949: Dynamic Instability of Two-Dimensional Nondivergent Flow in a Barotropic Atmosphere. *J. Meteor.*, **6**, 105—122.

— 1950: Dynamic aspects of the general circulation and the stability of zonal flow. Report No. 4, Contract AF 19—122—153, U.S.A.F. Cambridge Research Lab., Cambridge, Massachusetts.

— 1951: A note on the kinetic energy balance of the zonal wind systems. *Tellus* **3**, 3.

Lin, C. C., 1945: On the Stability of Two-Dimensional Parallel Flows. Parts I, II, III. *Quart. of App. Math.*, **3**, 117—142; 218—234; 277—301.

Machta, L., 1949: Dynamic Characteristics of a Tilted Trough Model. *J. Meteor.*, **6**, 261—265.

Mintz, Y., 1949: The Maintenance of the Mean Zonal Motion of the Atmosphere. Thesis for Ph. D. at University of California, Los Angeles.

Riehl, H., Yeh, T. C., and La Seur, N. E., 1950: A Study of Variations of the General Circulation. *J. Meteor.*, **7**, 181—194.

Rossby, C.-G., 1947: On the Distribution of Angular Momentum in Gaseous Envelopes Under the Influence of Large-Scale Horizontal Mixing Processes. *Bulletin American Meteor. Soc.*, **28**, 53—68.

— 1949: On the Nature of the General Circulation of the Lower Atmosphere. Chap. II of *The Atmospheres of the Earth and Planets*, edited by G. P. Kuiper, University of Chicago Press. 16—48.

Starr, V. P., 1948a: An Essay on the General Circulation of the Earth's Atmosphere. *J. Meteor.*, **5**, 39—43.

— 1948b: On the Production of Kinetic Energy in the Atmosphere. *J. Meteor.*, **5**, 193—196.

— 1950: Note on a recent study of stability by R. Fjörtoft. *Tellus*, **2**, 4, 321—323.

Wasow, W., 1947: On the Asymptotic Solution of the Differential Equation for Small Disturbances in a Laminar Flow. *Nat. Acad. Sci.*, U.S.A., **33**, 232—234.

White, R. M., 1950: Meridional Eddy Flux of Energy in the Northern Hemisphere. Report No. 3, Contract AF 19—122—153, U.S.A.F. Cambridge Research Lab., Cambridge, Mass.

Widger, W. K. Jr., 1949: A Study of the Flow of Angular Momentum in the Atmosphere. *J. Meteor.*, **6**, 291—299.

Willett, H. C., and Collaborators, 1947: Final Report of the Weather Bureau, M.I.T. Extended Forecasting Project for the fiscal year July 1, 1946—July 1, 1947, Cambridge and Washington.

Der Mechanismus des meteorologischen Lärmes

Von K. HINKELMANN
Zentralamt des Deutschen Wetterdienstes in der U. S. Zone, Bad Kissingen

(Manuscript received 16 June 1951)

Abstract

Using a simple atmospheric model, the difference between the solutions of the primitive and the quasi-hydrostatic equations is demonstrated. The results show that the quasi-hydrostatic processes are largely determined by the initial field of pressure wherever the meteorological "noise"-phenomena (in the form of short-period oscillations about a trend of the meteorological elements) depend on the initial field of the non-geostrophic windcomponents. This trend can be computed with sufficient accurracy also by a numerical integration of the primitive equations, which are mathematically simpler to handle than the quasi-hydrostatic equations.

In this case the initial wind fields can be computed from the observed pressure field by using the geostrophic approximation.

To find the trend the results have to be smoothed.

Die hydro- und thermodynamischen Differentialgleichungen erfassen bei ihrer Anwendung auf atmosphärische Vorgänge nicht nur die relativ langsam ablaufenden sogenannten quasistatischen Prozesse, sondern zwangsläufig auch gewisse kurzperiodischen Abläufe, bei denen Ausbreitungsgeschwindigkeiten in der Größenordnung der Schallgeschwindigkeit auftreten und die man deswegen als meteorologischen Lärm bezeichnet.

Im allgemeinen wirken sich diese kurzperiodischen Vorgänge mit relativ geringen Amplituden nur in Form einer Unruhe im zeitlichen Gang der meteorologischen Zustandsvariabeln aus und werden in den synoptischen Karten weitgehend weggeglättet, so dass man sich bei einer rechnerischen Vorhersage mit der Erfassung der quasistatisch verlaufenden Änderungsprozesse begnügen könnte. Beim numerischen Integrationsverfahren wird aber gerade der zeitliche Gang, also der partielle zeitliche Differentialquotient, dessen Berechnung auch ohne vollständige Integration aus den Differentialgleichungen verhältnismässig einfach ist, prognostisch zur Ermittlung der im nächsten Zeitintervall eintretenden Änderung der betrachteten Zustandsgrösse ausgewertet.

Benutzt man für den numerischen Rechenprozess die hydro- und thermodynamischen Grundgleichungen in unveränderter Form, so wird man bei Berechung der Tendenzen ungeglättete Momentanwerte erhalten. Aus den entsprechenden Differenzenquotienten lassen sich demzufolge nur Änderungen für die betreffende Variable für ein Zeitintervall entnehmen, das klein ist gegenüber der Schwingungsdauer der kurzperiodischen Lärmvorgänge, was einen Aufwand an Rechenarbeit erfordert, der eine rationelle Auswertung des numerischen Integrationsverfahren erschwert.

Die Anzahl der erforderlichen Zeitschritte kann wesentlich reduziert werden, wenn diese für die Rechnung unbequemen, meteorologisch uninteressanten kurzdauernden Vorgänge aus den Differentialgleichungen elimi-

niert werden, was allerdings auch eine grundlegende Änderung in der Gestalt der Differentialgleichungen zur Folge hat.

Im folgenden soll an Hand eines einfachen atmosphärischen Modells versucht werden, in den Lösungsfunktionen die kurzperiodischen Anteile von den quasistatischen zu separieren und abzuschätzen, für welche durch Druck- und Windfelder definierten Anfangszustände eine Elimination der meteorologischen Lärmvorgänge berechtigt erscheint.

I. Ausgangsgleichungen für das zugrundeliegende atmosphärische Modell

Als Ausgangsgleichungen sollen die bereits von J. G. Charney (1949) diskutierten linearisierten Gleichungen einer homogenen Atmosphäre zugrundegelegt werden. Bei Gültigkeit der hydrostatischen Grundgleichung und bei Annahme eines durch

$$U = -\frac{g}{l} H_y = \text{const}$$
$$V = 0$$

definierten Grundzustandes schreiben sich diese:

$$Du = -gh_x + lv \qquad (1)$$
$$Dv = -lu \qquad (2)$$

Bewegungsgleichungen

$$Dh = \frac{lU}{g} v - Hu_x \qquad (3)$$

Kontinuitätsgleichung,

wenn $u_z = v_z = u_y = v_y = h_y = 0$ vorausgesetzt, die geringe Abhängigkeit der Parameter l, H von y also als unerheblich betrachtet wird. In den Gleichungen bedeuten H Höhe der homogenen Atmosphäre, U, V Geschwindigkeitskomponenten des Grundzustandes; h, u, v die entsprechenden Grössen der Störungsfelder; $D = \frac{\partial}{\partial t} + U\frac{\partial}{\partial x}$, $l = 2\omega \sin\varphi$.

Das Gleichungssystem lässt sich in dieser einfachen Form allgemein integrieren. Wegen der vorgenommenen Vereinfachungen werden zwar die gefundenen Lösungen tatsächliche Wettervorgänge nur sehr weitgehend idealisiert wiedergeben. Zur Demonstration der charakteristischen Unterschiede in den Dimensionen und in der Abhängigkeit von den Anfangsfeldern zwischen kurz- und langperiodischen Prozessen dürfte jedoch das Modell ausreichend sein, so daß dieses zumindest einen Einblick in die Wirkungsweise des atmosphärischen Mechanismus vermittelt und einen Hinweis geben dürfte, auf welche Weise und unter welchen Voraussetzungen eine derartige Elimination auch in den nichtlinearen dreidimensionalen Diff. Gl. System möglich und berechtigt ist.

Das System (1—3) läßt sich auf eine Diff. Gl. der Variablen h reduzieren. Aus (1, 2) erhält man

$$(D^2 + l^2)u = -gDh_x$$

bzw. wegen $D\frac{\partial}{\partial x} = \frac{\partial}{\partial x}D$

$$(D^2 + l^2)u_x = -gDh_{xx} \qquad (4)$$
$$(D^2 + l^2)v = glh_x \qquad (5)$$

Führt man diese Gl. in (3) ein, so resultiert eine homogene lineare Diff. Gl. III. Ordnung in h allein:

$$D\left(D^2 - gH\frac{\partial^2}{\partial x^2}\right)h + l^2 h_t = 0; \qquad (6)$$

die im Falle $l \to 0$ in die Diff. Gl. für Schwerewellen $\left(D^2 - gH\frac{\partial^2}{\partial x^2}\right)h = 0$ übergeht. Das System (4—6) ist dem System (1—3) völlig äquivalent und soll allgemein integriert werden, wobei insbesondere der Einfluß einer Variation der beliebig vorgebbaren Windfelder u und v auf die zeitliche Entwicklung des durch die Größe h charakterisierten Druckfeldes untersucht werden soll.

Wir beschränken uns dabei auf das Anfangswertproblem, bei dem zu einem bestimmten Zeitpunkt $t = 0$ die Funktionen $h = h^0$, $u = u^0$, $v = v^0$ für alle x-Werte vorgegeben sind, wodurch $h(x, t)$, $u(x, t)$ und $v(x, t)$ eindeutig bestimmt sind.

II. Berechnung der Druckfunktion $h(x, t)$

Der Ansatz $h = h_0 A e^{i\nu(x-ct)}$ führt nach Einsetzen in Gl. (6) auf die Frequenzengleichung

$$-\nu^2(U-c)^3 + gH\nu^2(U-c) - l^2 c = 0$$

bzw. auf $\triangle^3 - m^2\triangle + \frac{Ul^2}{\nu^2} = 0$ (7)

wenn zur Abkürzung gesetzt wird

$$m^2 = gH + \frac{l^2}{\nu^2} \quad \text{und}$$

$$\triangle = U - c \tag{7a}$$

Für $U^2 < gH \sim 10^5$ $[m^2\,\mathrm{sec}^{-2}]$ existieren drei reelle Wurzeln ($\triangle_1$, $\triangle_2$, $\triangle_3$), wovon $\triangle_1$ nahe bei $\frac{Ul^2}{m^2\nu^2}$; $\triangle_2$, $\triangle_3$ nahe bei $\pm m$ liegen.

$\triangle_1$ läßt sich als Grenzwert eines Kettenbruches darstellen mit dem Bildungsgesetz

$$\triangle_{1,n+1} = \frac{\frac{Ul^2}{\nu^2}}{m^2 - \triangle_{1,n}^2}; \quad \triangle_{1,0} = \frac{Ul^2}{m^2\nu^2}$$

Der Grenzwert $\triangle_1 = \lim_{n\to\infty} \triangle_{1,n}$ werde mit d abgekürzt. Die beiden weiteren Wurzeln $\triangle_2$, $\triangle_3$ ergeben sich aus

$$\triangle^2 + d\triangle + (d^2 - m^2) = 0,$$

so daß

$$\triangle_1 = d \approx \frac{Ul^2}{m^2\nu^2}$$

$$\triangle_2 = -\frac{d}{2} + \sqrt{m^2 - \frac{3}{4}d^2} = -\frac{d}{2} + M;$$

$$M = +\sqrt{m^2 - \frac{3}{4}d^2}$$

$$\triangle_3 = -\frac{d}{2} - \sqrt{m^2 - \frac{3}{4}d^2} = -\frac{d}{2} - M \tag{8}$$

$$c_k = U - \triangle_k, \; k = 1, 2, 3. \tag{9}$$

Mit den drei Werten für c erhält man als allgemeineren Ansatz für h

$$h(x,t) = h_0 \sum_{k=1}^{3} A_k e^{i\nu(x - c_k t)} \tag{10}$$

Der Lösungsansatz (10) erfaßt alle Lösungen mit Anfangsfeldern in h^0, u^0, v^0 in Form harmonischer Funktionen in x der gleichen Wellenlänge $L = \frac{2\pi}{\nu}$. Eine Anpassung an beliebige Anfangsfunktionen ergibt sich leicht durch Superposition von particulären Lösungen der Form (10) mit verschiedener Frequenz ν zu Fourierreihen (bei periodischen Anfangsfeldern). Man erhält bei periodischen Anfangsfunktionen für h^0, u^0, v^0 mit der Intervallänge $L^\star$ wegen $L = \frac{L^\star}{n}$; $\nu = \frac{2\pi}{L^\star}\, n$ für

$$h(x,t) = \sum_{n=-\infty}^{+\infty} h_{0\nu} \sum_{k=1}^{3} A_{k\nu}\, e^{i\nu(x - c_{k\nu}t)},$$

$$n = \frac{L^\star}{2\pi}\,\nu = \pm 0, 1, 2 \ldots \tag{11}$$

worin noch die $A_{k\nu}$ aus den Anfangsbedingungen zu bestimmen wären. Da die Berechnungsgleichungen für $A_{k\nu}$ sich für alle ν entsprechen, genügt es, diese bei einer festgehaltenen Frequenz ν aufzustellen. Z. Zt. $t = 0$ muß gelten:

$$h(x,0) = h^0 \qquad \text{und wegen (1—3)}$$

$$Dh(x,0) = \frac{Ul}{g}\, v^0 - Hu_x^0$$

$$D^2h(x,0) = -\frac{Ul^2}{g}\, u^0 + H(gh_{xx}^0 - l\, v_x^0) \tag{12}$$

Denkt man sich die Anfangsfunktionen für h^0, u^0, v^0 nach Fourier zerlegt, so möge für ein bestimmtes ν gelten:

$$h_\nu^0 = h_{0\nu} e^{i\nu x} \qquad h_0, u_0, v_0 = \text{komplexe Amplituden der betrachteten Partialwelle } z \cdot Zt \cdot t = 0 \text{ mit}$$

$$u_\nu^0 = u_{0\nu} e^{i\nu x}$$

$$v_\nu^0 = v_{0\nu} e^{i\nu x} \qquad L = \frac{2\pi}{\nu}\,^1 \tag{13}$$

Setzt man (10) und (13) in (12) ein, so erhält man zur Bestimmung der A_k folgendes lineares Gleichungssystem:

$$\sum_{k=1}^{3} A_k = 1$$

---

1 Zur vereinfachten Schreibweise soll künftig der Index ν wieder fortgelassen werden.

$$\sum_{k=1}^{3} \triangle_k A_k = -H \frac{u_0}{h_0} - \frac{Ul}{gv} \frac{v_0}{h_0} i \equiv F$$

$$\sum_{k=1}^{3} \triangle_k^2 A_k = gH + \frac{Ul^2}{gv^2} \frac{u_0}{h_0} + H \frac{l}{v} \frac{v_0}{h_0} i \equiv G \qquad (14)$$

Mit den Bezeichnungen (8) für $\triangle_k$ erhält man anstelle von (11) für eine bestimmte Frequenz (siehe Fussnote [1]):

$$h(x,t) = h_0 \Big\{ A_1 e^{iv(x-ct)} + [(A_2 + A_3) \cos vMt + (A_2 - A_3)\, i \sin vMt] \cdot \cdot e^{iv\left[x-\left(U+\frac{d}{2}\right)t\right]} \Big\} \qquad (11a)$$

und anstelle von (14)

$$A_1 + (A_2 + A_3) = 1$$

$$d A_1 - \frac{d}{2}(A_2 + A_3) + M(A_2 - A_3) = F$$

$$d^2 A_1 + \left(M^2 + \frac{d^2}{4}\right)(A_2 + A_3) - dM(A_2 - A_3) = G \qquad (14a)$$

Für die Amplituden der Funktion h in Gl. (11a) erhält man daraus:

$$A_1 = \frac{\left(M^2 + \frac{d^2}{4}\right) - G - d\left(F + \frac{d}{2}\right)}{M^2 - \frac{9}{4} d^2}$$

$$A_2 + A_3 = 1 - A_1$$

$$A_2 - A_3 = \frac{1}{M}\left(F + \frac{d}{2} - \frac{3}{2} d A_1\right) \qquad (15)$$

Zwecks bequemerer Variation des Anfangszustandes in u und v soll angesetzt werden

$$u^0 = u_0 e^{ivx} = \delta i \frac{gv}{1} h_0 e^{ivx}$$

$$v^0 = v_0 e^{ivx} = (1 - \varepsilon)\, i \frac{gv}{1} h_0 e^{ivx} \qquad (16)$$

Da $v_g^0 = i \frac{gv}{1} h_0 e^{ivx}$, $u_g^0 = 0$ die Komponenten des zu $h^0 = h_0 e^{ivx}$ zugehörigen geostrophischen Windes bezeichnen, so stellen die dimensionslosen komplexen Zahlen δ und ε ein Maß dar für die Auslenkung des Anfangswindfeldes gegenüber dem geostrophischen. Die Beträge von δ, ε geben das Verhältnis der Amplituden der nichtgeostrophischen Komponenten zur geostrophischen wieder, die Winkel von ε, δ deren Phasenverschiebung gegenüber der geostrophischen Windkomponente.

Mit diesen Ansätzen (16) für u^0 und v^0 erhält man anstelle von (14)

$$\sum_{k=1}^{3} A_k = 1$$

$$\sum_{k=1}^{3} \triangle_k A_k = \left[(1 - \varepsilon) U - \frac{\delta i v}{l} gH\right] = F$$

$$\sum_{k=1}^{3} \triangle_k^2 A_k = \left[gH\varepsilon + \frac{\delta i l}{v} U\right] = G \qquad (14b)$$

Mit (14) und (15) ist die Funktion $h(x,t)$ in (11 bzw. 11a) bestimmt. Bevor die auftretenden Amplituden A_k numerisch berechnet werden, sollen die weiteren Funktionen u und v ermittelt werden.

III. Berechnung der horizontalen Windfelder u und v

Die Funktionen u, v gewinnt man nach Vorliegen der Lösung h aus Gln. (4 u. 5), in welchen die rechten Seiten als inhomogene Terme betrachtet werden können. Einsetzen von $h(x,t)$ aus (10) in (4) und (5) ergibt:

$$(D^2 + l^2) u = -gh_0 i^2 v^2 \cdot \cdot \sum_{k=1}^{3} A_k \triangle_k e^{iv(x-c_k t)} \text{ und}$$

$$(D^2 + l^2) v = gh_0 i l v \cdot \sum_{k=1}^{3} A_k \cdot e^{iv(x-c_k t)}$$

mit den Lösungen:

$$u = gh_0 \sum_{k=1}^{3} \frac{A_k \triangle_k}{\frac{l^2}{v^2} - \triangle_k^2} e^{iv(x-c_k t)} + (\alpha_u \cos lt + \beta_u i s \text{ in } lt)\, e^{iv(x-Ut)}$$

$$v = \frac{gli}{\nu}\, h_0 \sum_{k=1}^{3} \frac{A_k}{\frac{l^2}{\nu^2} - \triangle_k{}^2}\, e^{i\nu(x-c_k t)} + \\ + (\alpha_v \cos lt + \beta_v i \sin lt) e^{i\nu(x-Ut)}$$

Die Lösungen der homogenen Differentialgleichungen (4,5) verschwinden[2] jedoch, da $\alpha_u = \beta_u = \alpha_v = \beta_v = 0$, wie man erkennt, wenn man die Lösungsfunktionen in *Gln.* (1—3) einsetzt und die Frequenzengleichung (7) beachtet, so daß man für u und v schließlich erhält:

$$u = \frac{g\nu}{l} h_0 \sum_{k=1}^{3} \frac{l}{\nu} \frac{A_k \triangle_k}{D_k} e^{i\nu(x-c_k t)} = \\ = \frac{g\nu}{l} h_0 \sum_{k=1}^{3} B_k e^{i\nu(x-c_k t)} = \\ = \frac{g\nu}{l} h_0 \left\{ B_1 e^{i\nu(x-c_1 t)} + [(B_2 + B_3) \cos \nu M t + \right. \\ \left. + i(B_2 - B_3) \sin \nu M t] e^{i\nu\left[x-\left(U+\frac{d}{2}\right)t\right]} \right\} \quad (17)$$

$$v = \frac{g\nu}{l} h_0 i \sum_{k=1}^{3} \frac{l^2}{\nu^2} \frac{A_k}{D_k} e^{i\nu(x-c_k t)} = \\ = \frac{g\nu}{l} h_0 i \sum_{k=1}^{3} C_k e^{i\nu(x-c_k t)} = \\ = \frac{g\nu}{l} h_0 i \left\{ C_1 e^{i\nu(x-c_1 t)} + [(C_2 + C_3) \cos \nu M t + \right. \\ \left. + i(C_2 - C_3) \sin \nu M t] e^{i\nu\left[x-\left(U+\frac{d}{2}\right)t\right]} \right\} \quad (18)$$

worin bedeutet:

$$D_k = \frac{l^2}{\nu^2} - \triangle_k{}^2; \quad B_k = \frac{l}{\nu} \frac{A_k \triangle_k}{D_k};$$

$$C_k = \frac{l^2}{\nu^2} \frac{A_k}{D_k}.$$

Unter Benutzung der Frequenzengleichung in der Form:

$$K_n = \sum_{k=1}^{3} \frac{A_k \triangle_k^n}{D_k} = \frac{Ul^2}{gH\nu^2} \sum_{k=1}^{3} \frac{A_k \triangle_k^{n-1}}{D_k} - \\ - \frac{1}{gH} \sum_{k=1}^{3} A_k \triangle_k^n = \left[1 - \left(\frac{Ul}{gH\nu}\right)^2\right]^{-1} \frac{\nu^2}{l^2} \cdot \\ \cdot \sum_{k=1}^{3} A_k \left[\triangle_k^n - \frac{\triangle_k^{n+2}}{gH} - \frac{1}{U}\left(\frac{Ul}{gH\nu}\right)^2 \triangle_k^{n+1}\right]$$

ergibt sich für

$$K_0 = \frac{\nu^2}{l^2}(1-\varepsilon) = -\frac{\nu}{l}\frac{1}{g}\, i\, \frac{v_0}{h_0}$$

$$K_1 = \frac{\nu}{l}\, \delta i = \frac{1}{g}\frac{u_0}{h_0}$$

$$K_2 = -\varepsilon$$

und damit für die dimensionslosen Koeffizienten:

$$B_1 = \frac{l}{\nu}\frac{A_1 d}{D_1}, \quad C_1 = \frac{l^2}{\nu^2}\frac{A_1}{D_1}$$

$$B_2 + B_3 = \delta i - B_1, \quad C_2 + C_3 = 1 - \varepsilon - C_1$$

$$B_2 - B_3 = \frac{1}{M}\left\{ -\frac{l}{\nu}\,\varepsilon + \frac{d}{2}\,\delta i - \frac{3}{2}\, d B_1 \right\},$$

$$C_2 - C_3 = \frac{1}{M}\left\{ \frac{l}{\nu}\,\delta i + \frac{d}{2}(1-\varepsilon) - \frac{3}{2}\, d C_1 \right\}$$

Eine Vorstellung über die Größenverhältnisse der in den Funktionen h, u, v auftretenden Amplituden A_k, B_k, C_k in Abhängigkeit von der Wellenlänge $L = \frac{2\pi}{\nu}$ vermittelt die Tabelle 1, in welcher $l = 10^{-4}$ [sec^{-1}], $U = 15$ [$m \cdot$ sec^{-1}], $gH = 8 \cdot 10^4$ [m^2 sec^{-2}] angenommen wurde.

IV. Elimination des meteorologischen Lärmes

Die Abschätzung der Größenverhältnisse ergibt, daß in dem meteorologisch interessierenden Spektrum mit ausreichender Näherung gesetzt werden kann:

$$A_1 \approx 1 - \frac{gH}{m^2}\,\varepsilon; \quad B_1 \approx \frac{\nu}{l}\, d\left(1 - \frac{gH}{m^2}\,\varepsilon\right);$$

---

[2] Im Falle $\nu = 0$ tritt allerdings die inertiale Frequenz l auf. Man erhält für die Anfangsfelder: $h(x, 0) = u(x, 0) = 0$; $v(x, 0) = v_0 = \text{const}$ die Lösung:

$$u = v_0 \sin lt; \quad v = v_0 \cos lt; \quad h = v_0 \frac{u}{g} \sin lt.$$

Tab. 1. Amplituden der Funktionen h, u, v nach Gln. (11a, 17, 18); mit $U = 15$ [m sec^{-1}], $gH = 8 \cdot 10^4$ [m^2 sec^{-2}] und $l = 10^{-4}$ [sec^{-1}]

L 10^6 m	A_1	$A_2 + A_3$	$A_2 - A_3$
30	$1 + 2{,}61 \cdot 10^{-4} - 0{,}260\,\varepsilon - 0{,}0172\,\delta i$	$-2{,}61 \cdot 10^{-4} + 0{,}260\,\varepsilon + 0{,}0172\,\delta i$	$0{,}00701 - 0{,}0192\,\varepsilon - 0{,}302\,\delta i$
25	$1 + 2{,}06 \cdot 10^{-4} - 0{,}336\,\varepsilon - 0{,}0166\,\delta i$	$-2{,}06 \cdot 10^{-4} + 0{,}336\,\varepsilon + 0{,}0166\,\delta i$	$0{,}00103 - 0{,}0205\,\varepsilon - 0{,}412\,\delta i$
20	$1 + 0{,}82 \cdot 10^{-4} - 0{,}441\,\varepsilon - 0{,}0147\,\delta i$	$-0{,}82 \cdot 10^{-4} + 0{,}441\,\varepsilon + 0{,}0147\,\delta i$	$0{,}00155 - 0{,}0222\,\varepsilon - 0{,}590\,\delta i$
15	$1 - 1{,}15 \cdot 10^{-4} - 0{,}584\,\varepsilon - 0{,}0109\,\delta i$	$+1{,}15 \cdot 10^{-4} + 0{,}584\,\varepsilon + 0{,}0109\,\delta i$	$0{,}00237 - 0{,}0258\,\varepsilon - 0{,}905\,\delta i$
10	$1 - 2{,}67 \cdot 10^{-4} - 0{,}760\,\varepsilon - 0.0055\,\delta i$	$+2{,}67 \cdot 10^{-4} + 0{,}760\,\varepsilon + 0{,}0055\,\delta i$	$0{,}00351 - 0{,}0336\,\varepsilon - 1{,}549\,\delta i$
5	$1 - 1{,}63 \cdot 10^{-4} - 0{,}927\,\varepsilon - 0{,}0010\,\delta i$	$+1{,}63 \cdot 10^{-4} + 0{,}927\,\varepsilon + 0{,}0010\,\delta i$	$0{,}00473 - 0{,}0459\,\varepsilon - 3{,}422\,\delta i$
1	$1 - 0{,}09 \cdot 10^{-4} - 0{,}997\,\varepsilon - 0{,}0000\,\delta i$	$+0{,}09 \cdot 10^{-4} + 0{,}997\,\varepsilon + 0{,}0000\,\delta i$	$0{,}00528 - 0{,}0527\,\varepsilon - 17{,}743\,\delta i$
	B_1	$B_2 + B_3$	$B_2 - B_3$
30	$0{,}0233 - 0{,}00604\,\varepsilon - 4{,}00 \cdot 10^{-4}\,\delta i$	$-0{,}0233 + 0{,}00604\,\varepsilon + \delta i$	$-7{,}10^{-4} - 0{,}860\,\varepsilon + 1{,}00 \cdot 10^{-2}\,\delta i$
25	$0{,}0251 - 0{,}00841\,\varepsilon - 4{,}17 \cdot 10^{-4}\,\delta i$	$-0{,}0251 + 0{,}00841\,\varepsilon + \delta i$	$-8{,}66^{-4} - 0{,}815\,\varepsilon + 1{,}15 \cdot 10^{-2}\,\delta i$
20	$0{,}0263 - 0{,}01162\,\varepsilon - 3{,}87 \cdot 10^{-4}\,\delta i$	$-0{,}0263 + 0{,}01162\,\varepsilon + \delta i$	$-7{,}78^{-4} - 0{,}748\,\varepsilon + 0{,}98 \cdot 10^{-2}\,\delta i$
15	$0{,}0261 - 0{,}01527\,\varepsilon - 2{,}85 \cdot 10^{-3}\,\delta i$	$-0{,}0261 + 0{,}01527\,\varepsilon + \delta i$	$-6{,}62^{-4} - 0{,}645\,\varepsilon + 0{,}84 \cdot 10^{-2}\,\delta i$
10	$0{,}0227 - 0{,}01722\,\varepsilon - 1{,}24 \cdot 10^{-4}\,\delta i$	$-0{,}0227 + 0{,}01722\,\varepsilon + \delta i$	$-3{,}78^{-4} - 0{,}490\,\varepsilon + 0{,}56 \cdot 10^{-2}\,\delta i$
5	$0{,}0138 - 0{,}01281\,\varepsilon - 0{,}14 \cdot 10^{-4}\,\delta i$	$-0{,}0138 + 0{,}01281\,\varepsilon + \delta i$	$-0.78^{-4} - 0{,}271\,\varepsilon + 0{,}19 \cdot 10^{-2}\,\delta i$
1	$0{,}0030 - 0{,}00259\,\varepsilon - 0{,}00 \cdot 10^{-4}\,\delta i$	$-0{,}0030 + 0{,}00259\,\varepsilon + \delta i$	$-0{,}08^{-4} - 0{,}056\,\varepsilon + 0{,}01 \cdot 10^{-2}\,\delta i$
	C_1	$C_2 + C_3$	$C_2 - C_3$
30	$1 + 8{,}05 \cdot 10^{-4} - 0{,}260\,\varepsilon - 0{,}0172\,\delta i$	$-8{,}05 \cdot 10^{-4} - 0{,}740\,\varepsilon + 0.0172\,\delta i$	$-0{,}00200 - 0{,}0022\,\varepsilon + 0{,}860\,\delta i$
25	$1 + 8{,}36 \cdot 10^{-4} - 0{,}336\,\varepsilon - 0{,}0166\,\delta i$	$-8{,}36 \cdot 10^{-4} - 0{,}664\,\varepsilon + 0{,}0166\,\delta i$	$-0{,}00231 + 0{,}0001\,\varepsilon + 0{,}815\,\delta i$
20	$1 + 7{,}76 \cdot 10^{-4} - 0{,}441\,\varepsilon - 0{,}0147\,\delta i$	$-7{,}76 \cdot 10^{-4} - 0{,}559\,\varepsilon + 0{,}0147\,\delta i$	$-0{,}00197 + 0{,}0032\,\varepsilon + 0{,}748\,\delta i$
15	$1 + 5{,}63 \cdot 10^{-4} - 0{,}584\,\varepsilon - 0{,}0109\,\delta i$	$-5{,}63 \cdot 10^{-4} - 0{,}416\,\varepsilon + 0{,}0109\,\delta i$	$-0{,}00169 + 0{,}0063\,\varepsilon + 0{,}645\,\delta i$
10	$1 + 2{,}48 \cdot 10^{-4} - 0{,}760\,\varepsilon - 0{,}0055\,\delta i$	$-2{,}48 \cdot 10^{-4} - 0{,}240\,\varepsilon + 0{,}0055\,\delta i$	$-0{,}00111 + 0{,}0071\,\varepsilon + 0{,}490\,\delta i$
5	$1 + 0{,}28 \cdot 10^{-4} - 0{,}927\,\varepsilon - 0{,}0010\,\delta i$	$-0{,}28 \cdot 10^{-4} - 0{,}073\,\varepsilon + 0{,}0010\,\delta i$	$-0{,}00037 + 0{,}0033\,\varepsilon + 0{,}271\,\delta i$
1	$1 - 0{,}08 \cdot 10^{-4} - 0{,}997\,\varepsilon - 0{,}0000\,\delta i$	$+0{,}08 \cdot 10^{-4} - 0{,}003\,\varepsilon + 0{,}0000\,\delta i$	$-0{,}00002 + 0{,}0002\,\varepsilon + 0{,}056\,\delta i$

$$C_1 \approx 1 - \frac{gH}{m^2}\,\varepsilon$$

$$A_2 + A_3 \approx \frac{gH}{m^2}\,\varepsilon;\; B_2 + B_3 \approx -$$

$$-\frac{\nu}{l}\,d\left(1 - \frac{gH}{m^2}\,\varepsilon\right) + i;\; C_2 + C_3 \approx -$$

$$-\left(1 - \frac{gH}{m^2}\right)\varepsilon$$

$$A_2 - A_3 \approx -\frac{gH}{M}\,\frac{\nu}{l}\,\delta i;\; B_2; -B_3 \approx -$$

$$-\frac{l}{\nu}\,\frac{1}{M}\,\varepsilon;\; C_2 - C_3 \approx \frac{l}{\nu}\,\frac{1}{M}\,\delta i$$

Die Wellen h, u, v setzen sich aus zwei hinsichtlich der Schwingungsdauer wesentlich unterschiedlichen Anteilen zusammen. Die Terme mit den Amplituden A_1, B_1, C_1 mit einer Schwingungsdauer $T_1 = \frac{2\pi}{\nu c_1} = \frac{L}{c_1}$ stellen in reeller Schreibweise harmonische Funktionen dar, die ohne Formänderung mit der konstanten Verlagerungsgeschwindigkeit c_1 sich in positiver x-Richtung fortbewegen. Die Terme mit den Amplituden $A_2 \pm A_3$; $B_2 \pm B_3$; $C_2 \pm C_3$ ergeben in dem Koordinatensystem

$$x - \left(U + \frac{d}{2}\right) t = \text{const}$$

stehende Wellen mit einer Schwingungsdauer

$$T_{2,3} = \frac{2\pi}{\nu M} = \frac{L}{M}.$$

Tab. 2 gibt in Abhängigkeit von der Wellenlänge die Schwingungszeiten T_1 und $T_{2,3}$ wieder:

Tab. 2. Schwingungsdauer T_1 und $T_{2,3}$ in Abhängigkeit von der Wellenlänge L für $U = 15$ [m · sec^{-1}], $l = 10^{-4}$ [sec^{-1}], $gH = 8 \cdot 10^4$ [m^2 · sec^{-2}]

L [10^6 m[	$c_1 = U - d$ [m · sec^{-1}]	M [m · sec^{-1}]	T_1 [Std]	$T_{2,3}$ [Std]
30	3,89	555	2 140	15
25	5,03	488	1 380	14
20	6,61	426	840	13
15	8,76	370	475	11
10	11,39	325	244	9
5	13,90	294	100	5
1	14,95	283	19	1

Die Terme

$$h_Q = h_0 A_1 e^{i\nu(x - c_1 t)}$$

$$u_Q = \frac{g\nu}{l}\,h_0 B_1 e^{i\nu(x - c_1 t)}$$

$$v_Q = \frac{g\nu}{l}\,i h_0 C_1 e^{i\nu(x - c_1 t)}$$

charakterisieren also die eingangs als "quasistatisch verlaufend" bezeichneten Änderungsprozesse, während die Terme

$$h_L = h_0 \sum_{k=2}^{3} A_k e^{i\nu(x - c_k t)} =$$

$$= h_0 \left[(A_2 + A_3)\cos \nu M t + \right.$$

$$\left. + (A_2 - A_3) i \sin \nu M t\right] e^{i\nu\left[x - \left(U + \frac{d}{2}\right)t\right]}$$

$$u_L = \frac{g\nu}{l}\,h_0 \sum_{k=2}^{3} B_k e^{i\nu(x - c_k t)} =$$

$$= \frac{g\nu}{l}\,h_0 \left[(B_2 + B_3)\cos \nu M t + \right.$$

$$\left. + (B_2 - B_3) i \sin \nu M t\right] e^{i\nu\left[x - \left(U + \frac{d}{2}\right)t\right]}$$

$$v_L = \frac{g\nu}{l}\,h_0 \sum_{k=2}^{3} C_k e^{i\nu(x - c_k t i)} =$$

$$= \frac{g\nu}{l}\,h_0 \left[(C_2 + C_3)\cos \nu M t + \right.$$

$$\left. + (C_2 - C_3) i \sin \nu M t\right] e^{i\nu\left[x - \left(U + \frac{d}{2}\right)t\right]}$$

die wegen ihrer relativ geringen Schwingungsdauer als "meteorologischer Lärm" bezeichneten Änderungsprozesse wiedergeben.

In Fig. 1a, b, c sind die Verläufe von h, u, v sowie h_Q u_Q, v_Q für $L = 5 \cdot 10^6$ [m] und $\varepsilon = |\varepsilon| = 10^{-1}$, $\delta = |\delta| = 10^{-1}$ als Funktion von t an der Stelle $x = 0$ dargestellt.

Es ergibt sich die für die zeitliche Entwicklung atmosphärischer Felder allgemein charakteristische Tatsache, daß der Verlauf der kurzdauernden Schwankungen um einen zeitlich zügigen Gang in den meteorologischen Elementen wesentlich bestimmt wird durch die — im Modell durch ε und δ definierten — ageostrophischen Windfelder, die man in der Ausgangssituation vorfindet, während die —

durch h_Q, u_Q, v_Q wiedergegebenen — zügigen Verläufe weitgehend durch die Druckverteilung zur Ausgangszeit festgelegt werden.

So ergibt sich mit den Näherungen (19a) bei einer Auslenkung des Anfangswindfeldes v^0 gegenüber dem geostrophischen Windfelde v_g^0 um $\varepsilon = |\varepsilon| e^{i\nu\varphi_\varepsilon}$ für h_Q eine reelle Amplitude von

$$|A_1| = \sqrt{1 + \left(\frac{gH}{m}|\varepsilon|\right)^2 - \frac{2gH}{m^2}|\varepsilon| \cos \nu\varphi_\varepsilon}$$

und eine Phasenverschiebung $\nu\alpha$ gegenüber h_Q mit $\varepsilon = 0$, die sich bestimmt aus

$$\sin \nu\alpha = |A_1|^{-1} \cdot \frac{gh}{m^2} |\varepsilon| \sin \nu\varphi_2 ,$$

worin φ_ε den Winkel der im allgemeinen komplexen Zahl ε bedeutet. Bei einer Beschränkung von $|\varepsilon| \leq 10^{-1}$ ergibt sich, daß die Partialwelle in h_Q eines durch $\varepsilon = |\varepsilon| e^{i\nu\varphi_\varepsilon}$ charakterisierten Anfangsfeldes gegenüber einem durch $\varepsilon = 0$ definierten Anfangsfelde in v^0 eine Amplituden- und Phasenänderung erfährt, deren Betrag beschränkt bleibt durch

$$|\triangle A_1| \leq |\varepsilon| \frac{gH}{m^2}, \quad |\sin \nu\alpha| \leq |\varepsilon| \frac{gH}{m^2}.$$

Die gleichen Abschätzungen ergeben sich auch für die Amplituden B_1, C_1 der Funktionen u_Q, v_Q.

Die Tabelle 3 gibt diese maximalen Beträge für $|\varepsilon| = 10^{-1}$ in Abhängigkeit von der Wellenlänge wieder.

Tab. 3. Maximale Amplitudenänderung und Phasenverschiebung, hervorgerufen durch eine Auslenkung des Anfangswindfeldes v^0 um $= 10^{-1} e^{i\nu\varphi_\varepsilon}$ gegenüber dem geostrophischen Windfeld.

L $]10^6\ m[$	Maximale relative Amplitudenänderung $\lvert \triangle A_1 \rvert$	Maximale Phasenverschiebung10 $\lvert \nu\alpha \rvert$
30	2,6 %	1,5°
25	3,4 %	2,0°
20	4,4 %	2,5°
15	5,8 %	3,3°
10	7,6 %	4,4°
5	9,3 %	5,4°
1	10,0 %	5,7°

Der Einfluß der ageostrophischen Komponente u bzw. δ im Anfangswindfeld auf Amplitude und Phase der Funktionen h_Q, u_Q, v_Q ist unerheblich.

Dagegen wächst das Amplitudenverhältnis zwischen kurz- und langperiodischen Schwingungen der Druckfunktion h und der ageostrophischen Komponente u — für kurze Wellen näherungsweise ausdrückbar durch

$$\frac{|A_2 - A_3|}{A_1} \text{ bzw. } \frac{|B_2 + B_3|}{|B_1|} —$$

bei festgehaltenem δ — der Einfluß von ε ist bei kurzen Wellen unerheblich — mit abnehmender Wellenlänge stark an, so daß bereits bei Wellenlängen in der Größenordnung von einigen 1000 km, wie Fig. 1a, b veranschaulichen, nicht mehr lediglich von einer durch den meteorologischen Lärm bewirkten Unruhe im zeitlichen Gang der meteorologischen Elemente gesprochen werden kann.

Es muß jedoch beachtet werden, daß sowohl δ als auch ε nicht unabhängig von der Wellenlänge angenommen werden können, da sicherlich allgemein

$$\lim_{L \to 0} \delta = 0 \text{ und } \lim_{L \to 1} \varepsilon = 1 \text{ gilt.}$$

Das ergibt sich schon daraus, daß die Lösungen (11, 17, 18) mit $\delta \to 0$, $\varepsilon \to 1$ in die Lösungen der Differentialgleichungen für reine Gravitationswellen, bzw. bei Annahme adiabatischer Zustandsänderungen in die Lösungen der Diff. Gl. für Schallwellen konvergieren, die ja für sehr kleine Wellenlängen die tatsächlichen physikalischen Vorgänge richtig beschreiben.

Weiterhin dürfte durch Superposition mehrerer Wellenfunktionen verschiedener Wellenlänge und Phase eine Glättung der kurzperiodischen Lärmschwankungen bewirkt werden.

Da den kurzdauernden Schwankungen wegen der Ungenauigkeit in den Meßdaten für u, v, z. Zt. $t = 0$ keine meteorologische Bedeutung beigemessen werden kann, wird man sich bei der rechnerischen Prognose mit der Ermittlung des zeitlichen zügigen Grundverlaufs — im Modell charakterisiert durch die Funktionen h_Q, u_Q, v_Q — begnügen müssen.

Dieser zügige Grundverlauf soll abkürzend als "Trend" bezeichnet werden, analog der

Ausdrucksweise in der statistischen Konjunkturforschung.

Ignoriert man also diese kurzperiodischen Vorgänge h_L, u_L, v_L und sieht man von dem geringen Einfluß ab, den die Anfangsfelder der ageostrophischen horizontalen Windkomponenten auf den Verlauf der Funktionen h_Q, u_Q, v_Q ausüben, so bestimmt sich der Trend der Variabeln h, u, v in dem betrachteten Modell lediglich durch die Vorgabe der Druckfunktion h^0 zu einem bestimmten Zeitpunkt, und zwar erhält man mit diesen Vernachlässigungen für

$$\bar{h} = h_0\, e^{i\nu\,(x - c_1 t)}$$

$$\bar{u} = \frac{g\nu^2}{l^2}\, dh_0\, e^{i\nu(x - c_1 t)}$$

$$\bar{v} = \frac{g\nu}{l^2}\, ih_0\, e^{i\nu\,(x - c_1 t)}, \qquad (20)$$

wenn unter den gestrichenen Größen die oben definierten ausgeglichenen Variabeln verstanden werden. Für ein beliebiges Ausgangsfeld h^0 ergibt sich durch Summation über ν:

$$\bar{h} = \sum_{n=-\infty}^{\infty} h_{0\nu}\, e^{i\nu\,(x - c_{1\nu} t)}$$

$$\bar{u} = \frac{g}{l^2} \sum_{n=-\infty}^{\infty} \nu^2 d_\nu h_{0\nu}\, e^{i\nu(x - c_{1\nu} t)} \quad n = \frac{Lv^\star}{2\pi}$$

$$\bar{v} = \frac{g}{l} \sum_{n=-\infty}^{\infty} \nu h_{0\nu}\, e^{i\nu(x - c_{1\nu} t)} \qquad (20a)$$

In den Lösungen der linearisierten Gleichungen ergibt sich diese Darstellung einfach durch Wegstreichen der den meteorologischen Lärm zum Ausdruck bringenden Funktionen h_L, u_L, v_L sowie der die ageostrophischen Komponenten (ε, δ) enthaltenden Terme in den Amplituden A_1, B_1, C_1.

Da die Funktionen (20a) für alle Anfangslagen, bei denen die Felder der horizontalen Windgeschwindigkeiten nur unwesentlich aus dem geostrophischen Windfeld ausgelenkt sind, die Lösungen der Differentialgleichungen (1—3) mit für synoptische Belange ausreichender Genauigkeit beschreiben dürften, so ist es naheliegend, die Differentialgleichungen von vornherein so zu modifizieren, daß deren

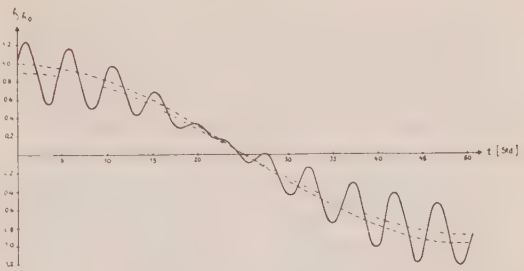

Fig. 1a. Lärm- und Trendkurven der Funktion h

——— h/h_0 $L = 5 \cdot 10^6\, m$, $\varepsilon = \delta = 10^{-1}$
- - - - - $\bar{h}/h_0$ $U = 15\, m\, \mathrm{sec}^{-1}$, $gH = 8 \cdot 10^4\, m^2\, \mathrm{sec}^{-2}$
– · – · – h_Q/h_0 $l = 10^{-4}\, \mathrm{sec}^{-1}$

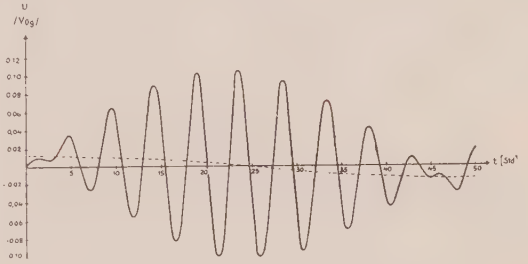

Fig. 1b. Lärm- und Trendkurven der Funktion u

——— $u/|v_{0g}|$ $L = 5 \cdot 10^6\, m$, $\varepsilon = \delta = 10^{-1}$
- - - - - $\bar{u}/|v_{0g}|$ $U = 15\, m\, \mathrm{sec}^{-1}$, $gH = 8 \cdot 10^4\, m^2\, \mathrm{sec}^{-2}$
$\approx u_Q/|v_{g0}|$ $l = 10^{-4}\, \mathrm{sec}^{-1}$

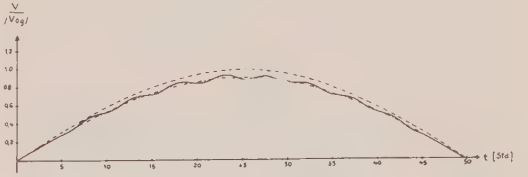

Fig. 1c. Lärm- und Trendkurven der Funktion v

——— $v/|v_{0g}|$ $L = 5 \cdot 10^6\, m$, $\varepsilon = \delta = 10^{-1}$
- - - - - $\bar{v}/|v_{0g}|$ $U = 15\, m\, \mathrm{sec}^{-1}$, $gH = 8 \cdot 10^4\, m^2\, \mathrm{sec}^{-2}$
– · – · – $v_Q/|v_{0g}|$ $l = 10^4\, \mathrm{sec}^{-1}$

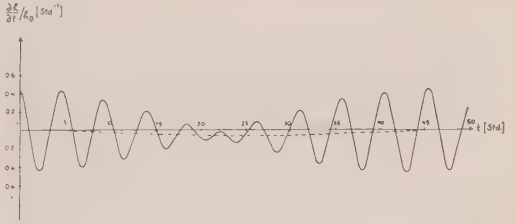

Fig. 1d. Lärm- und Trendkurven der Funktion $h = \dfrac{\partial h}{\partial t}$

——— h_t/h_0 $L = 5 \cdot 10^6\, m$, $\varepsilon = \delta = 10^{-1}$
- - - - - $\bar{h}_t/h_0$ $U = 15\, m\, \mathrm{sec}^{-1}$, $gH = 8 \cdot 10^4\, m^2\, \mathrm{sec}^{-2}$
$\approx (h_Q)_t/h_0$ $l = 10^4\, \mathrm{sec}^{-1}$

Lösungen nur die Trendkurven liefern, wie sie im benutzten Modell durch die Näherungen (20a) beschrieben werden, ein Rechenverfahren, das auf die direkte Messung oder Berechnung von Windfeldern der Ausgangswetterlage verzichtet.

Die zu den Lösungen (20a) zugeordneten Differentialgleichungen anstelle der Gln. (1—3) ergeben sich, wenn $c_1 = U - d$ durch $U\left(1 - \frac{l^2}{\nu^2 m^2}\right)$ angenähert wird, zu

$$\bar{u} = -\frac{g}{l^2} D\bar{h}_x \tag{21}$$

$$\bar{v} = \frac{g}{l} \bar{h}_x \tag{22}$$

$$D\bar{h} = \frac{lU}{g} \bar{v} - H\bar{u}_x \tag{23}$$

bzw. in auf die Variable h reduzierter Form

$$D\bar{h}_{xx} - \frac{l^2}{gH} \bar{h}_t = 0 \tag{24}$$

Die Mitnahme der ageostrophischen Windkomponente $\bar{u}$ in dem Vektor $\bar{v}$ ist in diesen Gleichungen nur erforderlich, wenn die zeitliche Entwicklung der meteorologischen Variabeln berechnet werden soll. Wie die Tab. 1 ausweist, macht die ageostrophische Komponente $\bar{u}$ nur wenige Prozent der geostrophischen Komponente $\bar{v}$ aus, so daßes bei Betrachtung des Windfeldes selbst ausreicht, aus der vorliegenden Lösung für h bzw. p den geostrophischen Wind durch Gradientbildung zu errechnen und den tatsächlichen Wind durch diesen zu approximieren.

V. Numerische Integration

Wegen der erheblichen mathematischen Schwierigkeiten, die der Lösung der allgemeinen nicht vereinfachten nichtlinearen hydro- und thermodynamischen Gleichungen entgegenstehen, wird man gezwungen sein, wenigstens näherungsweise eine Lösung durch eine numerische schrittweise Integration herbeizuführen.

Man begnügt sich zunächst mit der Errechnung der Tendenz der meteorologischen Variabeln $\frac{\partial \psi}{\partial t}$, wenn ψ eine beliebige meteorologische Variable bezeichnet, ersetzt dann näherungsweise den zeitlichen Differentialquotienten durch den entsprechenden Differenzenquotienten $\frac{\Delta \psi}{\Delta t}$ und ermittelt durch Annahme eines festen Wertes für Δt die während der Zeit Δt eintretende Änderung $\Delta \psi$, die man zu dem zur Zeit $t = 0$ vorgefundenen Wert von ψ addiert.

Durch fortgesetzte Anwendung dieses Rechenverfahrens erhält man eine diskrete Folge von Feldern ψ ($t = 0$; Δt; $2\Delta t$; $3\Delta t$ . .), die bei hinreichend klein gewählten Intervallen Δt die Lösung der Differentialgleichung hinreichend genau zu approximieren vermögen.

Es bieten sich dabei zwei hinsichtlich des Grades der Rechenschwierigkeit und des Umfanges der auszuführenden Integrationsschritte unterschiedliche Rechenverfahren an, je nachdem ob die zeitliche Änderung der Momentanwerte $\frac{\partial \psi}{\partial t}$ oder die zeitliche Änderung des Trends $\frac{\partial \bar{\psi}}{\partial t}$ berechnet wird.

Es besteht also die Möglichkeit, die Diff. Gln. in den Momentanwerten oder in den zeitlich ausgeglichenen Werten anzuschreiben.

1. Für das gewählte Modell einer homogenen Atmosphäre führt die erste Berechnungsmethode auf das folgende Rechenschema, das sich unmittelbar durch Auflösung der Gln. (1—3) nach den lokalen zeitlichen Differentialquotienten ergibt:

$$u_t = -Uu_x - gh_x + lv \approx \frac{\Delta u}{\Delta t} \tag{25a}$$

$$v_t = -Uv_x - lu \approx \frac{\Delta v}{\Delta t} \tag{25b}$$

$$h_t = -Uh_x + \frac{lU}{g} v - Hu_x \approx \frac{\Delta h}{\Delta t} \tag{25c}$$

Diese Gleichungen erfassen sowohl den ausgeglichenen zügigen Grundverlauf (Trend) als auch die kurzperiodischen Oszillationen (Lärm). Bei der Wahl des Zeitinkrementes Δt ist deshalb zu berücksichtigen, daß die ermittelten Differentialquotienten nur während einer relativ kurzen Zeitspanne als konstant betrachtet werden können.

In Fig. 1d ist $\frac{\partial h}{\partial t}$ und $\frac{\partial \bar{h}}{\partial t}$ als Funktion der Zeit dargestellt. Beide Werte unterscheiden sich in ihrer Größe erheblich, $\left|\frac{\partial h}{\partial t}\right| \gg \left|\frac{\partial \bar{h}}{\partial t}\right|$, weshalb auch bei der prognostischen Verwertung der entsprechenden Differenzenquotienten in gleicher Weise unterschiedliche Zeitintervalle verwendet werden müssen.

Zu einer sinnvollen Festsetzung des Inkrementes Δt gelangt man, wenn $\Delta t \ll T$ gewählt wird.

Bei Verwendung der Berechnungsgleichungen (25) führt dies zu

$$\Delta t \ll T_{2,3} = \frac{L}{M}.$$

Stellt $L_{\min}$ die kürzeste Wellenlänge dar, auf deren Erfassung gerade noch Wert gelegt wird, bzw. deren Ermittlung aus dem Beobachtungsmaterial des Stationsnetzes gerade noch möglich ist, so ergibt sich für

$$\Delta t \ll \frac{L_{\min}}{M}.$$

$L_{\min}$ wird für großräumige (zirkumpolare) Darstellungen in der Grössenordnung 10^6 [m] liegen, so daß — vgl. Tab. 2. — $\Delta t \ll 1$ [Std] zu wählen wäre. Der Vorteil dieses Berechnungsschemas liegt darin, daß zur Ermittlung der Tendenzen nur elementare Rechenprozesse (vier Spezies, räumliche Differentiationen I. Ordnung) erforderlich sind, die ohne sonderliche Schwierigkeiten durch automatische Rechenmaschinen ausgeführt werden können.

Die zwangsläufige Mitberechnung der kurzdauernden Lärmprozesse — ausgezogene Kurven der Fig. 1 — stellt dabei lediglich ein notwendiges Übel dar, da den ermittelten Funktionen h_L, u_L, v_L, die näherungsweise auch bei einer numerischen Integration der Gln. (25) erfaßt werden, so lange keinerlei physikalische Realität zukommt, als auch die Abweichung vom geostrophischen Windfeld im Ausgangsfelde meßtechnisch nicht erfaßt werden kann.

Um nicht eine übertriebene Genauigkeit vorzutäuschen, wird es notwendig sein, nach Ermittlung des zeitlichen Verlaufs der meteorologischen Variabeln diese völlig unsicheren Bestandteile durch Glättung mit den üblichen Methoden der Statistik wieder zu eliminieren.

Bei der praktischen Berechnung wird man also willkürliche, sich nur im Rahmen der Meßfehler haltende Werte für ε, δ annehmen können, ohne daß die Genauigkeit der mittleren Verläufe — $\bar{h}$, $\bar{u}$, $\bar{v}$ — merklich beeinträchtigt wird. Naheliegenderweise wird man als Ausgangsfeld für die horizontalen Windgeschwindigkeiten das geostrophische Windfeld zugrunde legen, ohne daß jedoch diese berechneten Winddaten für den Verlauf der Trendkurven oder -felder kritisch sind.

Der Nachteil des Rechenverfahrens besteht darin, daß nur relativ kurze Zeitintervalle (einige Minuten) verwendet werden können. Dieser Nachteil wird jedoch weitgehend ausgeglichen durch die Einfachheit der erforderlichen Rechenprozesse.

2. Bei Verwendung der hydro- und thermodynamischen Diff. Gln. mit ausgeglichenen Größen führt das Berechnungsschema bei Anwendung auf das betrachtete homogene Modell auf die Gln. (21—23) bzw. Gl. (24), aus welcher man die Tendenz des Trends in h durch Auflösung nach $\bar{h}_t$ mit der formalen Lösung

$$\bar{h}_t = \frac{U\bar{h}_{xx}}{\frac{\partial^2}{\partial x^2} - \frac{l^2}{gH}} \text{ gewinnt.}$$

Der Vorteil eines solchen Rechenverfahrens, in dem die Elimination der kurzperiodischen Schwankungen bereits in der differentiellen Form der Gleichungen, nicht erst in den Lösungsfunktionen vorgenommen wird, besteht darin, daß wesentlich größere Zeitintervalle Δt bei Ersatz des Differentialquotienten durch den Differenzenquotienten verwendet werden können.

Mit den gleichen Abschätzungen wie unter 1) ergibt sich wegen der größeren Schwingungsdauer T_1 für

$$\Delta t \ll \frac{L_{\min}}{c_1} \approx 19 \text{ Std.}$$

Die Anzahl der zur Überbrückung des gleichen Vorhersagezeitaums notwendigen Integrationsschritte nach Verfahern 2) reduziert sich also gegenüber dem Verfahren 1) um rund das 20-fache.

Andrerseits erfährt jedoch das Berechnungsschema insofern eine für den Rechenaufwand wesentlich ins Gewicht fallende Komplikation, als bereits zur Ermittlung der Tendenz die Lösung einer Differentialgleichung — im Modell Gl. (24) — erforderlich wird.

Die sinngemäßen nichtlinearisierten und nicht spezialisierten Diff. Gln., die sich nach Elimination des Lärmes ergeben, lauten entsprechend Gln. (21—23):

$$\overline{\mathfrak{V}} = \mathfrak{k}x \frac{g}{\bar{l}} \nabla\bar{h} - \frac{g}{\bar{l}^2} \frac{\bar{d}}{dt} \nabla\bar{h}, \text{ oder bei Verwendung der Druckfunktion } p.$$

$$\overline{\mathfrak{V}} = \mathfrak{k}x \frac{1}{\bar{l}\bar{\varrho}} \nabla\bar{p} - \frac{1}{\bar{l}^2} \frac{\bar{d}}{dt} \frac{1}{\bar{\varrho}} \nabla\bar{p}, \quad \frac{\bar{d}}{dt} = \frac{\partial}{\partial t} + \overline{\mathfrak{v}} \cdot \nabla_3 \text{ und} \tag{26a}$$

$$\frac{\partial\bar{\varrho}}{\partial t} = -\nabla_3 \bar{\varrho}\,\overline{\mathfrak{v}},$$

$\overline{\mathfrak{V}}, \nabla$ = 2 dimensionale Vektoren
$\overline{\mathfrak{v}}, \nabla_3$ = 3 dimensionale Vektoren (26b)

zu denen noch die dritte Komponente der Bewegungsgleichung, die in Form der statischen Grundgleichung eingeführt werden könnte, sowie eine thermodynamische Diff. Gl. tritt.

Die Elimination der Lärmvorgänge im allgemeinen Fall führt demnach darauf hinaus, in dem Diff. Gl. System die Bewegungsgleichungen für die horizontalen Komponenten zu ersetzen durch die durch H. Philipps (1939) aufgestellte sogenannte quasigeostrophische Windgleichung (26a), die nach Linearisierung unmittelbar auf die Form der Gln. (25a, 25b) führt.

Es kann zur Zeit nicht abgeschätzt werden, welches Verfahren für eine praktische rechnerische Wettervorhersage rationeller sein wird, da dies wesentlich von der technischen Leistungsfähigkeit der zur Verwendung gelangenden Rechenmaschinen abhängen wird. Jedoch dürfte auch das im allgemeinen als wenig aussichtsreich betrachtete Verfahren der numerischen Integration des ursprünglichen Gleichungssystems unter Mitnahme meteorologischer Lärmvorgänge bei Einsatz sehr schnell rechnender Automaten erfolgversprechend sein.

Bei einer Behandlung der Gleichungen im zweidimensionalen Rahmen wird die Auflösung einer immerhin sehr komplizierten Diff. Gl. erspart, im dreidimensionalen Falle — bei Ersatz der vertikalen Komponente der Bewegungsgleichung durch die statische Grundgleichung, der eine Elimination der in vertikaler Richtung verlaufenden kurzperiodischen Schallvorgänge bewirkt, — wird man lediglich auf die Notwendigkeit einer Integration über die vertikale Koordinate, also auf die Lösung einer gewöhnlichen Diff. Gl. geführt, in welcher die horizontalen Koordinaten als Parameter auftreten. Ein für eine numerische Integration geeignetes Gleichungssystem unter Einschluss meteorologischer Lärmvorgänge in der Horizontalen wurde von A. Eliassen (1949) angegeben.

Die Unkenntnis in den Ausgangsfeldern der Windgeschwindigkeit ist dabei, zumindest für höhere Breiten, kein ernsthaftes Hindernis, da diese Felder ohne Bedenken durch das durch den Kräftegleichgewichtszustand definierte geostrophische Windfeld ersetzt werden können.

LITERATUR

Charney, I. G., 1949: On a physical basis for numerical prediction of large-scale motions in the atmosphere. *Journ. of Met.*, **6**, 6, pp. 371—385.

Eliassen, A., 1949: The quasistatic equations of motion with pressure as independent variable. *Geof. Publ.* **12**, 3.

Phillipps, H., 1939: Die Abweichung vom geostrophischen Wind. *Meteor. Z.*, **56**, pp. 460—483.

Le bilan de la rotationnelle absolue dans l'atmosphère

Par J. VAN MIEGHEM, Université de Bruxelles

(Manuscrit reçu le 27 Juillet 1951)

Abstract

The equation of balance of the absolute vorticity is derived from V. Bjerknes' Circulation Theorem, formulated in an arbitrary moving frame of general coordinates. The flux and the rate of production of absolute vorticity are defined. The case of the component of absolute vorticity normal to the equiscalar surfaces of a meteorological quantity is considered. From the expression of the horizontal convective flux of the vertical component of the relative vorticity, a relation between the horizontal meridional flows of relative vorticity and angular momentum is deduced.

Rapportons l'atmosphère à un système de coordonnées curvilignes quelconques (x^1, x^2, x^3), animé d'un mouvement variable d'un point à un autre et d'un instant à un autre. Désignons respectivement par V_i, v_i et W_i, $(i = 1, 2, 3)$, les composantes covariantes en variables x^i de la vitesse $\mathbf{V}$ de l'air par rapport au système de référence inertial (système géocentrique fixe), de la vitesse $\mathbf{v}$ de l'air par rapport au référentiel mobile (x^1, x^2, x^3), et de la vitesse $\mathbf{W}$ du référentiel mobile par rapport au référentiel fixe, $(V_i = W_i + v_i)$. Soient $\gamma_{ij} \equiv \gamma_{ji}$ $(i, j = 1, 2, 3)$ les coefficients de la métrique en variables x^i et $\gamma^{ij} \equiv \gamma^{ji}$ les mineurs algébriques normés des éléments γ_{ij} du déterminant $\gamma \equiv \| \gamma_{ij} \|$. Les γ_{ij}, γ^{ij} et γ sont des fonctions des x^i et aussi du temps t lorsque le référentiel (x^1, x^2, x^3) se déforme tout en se mouvant; par contre, lorsque ce référentiel se meut à la manière d'un corps solide, les γ^{ij}, γ_{ij} et γ sont indépendants du temps t. Rappelons que $\frac{1}{\sqrt{\gamma}} \frac{\partial \gamma}{\partial t} = \operatorname{div} \mathbf{W}$ (Van Mieghem et Vandenplas, 1950).

Ensuite, introduisons les composantes contravariantes ξ^k de la rotationnelle absolue $\operatorname{rot} \mathbf{V}$, on sait que

$$\sqrt{\gamma}\ \xi^k \equiv V_{ij} \equiv \frac{\partial V_j}{\partial x^i} - \frac{\partial V_i}{\partial x^j} \equiv - V_{ji}, \quad (1)$$

où (i, j, k) représente une permutation tournante de (1, 2, 3) (loc. cit.). Rappelons que $\xi^k : \sqrt{\gamma^{kk}}$ est la projection orthogonale du vecteur $\operatorname{rot} \mathbf{V}$ sur la normale à la surface de coordonnées $x^3 = Cste$ au point considéré. Notons encore l'identité évidente

$$\frac{\partial \sqrt{\gamma}\ \xi^k}{\partial x^k} = 0, \quad (k = 1, 2, 3) \qquad (1')$$

en x^i et t.

Enfin, soient p la pression atmosphérique, α le volume spécifique de l'air et F_i les composantes covariantes de la force de frottement $\mathbf{F}$. Posons

$$\frac{\partial p}{\partial x^i} \frac{\partial \alpha}{\partial x^j} - \frac{\partial p}{\partial x^j} \frac{\partial \alpha}{\partial x^i} \equiv \sqrt{\gamma}\ s^k \text{ et}$$

$$\frac{\partial F_j}{\partial x^i} - \frac{\partial F_i}{\partial x^j} \equiv \sqrt{\gamma}\ f^k, \qquad (2)$$

où, comme dans (1), (i, j, k) est une permutation tournante quelconque déduite de (1, 2, 3).

Alors, le théorème de la circulation de V. Bjerknes s'écrit, (loc. cit.)

$$\frac{d(\xi_N \delta\sigma)}{dt} = (s_N + f_N)\,\delta\sigma, \qquad (3)$$

où ξ_N, s_N et f_N sont les projections orthogonales des vecteurs rot**V**, **s** et rot**F** sur la demi-normale N à l'élément $\delta\sigma$ de la surface σ prise à l'instant t, ($\delta t \equiv 0$).

En remarquant que

$$\xi_N \delta\sigma \equiv \xi^k N_k \delta\sigma = \sqrt{\gamma}\,\xi^k \delta x^i \delta x^j = V_{ij}\,\delta x^i \delta x^j, \qquad (4)$$

où (i, j, k) représente une permutation tournante de (1, 2, 3) et où N_k sont les composantes covariantes du vecteur-unité **N** porté par la normale N, on établit aisément (loc. cit.) que

$$\frac{d(\xi_N \delta\sigma)}{dt} = \left(\frac{dV_{ij}}{dt} + V_{lj}\frac{\partial v^l}{\partial x^i} + V_{il}\frac{\partial v^l}{\partial x^j}\right)\delta x^i \delta x^j. \quad (i, j, l = 1, 2, 3) \qquad (5)$$

En transformant $(s_N + f_N)\,\delta\sigma$ comme $\xi_N \delta\sigma$ a été transformé en (4) et en substituant (5) dans (3), on trouve la forme rotationnelle des équations de la dynamique atmosphérique en variables x^i, à savoir:

$$\frac{1}{\sqrt{\gamma}}\frac{d\sqrt{\gamma}\,\xi^k}{dt} + \frac{\partial v^i}{\partial x^i}\xi^k - \frac{\partial v^k}{\partial x^i}\xi^i = s^k + f^k; \quad (i, k = 1, 2, 3) \qquad (6)$$

d'où, finalement, grâce à (1'), l'équation du bilan de la composante ξ^k de la rotationnelle absolue rot**V**,

$$\frac{1}{\sqrt{\gamma}}\frac{\partial\sqrt{\gamma}\,\xi^k}{\partial t} + \frac{1}{\sqrt{\gamma}}\frac{\partial}{\partial x^i}\left[\sqrt{\gamma}\,(\xi^k v^i - v^k \xi^i)\right] = s^k + f^k, \quad (i, k = 1, 2, 3) \qquad (6a)$$

ou encore,

$$\frac{1}{\sqrt{\gamma}}\frac{\partial\sqrt{\gamma}\,\xi^k}{\partial t} + \operatorname{div}(\xi^k \mathbf{v} - v^k \operatorname{rot}\mathbf{V}) = s^k + f^k. \qquad (6b)$$

De ce bilan, il résulte que le flux, dans le référentiel mobile, de la composante ξ^k de la rotationnelle absolue rot**V** est défini par les composantes contravariantes

$$C^{ki} \equiv \xi^k v^i - v^k \xi^i, \qquad (7)$$

et que le taux de production de ξ^k, dans ce référentiel, s'exprime à l'aide de $s^k + f^k$, c'est-à-dire à l'aide des solénoïdes isobares-isostères et des tubes de tourbillon de la force de frottement **F**.

Remarquons que $C^{kk} \equiv 0$ et que, par suite, *le flux de ξ^k à travers la surface $x^k = C^{ste}$ est nul.* De plus, le flux C^{ki}, $(i \neq k)$, se décompose en un *flux convectif* $\xi^k v^i$ le long du courant atmosphérique dans la surface $x^k = C^{ste}$ et en un *flux non convectif* — $v^k \xi^i$ qui dépend du courant atmosphérique v^k à travers la surface $x^k = C^{ste}$. *Lorsque la surface $x^k = C^{ste}$ est une surface substantielle* $\left(\frac{dx^k}{dt} \equiv v^k \equiv 0\right)$ *le flux non convectif est nul.*

2. Supposons qu'à chaque instant t, les surfaces équiscalaires d'une grandeur météorologique, — la température potentielle Θ par exemple, — constituent une famille de surfaces à un paramètre. Identifions ces surfaces avec les surfaces de coordonnées $x^3 = Cste$ et, leurs trajectoires orthogonales avec les lignes de coordonnée $x^3 = \text{var}$. On a, alors, $\gamma_{31} \equiv \gamma_{32} \equiv \gamma^{31} \equiv \gamma^{32} \equiv 0$, $\gamma^{33}\gamma_{33} \equiv 1$, $\gamma \equiv \gamma_{33}\gamma_*$ avec $\gamma_* \equiv \gamma_{11}\gamma_{22} - (\gamma_{12})^2$, et

$$\zeta \equiv \frac{\xi^3}{\sqrt{\gamma^{33}}} \equiv \sqrt{\gamma_{33}}\,\xi^3 \equiv \operatorname{rot}_z \mathbf{V},\ v_z \equiv \sqrt{\gamma_{33}}\,v^3, \qquad (8)$$

où ζ et v_z ne sont autres que les projections orthogonales de rot**V** et de **v** sur la normale z à la surface $x^3 = Cste$ passant par le point considéré. Cette normale est tangente à la ligne de coordonnée $x^3 = \text{var}$. En particulier, lorsque $x^3 \equiv \Theta$, on a $v^3 \equiv \frac{d\Theta}{dt}$ et $\sqrt{\gamma^{33}} \equiv |\nabla\Theta|$ où $|\nabla\Theta|$ est la valeur algébrique de l'ascendant de la température potentielle Θ.

En substituant (8) dans (6a), on obtient le bilan de ζ,

$$\frac{1}{\sqrt{\gamma_*}}\frac{\partial\sqrt{\gamma_*}\,\zeta}{\partial t} + \frac{1}{\sqrt{\gamma_*}}\frac{\partial\left[\sqrt{\gamma_*}\,(\zeta v^\alpha - v_z \xi^\alpha)\right]}{\partial x^\alpha} = s_z + f_z, \quad (\alpha = 1, 2) \qquad (9)$$

ou encore,

$$\frac{1}{\sqrt{\gamma_*}}\frac{\partial\sqrt{\gamma_*}\zeta}{\partial t}+\frac{1}{\sqrt{\gamma_*}}\frac{\partial\left(\sqrt{\gamma_*}\zeta v^a\right)}{\partial x^a}+$$

$$+\frac{v_z}{\sqrt{\gamma_*}}\frac{\partial\left(\sqrt{\gamma_*}\zeta\right)}{\partial z}-\frac{\partial v^3}{\partial x^a}\sqrt{\gamma_{33}}\,\xi^a=s_z+f_z \tag{9a}$$

où $\partial z\equiv\sqrt{\gamma_{33}}\,\partial x^3$ et où s_z et f_z sont les nombres de solénoïdes isobares-isostères et de tubes-unités de tourbillon de la force de frottement par unité d'aire, dans les surfaces $x^3=Cste$. La somme s_z+f_z représente le taux de production de ζ dans $x^3=Cste$.

Lorsque, dans l'équation (9a), on néglige les termes en $\frac{1}{\sqrt{\gamma_*}}\frac{\partial\sqrt{\gamma_*}}{\partial t}$, $\frac{1}{\sqrt{\gamma_*}}\frac{\partial\sqrt{\gamma_*}}{\partial z}$ et en γ_{33}, on obtient une équation établie par S. Petterssen (1950). Cette remarque fixe le degré de validité de l'équation de Petterssen. Notons que $\frac{1}{\sqrt{\gamma_*}}\frac{\partial\sqrt{\gamma_*}}{\partial t}$ exprime la déformation subie par les surfaces $x^3=Cste$ et que $\frac{-1}{\sqrt{\gamma_*}}\frac{\partial\sqrt{\gamma_*}}{\partial z}$ représente la courbure moyenne de ces surfaces.

3. Proposons-nous d'étudier le flux de la composante ζ de la rotationnelle dans le cas de coordonnées curvilignes triorthogonales (x^1, x^2, x^3). Dans ce cas, on a: $\gamma_{ij}\equiv\gamma^{ij}\equiv 0$ pour $i\neq j$ et $\gamma^{ii}\gamma_{ii}\equiv 1$ respectivement pour $i=1, 2, 3$. Désignons par x, y, z les axes tangents aux lignes de coordonnée x^i et par v_x, v_y, v_z les composantes coordonnées de la vitesse relative $\mathbf{v}$ de l'air dans le trièdre trirectangle xyz, supposé dextrogyre. Les axes x, y, z sont normaux respectivement aux surfaces $x^1=Cste$, $x^2=Cste$, $x^3=Cste$. On a donc $v_x\equiv\sqrt{\gamma_{11}}\,v^1=v_1:\sqrt{\gamma_{11}}$, $v_y\equiv\sqrt{\gamma_{22}}\,v^2=v_2:\sqrt{\gamma_{22}}$, $v_z\equiv\sqrt{\gamma_{33}}\,v^3=v_3:\sqrt{\gamma_{33}}$, $\partial x\equiv\sqrt{\gamma_{11}}\,\partial x^1$, $\partial y\equiv\sqrt{\gamma_{22}}\,\partial x^2$, $\partial z\equiv\sqrt{\gamma_{33}}\,\partial x^3$,

et

$$\zeta\equiv 2\,\omega_z+\frac{1}{\sqrt{\gamma_{11}\gamma_{22}}}\left(\frac{\partial v_2}{\partial x^1}-\frac{\partial v_1}{\partial x^2}\right),$$

où ω_z désigne la composante coordonnée suivant l'axe z de la rotation instantanée du trièdre xyz par rapport au référentiel inertial. Nous avons vu que le flux de ζ se produit dans les surfaces $x^3=Cste$ et que la partie convective de ce flux s'exprime, dans le trièdre xyz, à l'aide des composantes coordonnées $(\zeta v_x, \zeta v_y, 0)$.

Si nous portons uniquement notre attention sur la partie ζ_* de ζ liée au mouvement de l'air par rapport au référentiel mobile; on voit que

$$\zeta_*\equiv\frac{1}{\sqrt{\gamma_{22}}}\frac{\partial\left(\sqrt{\gamma_{22}}\,v_y\right)}{\partial x}-$$

$$-\frac{1}{\sqrt{\gamma_{11}}}\frac{\partial\left(\sqrt{\gamma_{11}}\,v_x\right)}{\partial y}\equiv\mathrm{rot}_z\,\mathbf{v},$$

avec $\zeta\equiv\zeta_*+2\,\omega_z$.

Quant au flux convectif de ζ_* dans le référentiel mobile, il est défini par les composantes coordonnées $(\zeta_* v_x, \zeta_* v_y, 0)$ dans xyz. Remarquons que

$$\left\{\begin{aligned}\zeta_* v_x&=\frac{1}{\gamma_{22}}\frac{\partial}{\partial x}\left(\gamma_{22}v_x v_y\right)-v_y\,\mathrm{div}_h\,\mathbf{v}+\\&\quad+\frac{1}{2}\frac{1}{\gamma_{11}}\frac{\partial}{\partial y}\left\{\gamma_{11}\left[(v_y)^2-(v_x)^2\right]\right\},\\\zeta_* v_y&=\frac{-1}{\gamma_{11}}\frac{\partial}{\partial y}\left(\gamma_{11}v_x v_y\right)+v_x\,\mathrm{div}_h\,\mathbf{v}+\\&\quad+\frac{1}{2}\frac{1}{\gamma_{22}}\frac{\partial}{\partial x}\left\{\gamma_{22}\left[(v_y)^2-(v_x)^2\right]\right\},\end{aligned}\right.$$

où

$$\mathrm{div}_h\,\mathbf{v}\equiv\frac{1}{\sqrt{\gamma_{22}}}\frac{\partial}{\partial x}\left(\sqrt{\gamma_{22}}\,v_x\right)+$$

$$+\frac{1}{\sqrt{\gamma_{11}}}\frac{\partial}{\partial y}\left(\sqrt{\gamma_{11}}\,v_y\right).$$

On voit ainsi que, dans les surfaces $x^3=Cste$, le flux convectif de la composante normale $\zeta_*\equiv\mathrm{rot}_z\,\mathbf{v}$ de la rotationnelle relative rot$\mathbf{v}$, à travers les lignes $x^1=$ var et $x^2=$var, dépend en premier lieu de la corrélation, le long de ces lignes, entre les composantes v_x et v_y de la vitesse relative de l'air et de la corrélation, le long des mêmes lignes, entre chacune de ces

composantes et la divergence du courant dans les surfaces $x^3 = Cste$.

En particulier, lorsque le système de référence (x^1, x^2, x^3) est fixe par rapport à la terre et lorsque les coordonnées x^1, x^2, x^3 coïncident avec les coordonnées sphériques λ, φ, r, on a: $\gamma_{11} \equiv r^2 \cos^2\varphi$, $\gamma_{22} \equiv r^2$, $\gamma_{33} \equiv 1$. Le flux méridien Φ, vers le Nord, à travers le parallèle c, de la composante verticale $\zeta_* = \mathrm{rot}_z \mathbf{v}$ de la rotationnelle relative $\mathrm{rot}\,\mathbf{v}$ par rapport à la terre, est alors donné par

$$\Phi \equiv \oint_c \zeta_* v_y \, \delta x = -\frac{1}{r^2 \cos^2\varphi} \frac{\partial}{\partial y} \oint_c r^2 \cos^2\varphi \, v_x v_y \, \delta x + \oint_c v_x \, \mathrm{div}_h \mathbf{v} \, \delta x, \qquad (10)$$

où nous avons posé $\delta x \equiv r \cos\varphi \delta\lambda$ et $\frac{\partial}{\partial y} \equiv \frac{1}{r}\frac{\partial}{\partial\varphi}$.

La formule (10) montre que le flux Φ dépend 1°) de la corrélation, le long du parallèle c considéré, entre la composante zonale v_x du vent et la divergence horizontale du courant, et 2°) de la variation en latitude de la corrélation, le long du même parallèle, entre les composantes zonale (v_x) et méridienne (v_y) du vent $\mathbf{v}$. En particulier, lorsque les creux et les dorsales bariques sont orientés du SW vers le NE, ces deux corrélations sont positives; de plus, si la déviation vers l'E, par rapport aux méridiens, des creux et des dorsales, diminue lorsque la latitude augmente, la corrélation entre v_x et v_y, le long des parallèles, décroît vers le Nord. Dans ce cas, les termes du second membre de (10) sont positifs et il en est de meme du flux Φ qui est donc dirigé vers le Nord.

Enfin, notons que le flux méridien vers le Nord, à travers le parallèle c, du moment cinétique relatif de l'air par rapport à l'axe de la terre est donné par la formule de Jeffreys

$$\Psi \equiv \oint_c r^2 \cos^2\varphi \; \varrho \, v_x v_y \, \delta x,$$

où ϱ désigne la masse spécifique de l'air; par conséquent, *si l'on fait abstraction de la variation latitudinale de* ϱ, on a

$$\Phi \cong -\frac{1}{\bar{\varrho} r^2 \cos^2\varphi} \frac{\partial \Psi}{\partial y} + \oint_c v_x \, \mathrm{div}_h \mathbf{v} \, \delta x, \qquad (10a)$$

où $\bar{\varrho}$ désigne une valeur moyenne de ϱ au niveau r considéré. La relation (10a) fait apparaître le lien entre le flux méridien Φ de la composante verticale de la rotationnelle relative $\mathrm{rot}\,\mathbf{v}$ de l'air et le flux méridien Ψ du moment cinétique relatif de l'air par rapport à l'axe de la terre.

Le taux de production, par unité de surface horizontale, de la composante verticale $\mathrm{rot}_z \mathbf{v}$ de la rotationnelle relative $\mathrm{rot}\,\mathbf{v}$, est égal à $s_z + f_z$. Remarquons que s_z est positif ou négatif suivant que la rotation qui amène l'ascendant horizontal $\nabla_h \alpha$ de volume spécifique α de l'air sur le gradient horizontal $-\nabla_h p$ de la pression atmosphérique p est cyclonique ou anticyclonique. Comme $f_z \equiv \mathrm{rot}_z \mathbf{F}$, on en déduit que f_z est positif ou négatif suivant que la composante verticale $\mathrm{rot}_z \mathbf{F}$ de la rotationnelle de $\mathbf{F}$ est cyclonique ou anticyclonique, c'est-à-dire, d'après une remarque de S. Petterssen (1950), suivant que la circulation horizontale de l'air au point considéré est anticyclonique ou cyclonique.

BIBLIOGRAPHIE

Petterssen, S., 1950: Some aspects of the general circulation of the atmosphere. *Centenary Proc. Roy. Met. Soc.*, pp. 120—155.

Van Mieghem, J., et Vandenplas, A., 1950: Les équations de la dynamique atmosphérique en coordonnées généralisées. Application au cas des coordonnées sphériques. *Mém. Inst. Roy. Météor. de Belgique*, XLI, 57 p.

CORRESPONDENCE

Dear Sir:

The August 1951 issue of *Tellus* contains a very interesting article by Dr. F. A. Berson (1951) on some aspects of vortex motion on the earth. In the course of presenting a review of several existing theories on this general subject Dr. Berson refers to a result obtained by Rossby for the force acting on a solitary vortex in a resting environment (barotropic and non-divergent) on the earth. In particular, equation (1) of Dr. Berson's paper gives the value $\frac{1}{4} R^2 \omega \beta$ as the force per unit mass acting on a simple vortex. This value is obviously obtained from Rossby's equation

$$F = \beta \, p \, \pi \int_0^R r^3 \, \omega \, dr,$$

which occurs as equation (3) in Rossby's first paper on this subject (1948). The present writer would like to point out that this is merely the net *Coriolis* force acting on the vortex and that in the non-divergent model there will exist a net *pressure* force on the vortex *even initially* when the vortex has no translation and the environment it at rest. That this it so is indicated by Rossby's later result (1949) as well as by an analysis carried out by Long (1951). (Both of the latter indicate that the initial total force on the vortex is approximately one-half that given by Rossby's first result.)

Dr. Berson does not apply this formula in his paper, but it may be well to point out this distinction at this time.

REFERENCES

Berson, F. A., 1951: A synoptic-aerological study of interaction between vortices. *Tellus*, **3** 172—190.

Long, R. R., 1951: A theoretical and experimental study of the motion and stability of certain atmospheric vortices. *J. Meteor.*, **8**, 207—221 (see pp. 213—215).

Rossby, C. G., 1948: On displacements and intensity changes of atmospheric vortices. *J. Mar. Res.*, **7**, 175—187.

Rossby, C. G., 1949: On a mechanism for the release of potential energy in the atmosphere. *J. Meteor.*, **6**, 163—180 (see pp. 178—197).

Sincerely,

Norman A. Phillips

CORRIGENDUM

August issue uf Tellus 1951,

F. A. Berson on vortex interaction.

Due to regrettable mistake a wrong drawing has been substituted in Fig. 1. The downwards pointing arrow should point upward and to its right the minus sign be replaced by a plus sign. — In the text to Fig. 8a, p. 187, second line from the bottom read »corresponding broken symbols» instead of »primed numbers»,

INDEX

Volume 3, 1951

1. February
2. May
3. August
4. November

Italics indicate titles of articles or shorter contributions. Asterisks indicates notes, book reviews or letters to the editor. First figure refers to number, the second figure or number to page.

Aeromagnetic Survey: Lundbak 2, 69.
Age Determination: Arrhenius, Kjellberg, Libby 4, 222.
*Alpine Meteorology: Hovmöller 2, 114
ÅNGSTRÖM, A.: *The Blue Sun of September 1950*, 3, 135.
Angular Momentum (flux): Nyberg, Schmacke 2, 89; Mintz 3, 195.
Antarctic Circumpolar Current: Munk, Palmén 1, 53.
ARAKAWA, H.: *Possible Heavy Turbulent Exchange between the Extratropical Tropospheric Air and the Polar Stratospheric Air*, 3, 208.
ARRHENIUS, G.: *Age Determination of Pacific Chalk Ooze by Radiocarbon and Titanium Content*, 4, 222.

Barotropic Vorticity Equation: Bolin, Charney 4, 248.
BERSON, F. A.: *A Synoptic-Aerological Study of Interaction between Vortices*, 3, 172.
Bilan de la rotationelle absolue: Van Mieghem 4, 297.
Bjerknes, Vilhelm, (in memoriam): Sverdrup 4, 217.
Blocking Action: Rex 2, 100; Brezowsky, Flohn, Hess 3, 191.
Blue Sun (Blaue Sonne): Jenne 3, 129; Ångström 3, 135.
BMZ-apparatus: Lundbak 2, 69.
BOLIN, B: *Numerical Tendency Computations from the Barotropic Vorticity Equation*, 4, 248.
Boundary Conditions: Lowell 2, 78.
BRADBURY, D. L.: *Structure of Shear Lines near the Tropopause in Summer*, 3, 154.
BREZOWSKY, H : *Some Remarks on the Climatology of Blocking Action*, 3, 191.
BUSHBY, F. H.: *Note on the Numerical Integration of the Equations of Meteorological Dynamics*, 3, 201.

CARSON, J. E.: *Structure of Shear Lines near the Tropopause in Summer*, 3, 154.
Chalk Ooze: Arrhenius, Kjellberg, Libby 4, 222.
CHARNEY, J: *Numerical Tendency Computations from the Barotropic Vorticity Equation*, 4, 248.
Cloud Seeding: Leopold, Mordy 1, 44.
Complete Precipitation: Sherman 3, 203.
*Cooperative Research: Rossby 3, 212.
CRAYA, A.: *Critical Regimes of Flows with Density Stratification*, 1, 28.
Critical Regimes: Craya 1, 28.
Cumulus Clouds: Sherman 3, 203.

*DIETERICHS, H.: *Das Halophänomen in Nyköping am 3. Okt. 1580*, 2, 113.

*E Movements: Gerson 1, 56.
Eddy Diffusivity: Stommel 1, 43.
Eddy Flux of Heat: White 2, 82; Nyberg, Schmacke 2, 89.
Eddy Flux of Momentum: Nyberg, Schmacke 2, 89; Mintz 3, 195.
Effective Radiation: Lönnqvist 3, 148.
Energy Balance: Kuo 3, 205.
European Climate: Rex 2, 100.

Feldkomponentenmühle: Kasemir 4, 240.
FLOHN, H.: *Some Remarks on the Climatology of Blocking Action*, 3, 191.
Flows with density stratification: Craya 1, 28.
Flux of angular momentum: Nyberg, Schmacke 2, 89; Mintz 3, 195.
Flux of sensible heat: White 2, 82; Nyberg, Schmacke 2, 89.
Forecasting Minimum Temperature: Reuter 3, 141.

Fuglister, F. C.: *Some Results of a Multiple Ship Survey of the Gulf Stream*, 1, 1.
Fuglister, F. C.: *Multiple Currents in the Gulf Stream System*, 4, 230.
Fultz, D.: *Two-Dimensional Flow around a Circular Barrier in a Rotating Spherical Shell*, 2, 61.

General Circulation: Kuo 4, 268.
*Gerson, N. C.: *Sporadic E Movements on 21 June 1949*, 1, 56.
Gulf Stream: Fuglister, Worthington 1, 1; Stommel 1, 43; Fuglister 4, 230.

*Halophänomen: Dieterichs 2, 113.
Height Variations in Concentration of Ions: Norinder, Siksna 4, 234.
Hess, P.: *Some Remarks on the Climatology of Blocking Action*, 3, 191.
Hinkelmann, K.: *Der Mechanismus des meteorologischen Lärmes*, 4, 285.
*Hovmöller, E.: *International Congress on Alpine Meteorology*, 2, 114.

*International Congress: Hovmöller 2, 114.
Ions (Concentration): Norinder, Siksna 4, 234.

James, R. W.: *The Structure of Mean Circulations*, 4, 258.
Jenne, W.: *Das Phänomen »Blaue Sonne»*, 3, 129.
Jerlov, N. G.: *Optical Measurement of Particle Distribution in the Sea*, 3, 122.

Kasemir, H. W.: *Die Feldkomponentenmühle*, 4, 240.
Kinetic Energy Balance: Kuo 3, 205.
Kjellberg, G.: *Age Determination of Pacific Chalk Ooze by Radiocarbon and Titanium Content*, 4, 222.
Kuo, H.-L.: *A Note on the Kinetic Energy Balance of the Zonal Wind Systems*, 3, 205.
Kuo, H.-L.: *Dynamical Aspects of the General Circulation and the Stability of Zonal Flow*, 4, 268.

Lateral Eddy Diffusivity: Stommel 1, 43.
Length of the Day: Mintz, Munk 3, 117.
Leopold, L. B.: *1948—1949 Trials of the Schaefer-Langmuir Cloud-Seeding Technique in Hawaii*, 1, 44.
Libby, W. F.: *Age Determination of Pacific Chalk Ooze by Radiocarbon and Titanium Content*, 4, 222.
Long, R. R.: *Two-Dimensional Flow around a Circular Barrier in a Rotating Spherical Shell*, 2, 61.
Lönnqvist, O.: *On the Effective Radiation to Various Parts of a Cloudless Sky*, 3, 148.
Lowell, S. C.: *The Boundary Conditions at the Tropopause*, 2, 78.
Lundbak, A: *Aeromagnetic Survey of Vertical Intensity over the Sound with Apparatus of the BMZ Type*, 2, 69.

Mean Circulation: James 4, 258.
Meteorologischer Lärm: Hinkelmann 4, 285.
Van Mieghem, J: *Le mouvement des tourbillons atmosphériques*, 2, 75.
Van Mieghem, J.: *Le bilan de la rotationnelle absolue dans l'atmosphère*, 4, 297.
Minimum Temperature: Reuter 3, 141.
Mintz, Y: *The Effect of Winds and Tides on the Length of the Day*, 3, 117.
Mintz, Y.: *The Geostrophic Poleward Flux of Angular Momentum in the Month of January 1949*, 3, 195.
Mordy, W. A.: *1948—1949 Trials of the Schaefer-Langmuir Cloud-Seeding Technique in Hawaii*, 1, 44.
Momentum Concentration: Rossby 1, 15.
Momentum Flux: Nyberg, Schmacke 2, 89; Mintz, 3, 195.
Multiple Currents: Fuglister 4, 230.
Munk, W. H.: *Notes on the Dynamics of the Antarctic Circumpolar Current*, 1, 53.
Munk, W. H.: *The Effect of Winds and Tides on the Length of the Day*, 3, 117.

Newton, C. W.: *Structure of Shear Lines near the Tropopause in Summer*, 3, 154.
Norinder, H.: *Height Variations in the Concentration of Ions near the Ground during Quiet Summer Nights at Uppsala*, 4, 234.
Numerical Integration: Sawyer, Bushby 3, 201; Bolin, Charney 4, 248.
Nyberg, A.: *Eddy Flux of Heat and Momentum during Two Years at Stockholm-Bromma*, 2, 89.

Ocean Currents: Fuglister, Worthington 1, 1; Rossby 1, 15; Stommel 1, 43; Fuglister 4, 230.
Optical Measurement: Jerlov 3, 122.

Pacific Chalk Ooze: Arrhenius, Kjellberg, Libby 4, 222.
Palmén, E.: *Notes on the Dynamics of the Antarctic Circumpolar Current*, 1, 53.
Particle Distribution in the Sea: Jerlov 3, 122.
Phillips, N. A.: *Structure of Shear Lines near the Tropopause in Summer*, 3, 154.
Precipitation: Sherman 3, 203.

Radiation: Lönnqvist 3, 148.
Radiocarbon Content: Arrhenius, Kjellberg, Libby 4, 222.
*Research Projects: Rossby 3, 212.

Reuter, H.: *Forecasting Minimum Temperatures*, 3, 141.
Rex, D. F.: *The Effect of Atlantic Blocking Action upon European Climate*, 2, 100.
Rossby, C.-G.: *On the Vertical and Horizontal Concentration of Momentum in Air and Ocean Currents. I. Introductory Comments and Basic Principles, with Particular Reference to the Vertical Concentration of Momentum in Ocean Currents*, 1, 15.
*Rossby, C.-G.: *Note on Cooperative Research Projects*, 3, 212.
Rotating Spherical Shell: Fultz, Long 2, 61.
Rotationnelle absolue: Van Mieghem 4, 297.

Sawyer, J. S.: *Note on the Numerical Integration of the Equations of Meteorological Dynamics*, 3, 201.
Schmacke, E.: *Eddy Flux of Heat and Momentum during Two Years at Stockholm—Bromma*, 2, 89.
Sensible Heat: White 2, 82; Nyberg, Schmacke 2, 89.
Shear Lines: Newton, Phillips, Carson, Bradbury 3, 154.
Sherman, L.: *Photographs of the "Complete Precipitation" of a Cumulus Cloud*, 3, 203.
Siksna, E.: *Height Variations in the Concentration of Ions near the Ground during Quiet Summer Nights at Uppsala*, 4, 234.
Stability of zonal flow: Kuo 4, 268.
Stommel, H.: *Determination of the Lateral Eddy Diffusivity in the Climatological Mean Gulf Stream*, 1, 43.
Sverdrup, H.: *Vilhelm Bjerknes in memoriam*, 4, 217.
Synoptic-aerological Study: Berson 3, 172.

Tides: Mintz, Munk 3, 117.
Titanium Content: Arrhenius, Kjellberg, Libby 4, 222.
Tourbillons atmosphériques: Van Mieghem 2, 75.
Tropopause: Lowell 2, 78.
Turbulent Exchange: Arakawa 3, 208.
Two-Dimensional Flow: Fultz, Long 2, 61.

Vortices: Berson 3, 172.
Vorticity Equation: Bolin, Charney 4, 248.

White, R. M.: *The Meridional Flux of Sensible Heat over the Northern Hemisphere*, 2, 82.
Worthington, L. V.: *Some Results of a Multiple Ship Survey of the Gulf Stream*, 1, 1.

Zonal Flow: Kuo 4, 268.
Zonal Wind Systems: Kuo 3, 205.